

Cherry Creek Reservoir Water-Quality Model Documentation



Prepared for:

The Cherry Creek Basin Water Quality Authority



CHERRY CREEK BASIN WATER QUALITY AUTHORITY

c/o Clifton Larson Allen, LLP
8390 East Crescent Parkway, Suite 500
Greenwood Village, CO 80111

Prepared by:

Christine Hawley and Dr. Jean Marie Boyer, PE
Hydros Consulting Inc.



1628 Walnut St.
Boulder, CO 80302

And Dr. Brett Johnson (Colorado State University)

April 5, 2017

Table of Contents

Executive Summary.....	ES-1
1 Introduction.....	1
2 System Understanding Highlights	3
2.1 Bathymetry and Storage.....	3
2.2 Hydrology	5
2.3 Inflow Water Quality	9
2.4 Meteorology.....	12
2.5 In-Reservoir Water Quality.....	15
2.5.1 Temperature.....	15
2.5.2 Dissolved Oxygen.....	16
2.5.3 Nutrients.....	17
2.5.4 Chlorophyll a.....	19
2.5.5 Cyanobacteria.....	21
2.5.6 Zooplankton.....	27
2.5.7 Clarity.....	29
2.5.8 pH and Conductivity	29
2.6 Fish.....	32
3 Model Development.....	33
3.1 Bathymetry	34
3.2 Water Balance	38
3.3 Algae and Zooplankton.....	39
3.4 Sediment.....	40
3.5 Destratification System	41
3.6 Model Code Adjustments.....	42
4 Model Calibration.....	43
4.1 Surface Water Elevation	43
4.2 Temperature.....	45
4.3 Nutrients.....	48
4.3.1 Total Ammonia	49
4.3.2 Nitrate.....	50
4.3.3 Orthophosphate	51
4.4 Dissolved Oxygen.....	52
4.5 Algae.....	56
5 Sensitivity Analysis	60
5.1 Approach	60
5.2 Results	61
5.2.1 Destratification System Mixing Effects.....	61
5.2.2 Wind Mixing Effects.....	65
5.2.3 Inflow Nutrient Loading.....	69
5.2.4 Internal Loading and SOD.....	72
6 Management Runs	76
6.1 Run 1 – Best Anticipated Watershed Control of Nutrients	77

6.2	Run 2 – Increased Destratification System Mixing	79
6.3	Run 3 – Increased Destratification System Mixing and Best Anticipated Watershed Control of Nutrients	81
6.4	Run 4 – Reduction in Inflow Phosphorus Concentration Needed to Meet Chlorophyll a Standard	83
6.5	Run 5 – Nitrogen-to-Phosphorus Ratio	85
7	Summary of Findings, Recommendations, and Next Steps.....	88
7.1	Study Findings.....	88
7.2	Recommendations.....	90
7.3	Next Steps.....	91
8	References.....	92

ATTACHMENTS

Attachment A – Environmental Conditions for Walleye in Cherry Creek Reservoir

Attachment B – Temperature Profiles and Thermistors – Observed versus Simulated

Attachment C – Dissolved Oxygen Profiles – Observed versus Simulated

Attachment D – Sensitivity Analysis Results

Attachment E – Simplifying Assumptions in W2 Noted in Main Report Section 4.3

Attachment F – Assumed Inflow Concentrations for Management Runs 1, 3, and 5 Compared to Observed Concentrations

Attachment G – Peer Review Comments and Updated Response to Comments

LIST of FIGURES

Figure 1.	Image of Cherry Creek Reservoir Looking South (Photo by Harry Weddington, USACE)	1
Figure 2.	Approximate Aerator Footprint; Based on Image from GEI Presentation, April 30, 2013	2
Figure 3.	Cherry Creek Average Summer Chlorophyll <i>a</i> Compared to Site-Specific Standard, 1987-2013; Graph from GEI, 2015	2
Figure 4.	Cherry Creek Reservoir Bathymetry, 1 Ft. Contours, and In-Reservoir Sampling Locations	4
Figure 5.	Observed Reservoir Water Level, 2003-2013.....	5
Figure 6.	Cherry Creek Reservoir Gaged Inflows and Outflows	5
Figure 7.	Relative Fractions of Cherry Creek Inflows, 2003-2013	7
Figure 8.	Relative Fractions of Cherry Creek Outflows, 2003-2013	7
Figure 9.	Cherry Creek Reservoir Daily Inflow Rates, 2003-2013.....	8
Figure 10.	Cherry Creek Reservoir Annual Balance, 2003-2013.....	8
Figure 11.	Annual Hydraulic Residence Time (Flow Based on Reservoir Releases)	9

Figure 12. Inflow Soluble Reactive Phosphorus Concentrations, 1999-2013	10
Figure 13. Inflow Nitrate + Nitrite Concentrations, 2003-2013	10
Figure 14. Inflow Ammonia Concentrations, 2003-2013	11
Figure 15. Observed Ratios of TIN to SRP for Cherry Creek (CC-10) and Cottonwood Creek (CT-2), 2000-2013; Note Different Scales	11
Figure 16. TSS Concentrations in Cottonwood Creek (CT-2) and Cherry Creek (CC-10). 2000- 2013	12
Figure 17. Locations of Met Stations Used to Compile Meteorological Inputs.....	13
Figure 18. Hourly Air Temperature (Compiled from CPW and KAPA), 2003-2013.....	13
Figure 19. Monthly Precipitation, 2003-2013	14
Figure 20. Wind Rose, 2003-2013, KAPA Data from 10 m	14
Figure 21. Water Temperature at CCR1 and CCR2, Photic Zone, 2003-2013.....	15
Figure 22. June through September Temperature Profiles at CCR2, 2005 and 2010	16
Figure 23. Thermistor-Measured Temperature Difference between 1 m and 7 m at CCR2, 2007-2013	16
Figure 24. Dissolved Oxygen Concentration at 1 m and Near the Bottom of the Reservoir at CCR2 and CCR3; Red Line Indicates Start of Destratification System Operations	17
Figure 25. Nitrate and Ammonia Observations from the Top and Bottom of the Reservoir, 2003-2013; Red Line Indicates Start of Destratification System Operations	18
Figure 26. SRP Observations from the Top and Bottom of the Reservoir, 2003-2013; Red Line Indicates Start of Destratification System Operations.....	19
Figure 27. Observed Chlorophyll a Concentrations from CCR2 (2003-2013) and Comparison to Standard; Red Line Indicates Start of Destratification System Operations.....	20
Figure 28. Average Summer Chlorophyll <i>a</i> , Biovolume, and Algal Density, 2009-2015.....	21
Figure 29. Figure 24 from the 2013 Monitoring Report (GEI, 2014); <i>Data in these Pie Charts Reflect Relative % Density of Algal Species on a Calendar-Year Basis, Using Composite Samples of the Photic Zone (0-3 m)</i>	22
Figure 30. Algal Density Reported for 2006-2013. CU Data (2006-2008); Aquatic Analysts Data (2009-2013)	23
Figure 31. Cyanophyta Density (2003-2010). All CU Data. Data in July 2010 from a Separate WQCD Study (May, 2014)	23
Figure 32. Biovolume and Density of Major Taxonomic Groups of Algae in Cherry Creek Reservoir, 2009-2015.....	25
Figure 33. TIN and Dissolved Phosphorus Concentrations in the Photic Zone with Cyanobacteria Biovolume, 2010-2014.....	26
Figure 34. TIN:Dissolved Phosphorus Ratio and Cyanobacteria Biovolume, 2010-2014	26
Figure 35. Cherry Creek Reservoir Zooplankton Density and Biomass, 2011-2015	27
Figure 36. Comparison of Total Zooplankton and Total Algae, Densities, Biomass, and Biovolume	28
Figure 37. Secchi Depth at CCR2.....	29
Figure 38. In-Reservoir pH and Conductivity at 1 m at CCR2, 2003-2015.....	30
Figure 39. Inflow pH and Conductivity, 2002-2015	31
Figure 40. Chlorophyll <i>a</i> at CCR1 and CCR2, Photic Zone, 2003-2013	34

Figure 41. Model Segment Layout Shown with Bathymetric Contours, Destratification System (Pink Circles), and Sampling Locations (Three Black Stars).....	35
Figure 42. Example of Profile Data Considerations in Selecting Vertical Discretization of Model Layers.....	35
Figure 43. Profile View of Model Grid	36
Figure 44. Model Profile without Exaggerated Vertical Scale	36
Figure 45. Plan View of Model Grid (Left) and Section View of Segment 12 (Right)	36
Figure 46. Comparison of Model Bathymetry and Contour Data Elevation - Volume Relationship	37
Figure 47. Comparison of Model Bathymetry and Contour Data Elevation - Volume Relationship	38
Figure 48. Location of Inflows and Outflows Applied in Model	39
Figure 49. Maximum Growth Rate as a Function of Water Temperature for Algal and Zooplankton Groups in the Model.....	40
Figure 50. Actual Location of Aerators on Reservoir Footprint (Left) and Model Segments Designated to Contain Aerator Heads (Right)	41
Figure 51. Comparison of Simulated and Observed Daily Water Levels, 2003-2013.....	44
Figure 52. Simulated Water Age at 1 m and at the Bottom at CCR2, 2003-2013	44
Figure 53. Example Calibration Profiles at CCR2 from 2007	46
Figure 54. Observed and Simulated Hourly Temperatures at 1 m at CCR2, 2008	47
Figure 55. Observed and Simulated Hourly Temperatures at 7 m at CCR2, 2008	47
Figure 56. Observed and Simulated Hourly Temperature Differences between 7 m and 1 m at CCR2, 2008.....	48
Figure 57. Simulated and Observed Ammonia Concentrations at CCR2 (Top and Bottom), 2003-2013	50
Figure 58. Simulated and Observed Nitrate Concentrations at CCR2 (Top and Bottom), 2003-2013	51
Figure 59. Simulated and Observed Orthophosphate Concentrations at CCR2 (Top and Bottom), 2003-2013.....	52
Figure 60. Observed and Simulated Dissolved Oxygen at the Top, CCR2, 2003-2013	53
Figure 61. Observed DO Profiles at CCR1, CCR2, and CCR3 on April 13, 2005 and October 16, 2008	53
Figure 62. Observed and Simulated Dissolved Oxygen at the Bottom, CCR2, 2003-2013	54
Figure 63. Observed and Simulated Dissolved Oxygen at the Bottom, CCR3, 2003-2013	54
Figure 64. Observed and Simulated Dissolved Oxygen Gradient from Top to Bottom, CCR2, 2003-2013	55
Figure 65. Simulated and Observed Chlorophyll <i>a</i> Concentrations in the Photic Zone, 2003-2013	56
Figure 66. Comparison of Simulated and Observed Algal Biomass.....	57
Figure 67. Simulated and Observed Summer Average Chlorophyll <i>a</i> Concentrations in the Photic Zone, 2003-2013, July – September, CCR1 and CCR2.....	58
Figure 68. Comparison of Observed and Simulated Cyanobacteria Peak Timing, 2009-2013	59
Figure 69. Comparison of Observed and Simulated Zooplankton Biomass	59

Figure 70. Hourly Simulated Water Temperature at 1 m for Aerator Mixing Simulations, CCR2, 2009	62
Figure 71. Hourly Simulated Water Temperature at the Bottom for Aerator Mixing Simulations, CCR2, 2009	62
Figure 72. Hourly Simulated Difference in Water Temperature from 1 m to 7 m for Aerator Mixing Simulations, CCR2, 2009	63
Figure 73. Simulated DO at the Bottom of the Reservoir (CCR1,2), Aerator Mixing Simulations, 2003-2013	63
Figure 74. Simulated Total Ammonia at the Bottom of the Reservoir (CCR1,2), Aerator Mixing Simulations, 2003-2013	64
Figure 75. Simulated Average Summer (July-September) Chlorophyll <i>a</i> (CCR1,2), Aerator Mixing Simulations, 2003-2013	65
Figure 76. Hourly Simulated Water Temperature at 1 m for the No Wind and Baseline Simulations, CCR2, 2009	66
Figure 77. Hourly Simulated Water Temperature at the Bottom for No Wind and Baseline Simulations, CCR2, 2009	66
Figure 78. Hourly Simulated Difference in Water Temperature from 1 m to 7 m for No Wind and Baseline Simulations, CCR2, 2009	67
Figure 79. Simulated DO at the Bottom of the Reservoir (CCR1,2), No Wind and Baseline Simulations, 2003-2013	67
Figure 80. Simulated Ammonia Concentration at the Bottom of the Reservoir (CCR1,2), No Wind and Baseline Simulations, 2003-2013	68
Figure 81. Simulated Chlorophyll <i>a</i> (CCR1,2), No Wind and Baseline Simulations, 2003-2013	69
Figure 82. Simulated Average Summer (July-September) Chlorophyll <i>a</i> (CCR1,2), No Wind and Baseline Simulations, 2003-2013	69
Figure 83. Simulated DO at the Bottom of the Reservoir (CCR1,2), Half Tributary Nutrient Loading and Baseline Simulations, 2003-2013	70
Figure 84. Simulated PO ₄ at the Top (0-3 m) of the Reservoir (CCR1,2), Half Tributary Nutrient Loading and Baseline Simulations, 2003-2013	71
Figure 85. Simulated Average Summer (July-September) Chlorophyll <i>a</i> (CCR1,2), Half Tributary Nutrient Loading and Baseline Simulations, 2003-2013	71
Figure 86. Simulated DO at the Bottom of the Reservoir (CCR1,2), Aerobic and Anaerobic Internal Loading and Baseline Simulations, 2003-2013	73
Figure 87. Simulated Ammonia at the Bottom of the Reservoir (CCR1,2), Excluding Aerobic and Anaerobic Internal Loading and Baseline Simulations, 2003-2013	73
Figure 88. Simulated Orthophosphate at the Bottom of the Reservoir (CCR1,2), Excluding Aerobic and Anaerobic Internal Loading and Baseline Simulations, 2003-2013	74
Figure 89. Simulated Average Summer (July-September) Chlorophyll <i>a</i> (CCR1,2), Aerobic and Anaerobic Internal Loading and Baseline Simulations, 2003-2013	74
Figure 90. Comparison of Average Annual Cherry Creek Nutrient Loads for Management Runs 1, 3, and 5 (Model Runs Involving Provided Watershed Control Estimates)	77
Figure 91. Comparison of Average Annual Cottonwood Creek Nutrient Loads for Management Runs 1, 3, and 5 (<i>Shown at same vertical scale as Cherry Creek, Figure 1, to support comparison</i>)	77

Figure 92. Simulated Average July-September Chlorophyll <i>a</i> – Maximum Watershed Controls on Nutrients (NP) (<i>Baseline and Hypothetical Best-Case Reduced Inflow Nutrient Concentrations</i>)	78
Figure 93. Simulated Average Summer Cyanobacteria Biomass – Maximum Watershed Controls (<i>Baseline and Hypothetical Best-Case Reduced Inflow Nutrient Concentrations</i>).....	79
Figure 94. Simulated Dissolved Oxygen Concentrations at the Bottom at CCR1,2 – Destratification Run (<i>Baseline [Existing Destratification Operation] and Hypothetical Destratification System with Three Times the Vertical Mixing of the Current System - Applied to All Years</i>)	80
Figure 95. Simulated Average July-September Chlorophyll <i>a</i> – Destratification Optimization Run (<i>Baseline [Existing Destratification Operation] and Hypothetical Destratification System with Three Times the Vertical Mixing of the Current System - Applied to All Years</i>)	81
Figure 96. Simulated Average Summer Cyanobacteria Biomass – Destratification Optimization Run (<i>Baseline [Existing Destratification Operation] and Hypothetical Destratification System with Three Times the Vertical Mixing of the Current System - Applied to All Years</i>)	81
Figure 97. Simulated Average July-September Chlorophyll <i>a</i> – Max Watershed, 3x Destratification (<i>Baseline Compared to Best-Case Reduced Inflow Nutrients and Hypothetical Destratification System with Three Times the Vertical Mixing - Applied to All Years</i>).....	82
Figure 98. Simulated Average Summer Cyanobacteria Biomass – Max Watershed, 3x Destratification (<i>Baseline Compared to Best-Case Reduced Inflow Nutrients and Hypothetical Destratification System with Three Times the Vertical Mixing - Applied to All Years</i>).....	82
Figure 99. Simulated Zooplankton Biomass Concentrations– Max Watershed, 3x Destratification (<i>Baseline Compared to Best-Case Reduced Inflow Nutrients and Hypothetical Destratification System with Three Times the Vertical Mixing - Applied to All Years</i>).....	83
Figure 100. Comparison of Average Annual Cherry Creek Nutrient Loads for Management Runs 1, 3, 4, and 5.....	84
Figure 101. Simulated Average July-September Chlorophyll <i>a</i> – Reduced PO ₄ in Inflow (<i>Baseline [Existing Destratification Operation] and Hypothetical Destratification System with Three Times the Vertical Mixing of the Current System - Applied to All Years</i>)	84
Figure 102. Simulated Average Summer Cyanobacteria Biomass – Reduced PO ₄ in Inflow (<i>Baseline [Existing Destratification Operation] and Hypothetical Destratification System with Three Times the Vertical Mixing of the Current System - Applied to All Years</i>)	85
Figure 103. Simulated Average July-September Chlorophyll <i>a</i> – N-to-P Ratio Run (<i>Baseline and Hypothetical Minimum Nitrogen-to-Phosphorous Inflow Ratio</i>)	86
Figure 104. Simulated Average Summer Cyanobacteria Biomass – N-to-P Ratio Run (<i>Baseline and Hypothetical Minimum Nitrogen-to-Phosphorous Inflow Ratio</i>)	87

Figure 105. Simulated Average Spring/Fall Cyanobacteria Biomass – N-to-P Ratio Run
(Baseline and Hypothetical Minimum Nitrogen-to-Phosphorous Inflow Ratio)87

LIST of TABLES

Table 1. Comparison of Volume-Weighted Average Nutrient Concentrations for Inflows, 2003-2009 and 2010-2013.....	12
Table 2. Summary Calibration Statistics for Temperature Profiles, 2003-2013	46
Table 3. Summary Calibration Statistics for Thermistors at CCR2, 2007-2013	48
Table 4. Average Error, MAE, and RMSE Calibration Statistics for Nutrients, 2003-2013	49
Table 5. MAE as a Percent of Observed Range for CCR1, CCR2, and CCR3 for Nutrients, 2003-2013	49
Table 6. Summary Calibration Statistics for Dissolved Oxygen Profiles, 2003-2013.....	55
Table 7. Summary Calibration Statistics for Chlorophyll <i>a</i> Concentrations in the Photic Zone, 2003-2013, All Months	57
Table 8. Summary Calibration Statistics for Summer Average Chlorophyll <i>a</i> Concentrations in the Photic Zone, 2003-2013, July – September, CCR1 and CCR2	58
Table 9. Sensitivity Analysis Runs	61
Table 10. Management Runs.....	76

Executive Summary

Cherry Creek Reservoir is a 13,000 acre-ft flood-control reservoir near Denver, Colorado. The reservoir is a popular recreation area and a high-quality walleye fishery, which is heavily relied upon for providing eggs to hatcheries for subsequent stocking throughout the state. The Cherry Creek Basin Water Quality Authority (Authority) exists to protect and improve water quality in the reservoir to meet applicable water-quality standards. The reservoir exhibits periodic nuisance cyanobacteria (blue-green algae) blooms and high chlorophyll *a* concentrations. The reservoir has failed to consistently meet the current site-specific chlorophyll *a* standard of 18 ug/L, assessed as a July – September average.

In efforts to improve water quality, Cherry Creek Reservoir has been the focus of major watershed and in-reservoir monitoring and mitigation projects. In-reservoir efforts include installation of a destratification system in 2008. Mixing from the destratification system was intended to increase dissolved oxygen at the bottom, thereby reducing internal loading of nutrients. The mixing from the destratification system was also intended to reduce cyanobacteria concentrations by disrupting their buoyancy advantage over other algal types.

The destratification system, however, has not met those objectives. Of the six years of destratification system operations (2008-2013), the site-specific standard for chlorophyll *a* (18 ug/L as a July through September average) was only met in two years. Further, there is no evidence in the data that cyanobacteria blooms have been reduced by the destratification system.

Based on ongoing water-quality concerns, the Authority identified a need to develop a water-quality model of the reservoir to:

- Better understand the causes of chlorophyll *a* standard exceedances and cyanobacteria blooms;
- Determine the impacts of the destratification system; and
- Provide a tool to help predict the effects of future management strategies.

This report documents the development, calibration, initial applications, findings, and recommendations from that effort.

Model Development and Calibration

A two-dimensional hydrodynamic and water-quality model of Cherry Creek Reservoir has been developed using CE-QUAL-W2 (Figure E-1). Model development was based on a detailed review of observed data. The model simulates the years 2003 through 2013 and was calibrated to observed data.

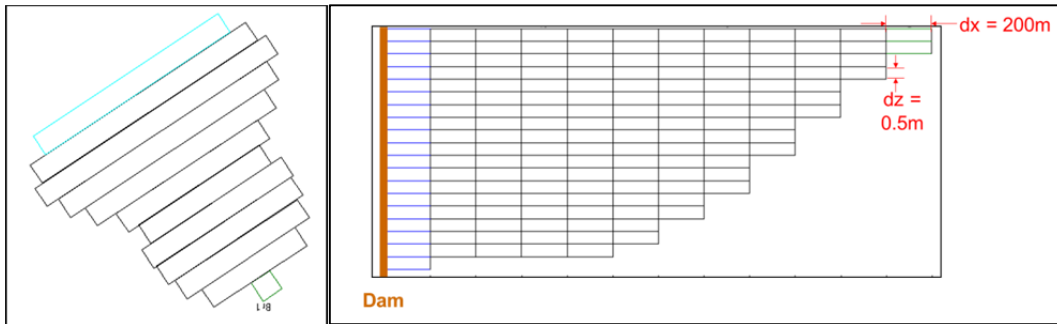


Figure E-1. Plan and Profile Views of Cherry Creek Reservoir Model

The ultimate calibration target was average summer chlorophyll *a* concentration (the metric for the site-specific chlorophyll *a* standard). Simulated summer (July through September) average chlorophyll *a* concentrations are compared to observed concentrations in Figure E-2. Results show good pattern and value matches for all simulated years. Mean absolute error (MAE), average error, and root mean squared error are all less than 4 ug/L for the summer average prediction.

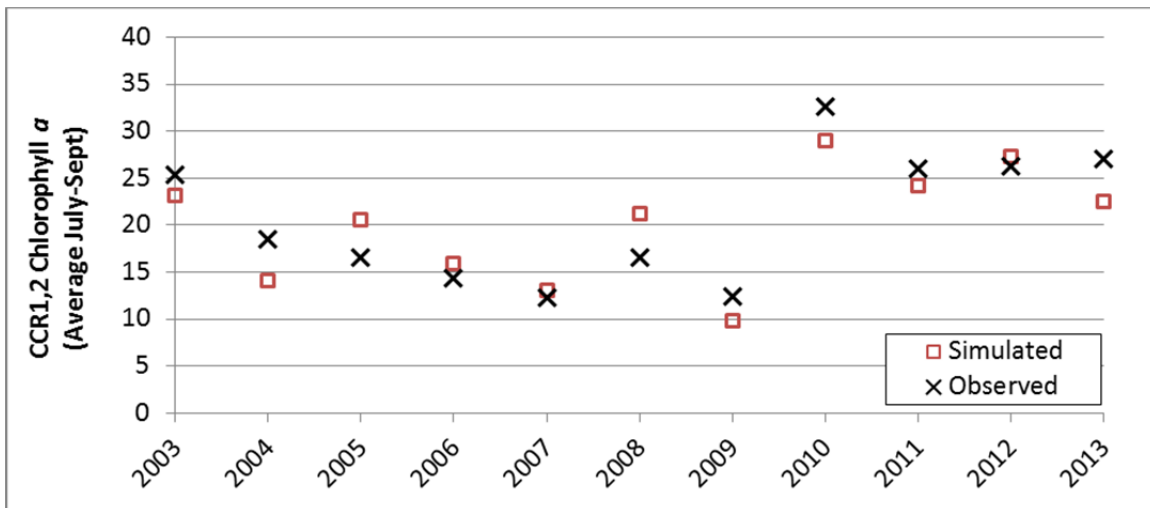


Figure E-2. Simulated and Observed Summer Average Chlorophyll *a* Concentrations in the Photic Zone, 2003-2013, July – September, CCR1 and CCR2

The calibration also focused on the simulation of surface water elevation, water temperature, summer cyanobacteria bloom timing and magnitude, nutrients, and dissolved oxygen. In addition to good range and pattern matches for these, all numerical calibration targets were met.

Sensitivity Analysis and Model Application Runs

A sensitivity analysis was conducted with the model. The sensitivity analysis focused on assessing modeled water-quality response to major forcing functions for this system. Forcing functions are external forces that can cause a water-quality response (e.g., wind, inflow concentrations, changes in operations, etc.). Specifically, effects of the following factors were evaluated:

- Destratification system mixing;
- Wind;
- Nutrient loading from major tributaries; and
- Internal loading.

Some of these forcing functions can be managed, and some cannot (e.g., wind). As such, these do not represent realistic management scenarios, but they were defined to provide an understanding of the system and modeling tool to ultimately support selection of management model runs.

Following completion of sensitivity analysis runs, the Authority identified five model application runs. These five management runs simulated variations on:

- Reducing inflow nutrient concentrations from the watershed; and
- Increasing vertical mixing by the destratification system.

Key Findings

This study yielded an improved understanding of nutrient loading and algal response in the reservoir, as well as the effectiveness of the current destratification system.

What Drives/Affects Algal Growth in Cherry Creek Reservoir?

- **Polymictic:** Cherry Creek Reservoir is a shallow, eutrophic reservoir that exhibits significant mixing by wind throughout the year (polymictic), resulting in vertical nutrient cycling and increased algal growth throughout the summer.
- **High Internal and External Nutrient Loading:** Both high internal (from sediments) and external (from inflows) loading of nutrients are important drivers with respect to algal growth. Of the external loading terms, Cherry Creek provides the majority of the inflowing nutrient load.
- **Anaerobic and Aerobic Internal Loading:** Both anaerobic and aerobic internal loading from sediments are significant for algal growth, though anaerobic loading is currently greater. This is relevant in consideration of in-reservoir management options.
- **Flushing Flows:** Large spring inflows (flushing flows reducing residence time in the reservoir), such as those observed in 2007, 2009, and 2015, appear to affect summer algal dynamics, resulting in lower chlorophyll *a* concentrations, though not necessarily lower algal biomass.

What Causes Cyanobacteria Blooms in Cherry Creek Reservoir?

- **Nitrogen Limitation:** Cherry Creek Reservoir tends to be nitrogen-limited, with elevated orthophosphate and near-absence of inorganic nitrogen at times. This gives a competitive advantage to nitrogen-fixing cyanobacteria.
- **Calm, Warm Conditions:** Summer cyanobacteria blooms tend to occur when the reservoir is calm (low wind and minimal inflows) with warm water temperatures. These

conditions set up weak stratification which leads to depletion of inorganic nitrogen in the photic zone, while excess orthophosphate remains.

What is the Current and Potential Effectiveness of the Destratification System?

- **Current System is Under-sized:** The current destratification system is under-sized to achieve the mixing needed to maintain oxic conditions at the bottom of the reservoir. As a result, the current system is not effectively reducing anaerobic internal loading of nutrients.
- **Minimal to No Effect on Cyanobacteria, Algae, or Walleye:**
 - Existing data and modeling indicate there has not been a noteworthy reduction in cyanobacteria since installation of the destratification system.
 - The current destratification system has only a very small effect on algal growth and chlorophyll *a*.
 - There is no clear impact (adverse or beneficial) of the current destratification system on the walleye fishery.
- **Redesign with Increased Mixing Could Have the Desired Effects:**
 - Model runs indicate that a destratification system with three times the vertical mixing effect of the current destratification system is needed to meet the original design target dissolved oxygen (DO) of 5 mg/L at the bottom of the reservoir.
 - This increased mixing would also decrease average summer chlorophyll *a* below the standard and reduce cyanobacteria blooms.
 - A separate study would be needed to appropriately size and design a system to meet these objectives.

*What is the Potential Effectiveness of Watershed Nutrient Controls on Chlorophyll *a*?*

- **Major Inflow Nutrient Concentration Reductions Needed to Meet Chl *a* Standard:**
 - A 50% reduction in nutrient loading from either Cherry Creek or Cottonwood Creek alone would not be adequate to meet the chlorophyll *a* standard in all years.
 - The Authority's best-case estimated reductions in inflow nutrient concentrations (47% decrease in orthophosphate and 72% decrease in inorganic nitrogen from the combined tributary load) would result in meeting the site-specific chlorophyll *a* standard in all the simulated years. Further, peak cyanobacteria concentrations would be reduced.
- **Drastic Changes Predicted for Combined Maximum Watershed Controls *plus* Redesigned Destratification System:** The combined effect of sharply reducing inflow nutrient concentrations (Authority-predicted maximum controls) and tripling the vertical mixing of the destratification system would result in summer chlorophyll *a* well

below the standard in all simulated years (an average reduction of 9.4 ug/L) and sharply reduced peak cyanobacteria concentrations.

- **Caution on N:P Ratios and Cyanobacteria:** Major changes to the inflow nutrient ratios (reduced inorganic nitrogen inflow concentrations in the absence of corresponding reductions to inflow orthophosphate) could increase spring cyanobacteria blooms of *Anabaena flos-aquae*. There are not similar concerns for the summer cyanobacteria (typically *Aphanizomenon flos-aquae*).

Recommendations and Next Steps

Through the course of the study, critical areas of remaining uncertainty were identified that merit ongoing evaluation and/or additional monitoring. From those, the following higher-priority recommendations are provided:

- **Collect Continuous / High-Frequency In-Reservoir DO Measurement** – The greatest area of remaining uncertainty in the modeling is for dissolved oxygen. It is strongly recommended that the Authority install continuous DO probes at 1 m below the surface and at 0.5 m above the bottom of the reservoir at CCR2. Alternatively, a buoy-based automated profiler, including DO measurement, located at CCR2 would greatly contribute to understanding of DO and mixing dynamics. Even a single year of such data would be invaluable.
- **Collect Wind Data** – It is recommended that the Authority install a meteorological station at the reservoir, perhaps on the dam. Wind speed and direction data are of primary importance, but including air temperature, relative humidity, and solar radiation would also be helpful.
- **Investigate pH and Specific Conductivity Trends:** Investigate and continue to track the multi-year trend of increasing specific conductivity and decreasing pH observed in the reservoir and inflows. Ideally, the explanation for these trends will be a finding of the pending watershed modeling.

It is expected that the next application of the reservoir model will be conducted in conjunction with the watershed model (in development). The watershed model is expected to provide refined predictions of potential improvements to inflow water quality. The reservoir model can then use watershed model predictions as input to generate updated predictions of reservoir response to watershed controls.

1 Introduction

Cherry Creek Reservoir (Figure 1) is a 13,000 acre-ft (AF; ~ 16 million m^3) reservoir located near Denver, Colorado. It was constructed in 1950 by the U.S. Army Corps of Engineers (USACE) for flood control purposes. Cherry Creek Park is comprised of the reservoir and surrounding land. The park is a popular recreation area, receiving approximately 1.5 million visitors per year to enjoy boating, fishing, camping, swimming, hiking, and more (Colorado Parks and Wildlife [CPW], 2013). The reservoir is also considered a high-quality walleye fishery and is heavily relied upon for providing eggs to fish hatcheries for subsequent stocking in lakes throughout the state.

The Cherry Creek Basin Water Quality Authority (Authority) exists to protect and improve water quality in the reservoir to meet applicable water-quality standards. Cherry Creek Reservoir has been the focus of major watershed and in-reservoir monitoring and mitigation projects to improve water quality for its designated beneficial uses. The reservoir exhibits high chlorophyll *a* concentrations and has failed to consistently meet the current site-specific state standard of 18 $\mu g/L$, assessed as a July – September average.



Figure 1. Image of Cherry Creek Reservoir Looking South (Photo by Harry Weddington, USACE)

In 2008, a destratification system was installed in the reservoir to mix oxygen from the surface to the bottom with the intention of reducing internal loading of nutrients and ultimately chlorophyll *a* concentrations. Mixing from the destratification system was also intended to reduce cyanobacteria concentrations by disrupting their buoyancy advantage over other algal groups. In total, 123 aerator heads were installed covering roughly 350 of the 850 acres (1.4 of the 3.4 million m^2) of the reservoir (Figure 2). The aerators release air roughly 0.75 m above the sediment-water interface and, when operated, are generally run from April through November.



Figure 2. Approximate Aerator Footprint; Based on Image from GEI Presentation, April 30, 2013

Of the six years of destratification system operations (2008-2013), the site-specific standard for chlorophyll *a* was only met in two years (Figure 3).

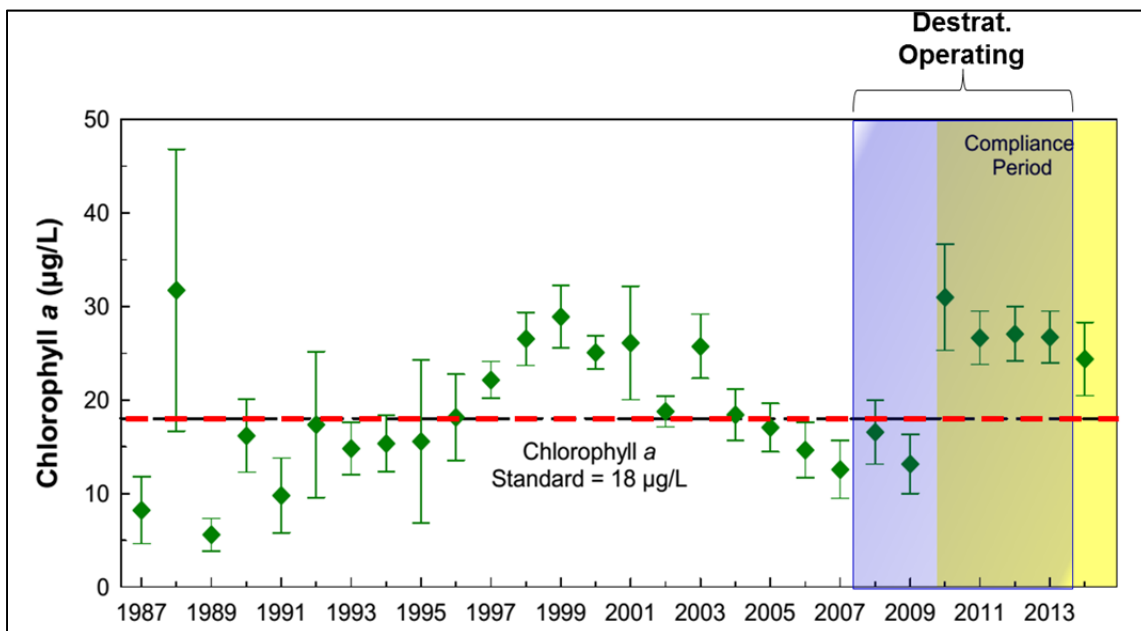


Figure 3. Cherry Creek Average Summer Chlorophyll *a* Compared to Site-Specific Standard, 1987-2013; Graph from GEI, 2015

Based on this, the Authority identified a need to develop a water-quality model of the reservoir to:

- Better understand the mechanisms behind chlorophyll *a* standard exceedances,
- Determine the impacts of the destratification system, and
- Provide a tool that can help predict effects of future management strategies.

To address this need, the Authority commissioned development of a water-quality model to simulate reservoir response from 2003 through 2013. Development, calibration, and initial application of the model are the subjects of this report.

Following the Executive Summary and this introductory section, the report is organized as follows:

- **Section 2 – System Understanding Highlights** – Key findings from review of observed data prior to model development
- **Section 3 – Model Development** – Model setup, development of inputs, key assumptions and code modifications
- **Section 4 – Model Calibration** – The approach to and results of calibration of the model
- **Section 5 – Sensitivity Analysis** – The goals, design and findings of the sensitivity analysis conducted with the model
- **Section 6 – Management Runs** – Findings of model application runs defined by the Authority to support reservoir management
- **Section 7 – Summary of Findings, Recommendations, and Next Steps**
- **Section 8 – References.**

2 System Understanding Highlights

A conceptual system understanding was developed based on review of existing observed data to support model selection and development. This included review of reservoir bathymetry, hydrology, inflow water-quality, meteorology, in-reservoir water-quality, and fish data. The discussion focuses primarily on observed data from the model simulation period (2003 and 2013), but considers data through 2015 in some cases, reflecting analysis updates through the course of the project, particularly in areas with limited datasets before 2013.

2.1 Bathymetry and Storage

The 13,522 AF reservoir covers 876 acres (3.4 million m²) at capacity. The average depth of the reservoir is ~15.4 ft (~4.7 m), with a maximum depth of ~27 ft (~8.2 m). The bathymetry of the reservoir is presented in 1 ft contours in Figure 4, along with the location of the three main in-reservoir, water-quality sampling locations.

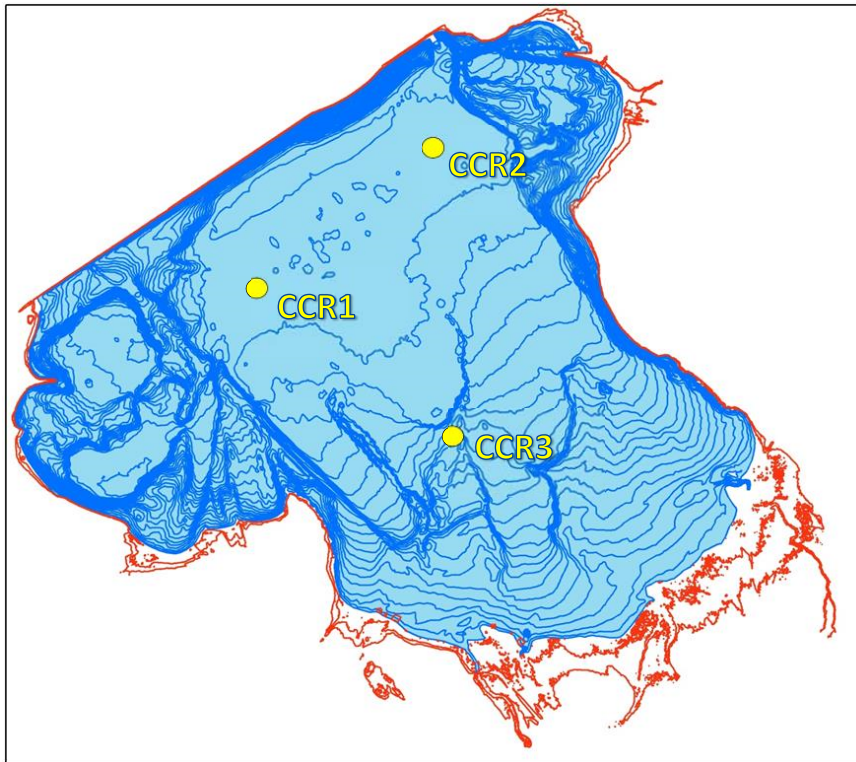


Figure 4. Cherry Creek Reservoir Bathymetry, 1 Ft. Contours¹, and In-Reservoir Sampling Locations

The reservoir water surface elevation is recorded daily by the USACE (Figure 5). These data show that the water surface elevation has varied by ~6.5 ft (2 m) between 2003 and 2013. Due to changes in reservoir operations, there has been a general decrease in the average annual storage over that period of time. The effect on water surface elevation from the September 2013 flood event is also evident in Figure 5, with the lowest and highest water levels occurred in September of 2013.

¹ The elevation contours shown here were measured as part of two separate studies. Contours from elevation 5,512' to 5,550' (Local Project Datum) were measured at one-foot intervals by Absolute Natural Resources (ANR) in 2013, and contours from elevation 5,552.2' to 5,558.2' at two-foot intervals were from a LiDAR survey carried out by Southeast Metro Stormwater Authority (SEMSWA) in 2008. These two sets of contours were merged by Shane Michael of Leonard Rice Engineers and delivered to Hydros by email on 3/28/14 as a shapefile.

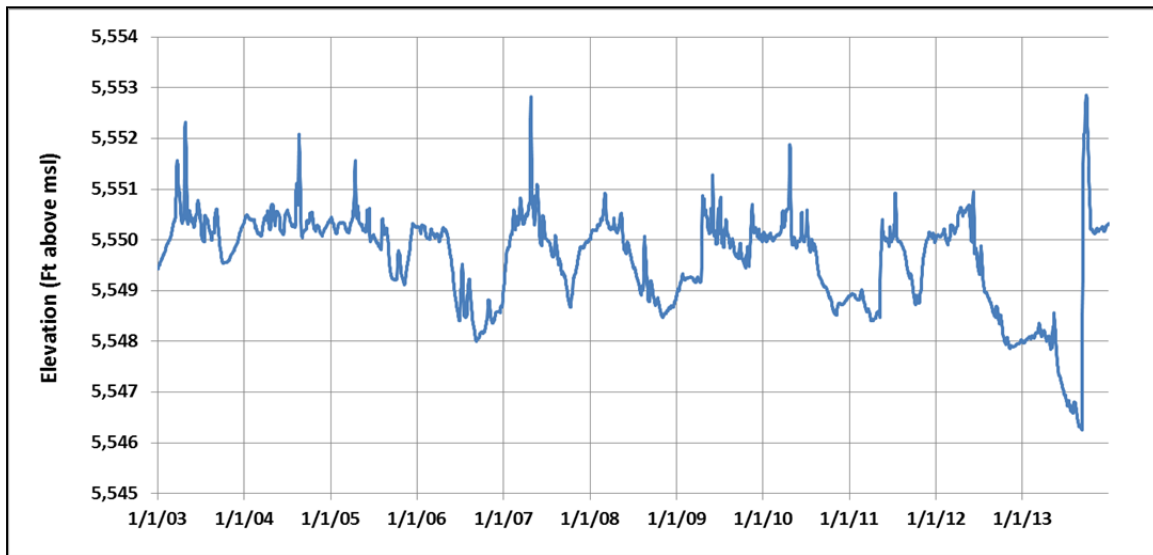


Figure 5. Observed Reservoir Water Level, 2003-2013

2.2 Hydrology

There are two major gaged tributaries flowing into Cherry Creek Reservoir: Cherry Creek and Cottonwood Creek (Figure 6). Other inflows include alluvial inflow, ungaged surface inflow, and precipitation. Water is released from the reservoir on the northwest end of dam from the bottom of the reservoir. Water is also lost through evaporation and outflow seepage.

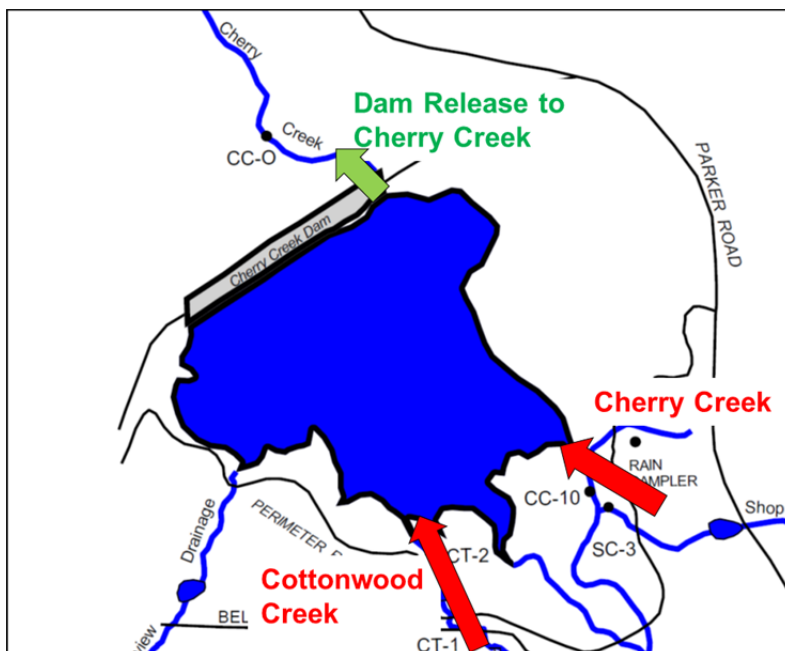


Figure 6. Cherry Creek Reservoir Gaged Inflows and Outflows

To evaluate the system hydrology and develop a water balance for the model, observed precipitation and daily flow data were compiled. For ungaged flows, the following calculations and assumptions were made:

- **Outflow seepage** was estimated from USACE measurements conducted during dam construction².
- **Ungaged surface inflows** for the 5.2 square mile direct watershed were estimated from precipitation, applying averaged runoff parameters developed by Brown and Caldwell for watershed phosphorus modeling (Brown and Caldwell, 2009).
- **Evaporation** was estimated by applying the methodology outlined in the ASCE Standardized Reference Evapotranspiration Equation (Walter et al., 2001) and the FAO Irrigation and Drainage Paper 56 (Allen et al., 2006). The long-term average annual evaporation rate resulting from these calculations is ~42 in/yr (107 cm/yr), which is very close to the expected value for this region and close to the value reported by USACE in for the reservoir.
- **Alluvial inflow seepage** was assumed to be constant and equal to the 2,200 AF/ yr (~2.7 million m³/yr) estimate developed by Lewis et al. (2005). Attempts to solve for alluvial inflow seepage as the closure term of the water balance produced similar seepage estimates in some years. However, there were seasons when increases in the closure term did not correlate with times when inflow seepage would be expected to increase. This suggested other sources of error in the water balance and led to assumption of constant inflow seepage.

Compiling these terms on a daily basis, along with daily reservoir storage, a water balance was developed. The closure term from these inputs was assumed to be error in the reported gaged inflows. Errors were smoothed and split proportionately between Cherry Creek and Cottonwood Creek inflows, adjusting these terms on a daily basis to close the water balance. The resulting adjustments to Cherry Creek and Cottonwood Creek flow rates were less than 5% of the observed flow data, which is well below the typical 10 to 15% estimate of accuracy for good to fair streamflow monitoring (Risley and Gannett, 2006).

The water balance inflows for 2003-2013 in Figure 7 show that Cherry Creek is the dominant source of water into the reservoir, averaging more than 60%. Cottonwood Creek is the next largest term at 20%, and is nearly twice the next highest term, alluvial inflow. The water balance outflows for 2003-2013 are summarized in Figure 8, and show outflow seepage to be relatively small compared to outflow released at the dam and evaporation.

² As part of a supplemental design analysis carried out during preparation for reservoir construction in 1947, USACE calculated the horizontal and vertical hydraulic conductivity of the soils underlying Cherry Creek Reservoir. These conductivity estimates used to develop a linear relationship between reservoir surface elevation and seepage outflow. Application of this elevation-seepage relationship results in a relatively constant estimated outflow seepage.

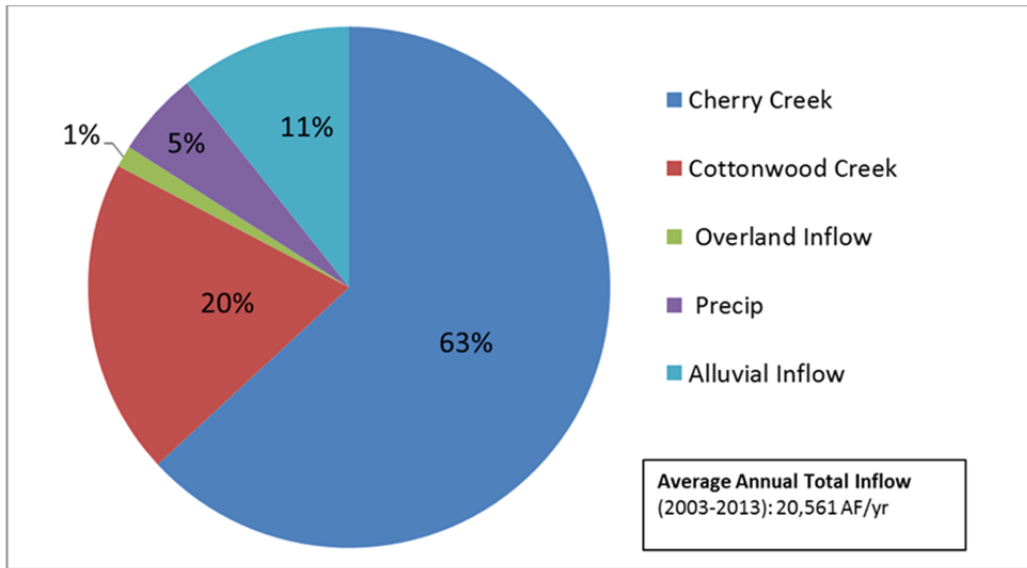


Figure 7. Relative Fractions of Cherry Creek Inflows, 2003-2013

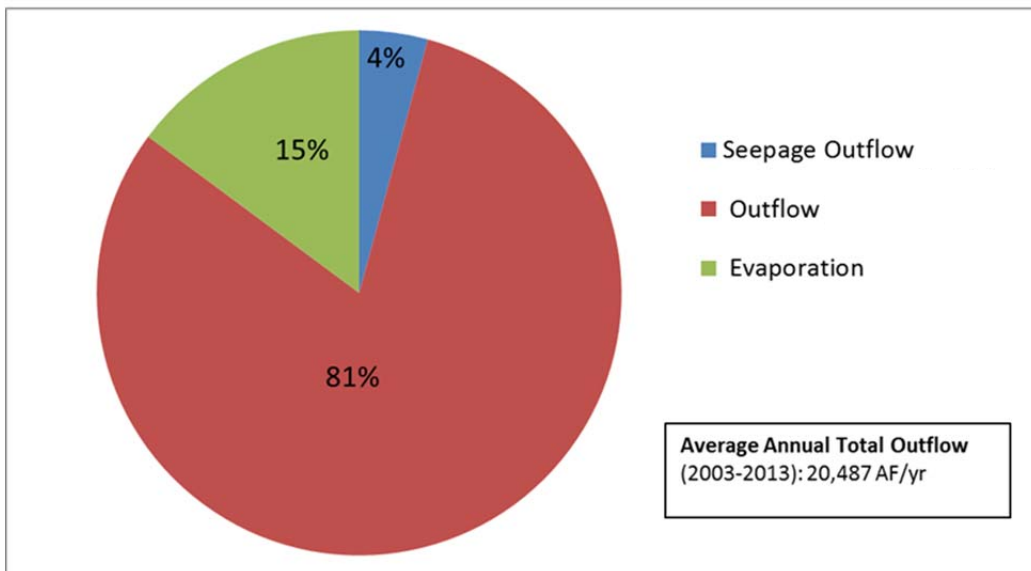


Figure 8. Relative Fractions of Cherry Creek Outflows, 2003-2013

The daily inflow pattern exhibits a wide range of inflow rates, characterized by periodic storm event hydrograph peaks (Figure 9). Over the modeled years (2003-2013), total annual inflows tended to be similar to total annual outflows each year (Figure 10). Variability among the years is apparent in the ratio of Cherry Creek to Cottonwood Creek flows and in the total volume of water moving through the reservoir.

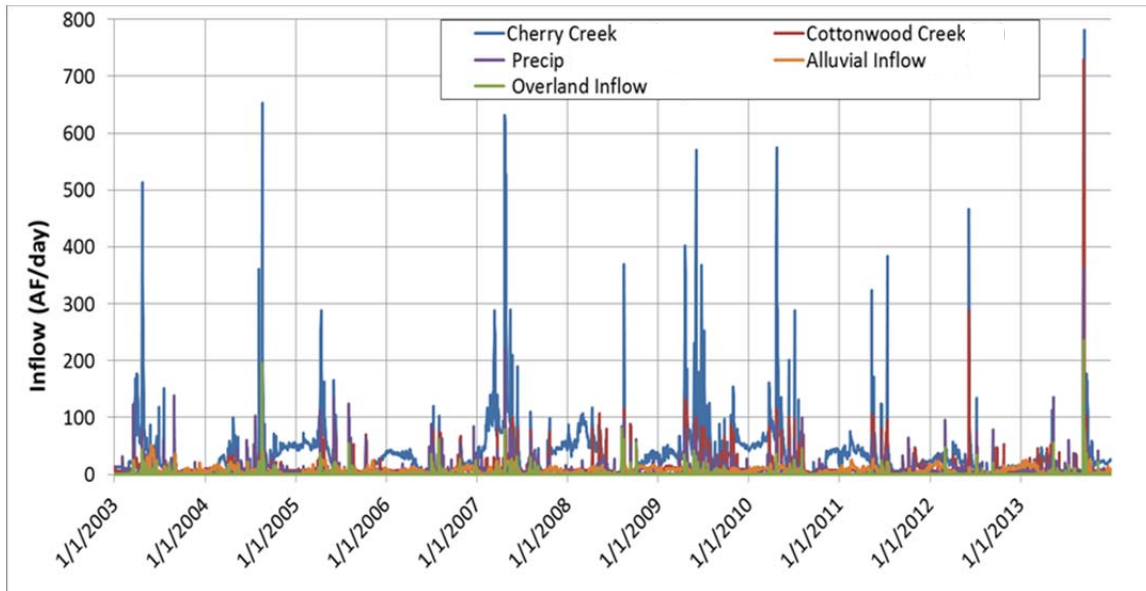


Figure 9. Cherry Creek Reservoir Daily Inflow Rates, 2003-2013

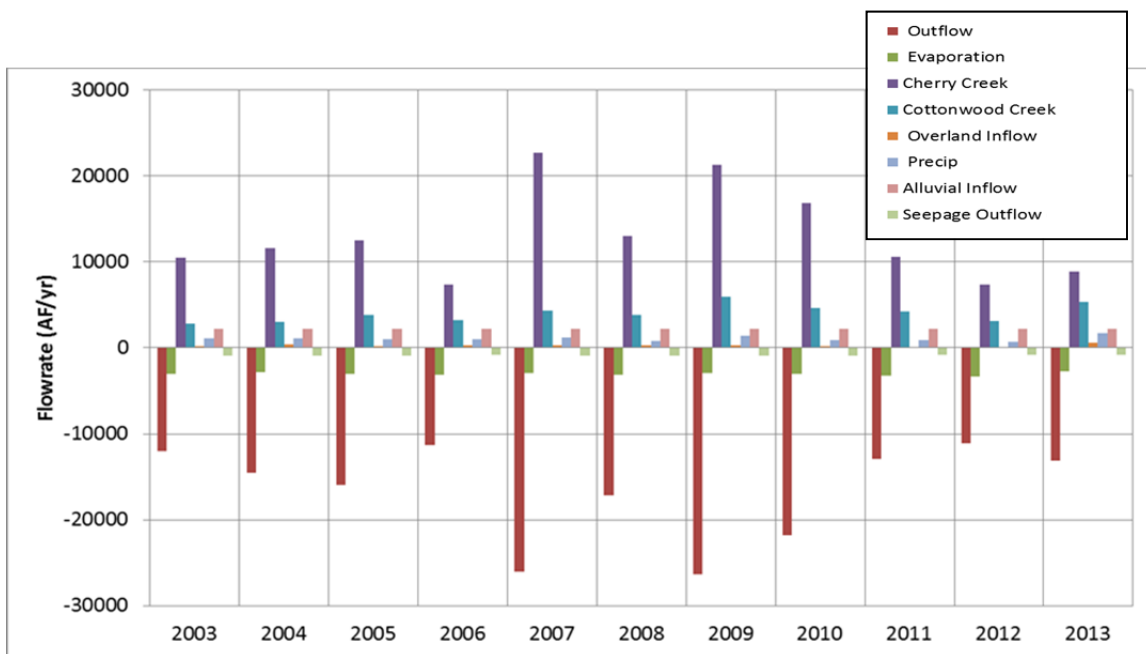


Figure 10. Cherry Creek Reservoir Annual Balance, 2003-2013

Estimated annual hydraulic residence time, based on observed outflows, averaged 10.4 months from 2003-2013 (Figure 11). The average annual residence time ranged from six months in 2009 to 14 months in 2012.

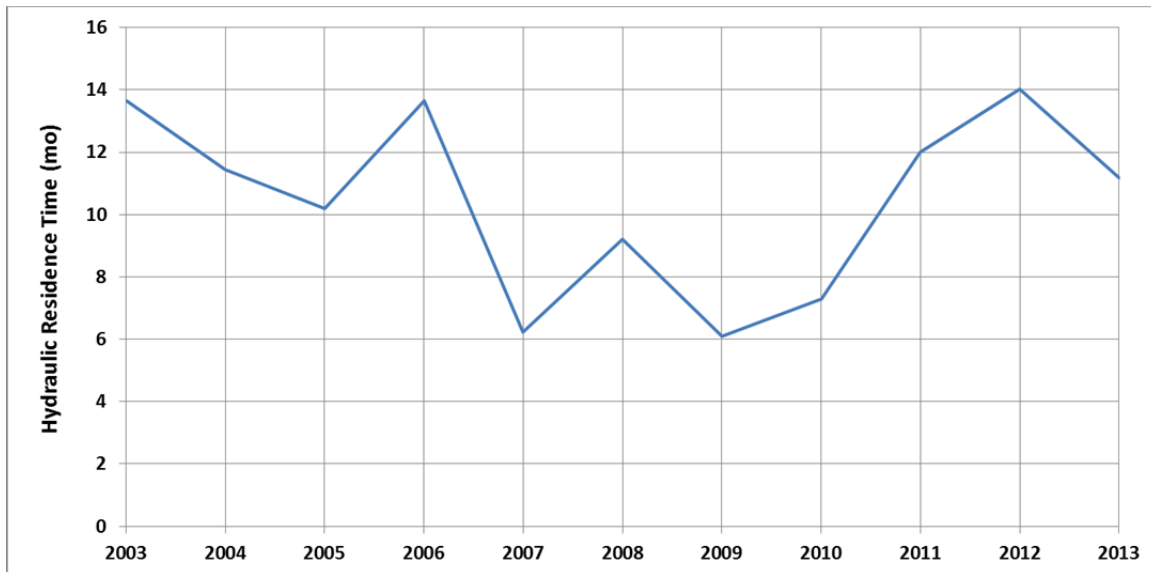


Figure 11. Annual Hydraulic Residence Time (Flow Based on Reservoir Releases)

2.3 Inflow Water Quality

Water-quality data are collected at the inflow locations to Cherry Creek Reservoir on Cherry Creek and Cottonwood Creek at gages CC-10 and CT-2, respectively. Groundwater-quality samples are also collected at MW-9, located approximately 440 ft (~130 m) up-gradient of the reservoir next to Cherry Creek. Inflow water quality is characterized by high nutrient and TSS concentrations and has been the subject of numerous water-quality improvement projects implemented by the Authority.

Surface inflow and groundwater soluble reactive phosphorus (SRP) concentrations are presented in Figure 12. Groundwater SRP concentrations are consistently high, averaging 188 ug/L. SRP concentrations in Cherry Creek at CC-10 are also relatively high but vary more, ranging from less than 100 ug/L to over 350 ug/L, with an average concentration of 170 ug/L. In Cherry Creek, there is a seasonal pattern of higher SRP concentrations in the summer months. Cottonwood Creek (CT-2) exhibits much lower SRP concentrations, averaging 18 ug/L. The combined, volume-weighted average concentration for Cherry and Cottonwood Creeks is approximately 120 ug/L SRP for 2003-2013 (~190 ug/L for total phosphorus [TP]).

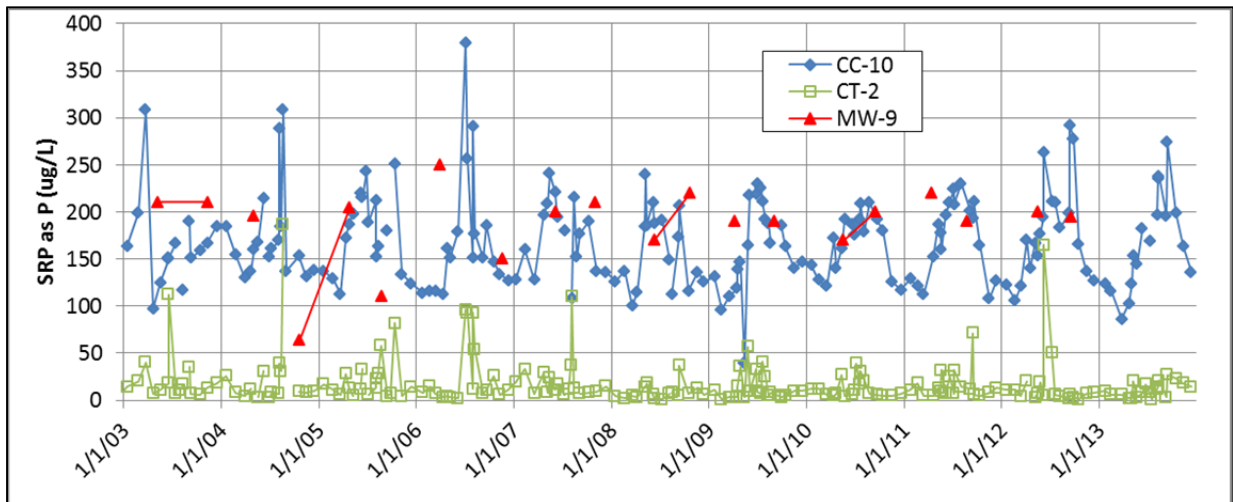


Figure 12. Inflow Soluble Reactive Phosphorus Concentrations, 1999-2013

Inflow nitrate and ammonia (ammonia is used throughout this document to indicate total ammonia, i.e., ammonia plus ammonium) concentrations exhibit different patterns compared to SRP. For ammonia and nitrate, Cottonwood Creek concentrations are higher than those in Cherry Creek, particularly before 2009. Peak nitrate concentrations tend to occur in winter months in both Cherry Creek and Cottonwood Creek. The average combined Cherry and Cottonwood Creek volume-weighted inflow concentrations from 2003-2013 are estimated to be 840 ug/L and 83 ug/L for nitrate and ammonia, respectively. Note that MW-9 ammonia data from 2004-2009 (shown on Figure 14) are considered suspect.

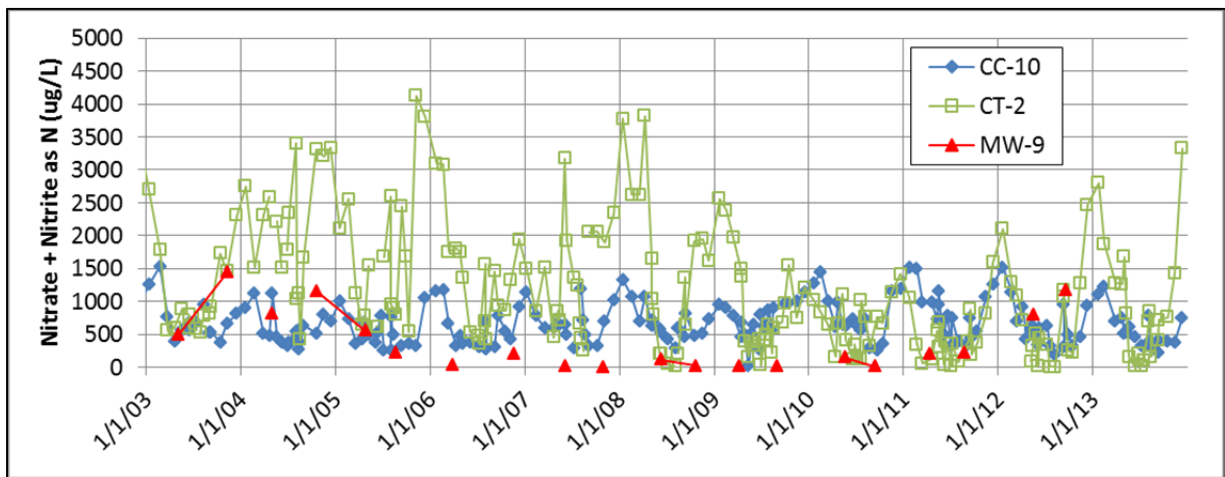


Figure 13. Inflow Nitrate + Nitrite Concentrations, 2003-2013

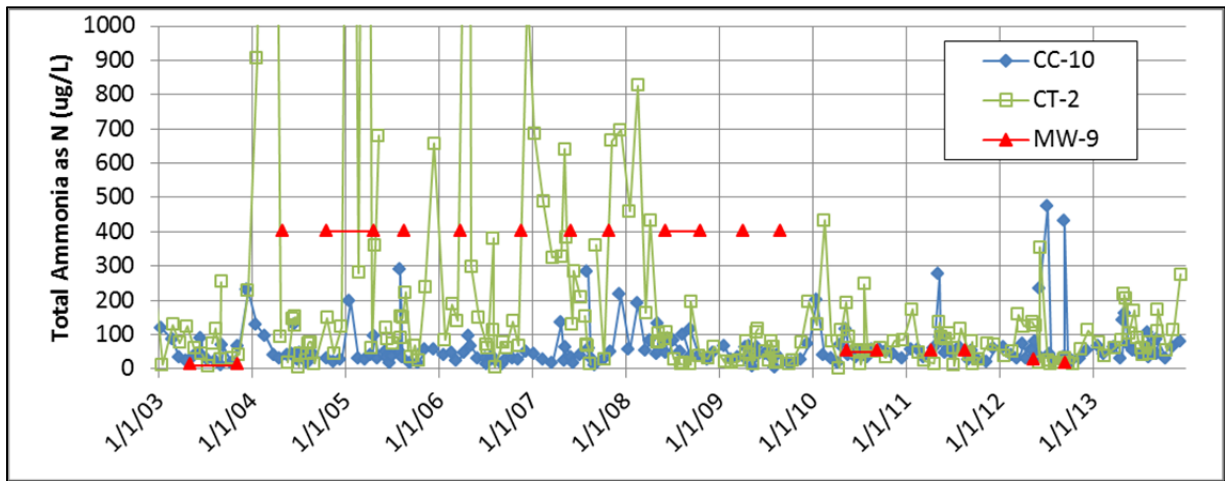


Figure 14. Inflow Ammonia Concentrations, 2003-2013

Looking more closely at the change in nitrate and ammonia concentrations in 2009, Figure 15 presents the ratios of TIN (total inorganic nitrogen = nitrate plus ammonia) to SRP for Cottonwood Creek and Cherry Creek from 2000 through 2013. A period of higher relative TIN:SRP ratios for Cottonwood Creek is apparent between roughly 2004 and 2009. The volume-weighted average concentrations for SRP were fairly consistent comparing periods before and after 2009, but there was a shift in ammonia after 2009, as shown in Table 1. A shift in TIN:SRP ratios is relevant because it can affect the in-reservoir algal response and assemblages in eutrophic lakes (e.g., Barica et al., 1980; Smith, 1983; Schindler et al., 2008).

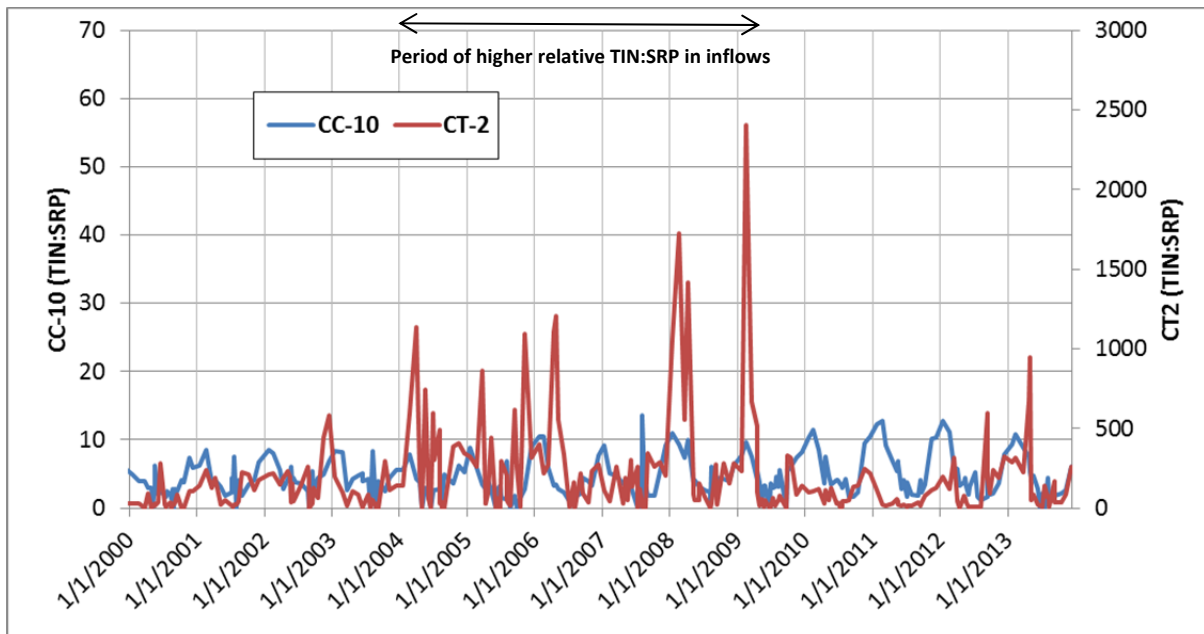
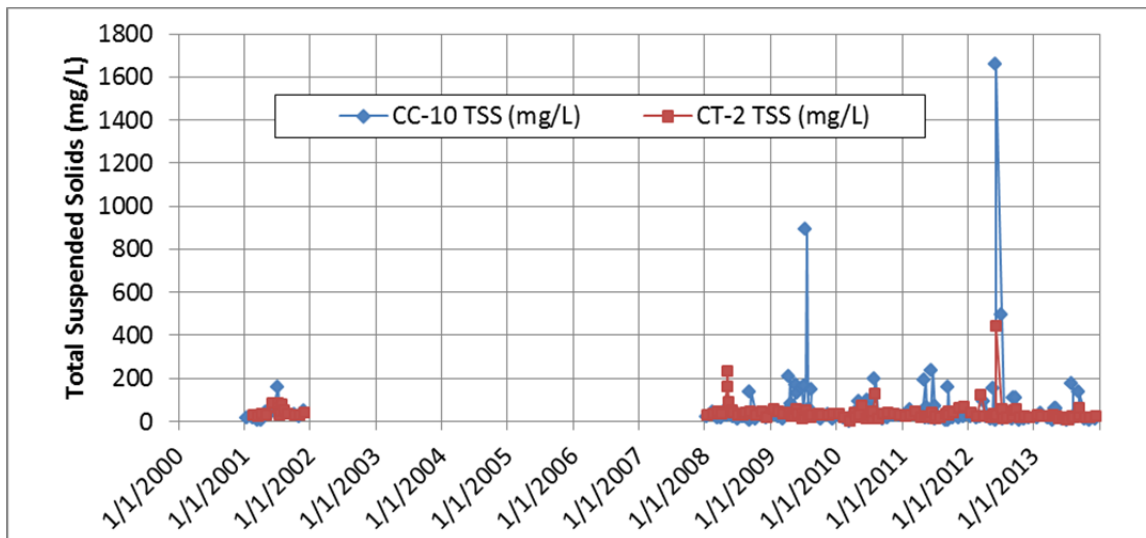


Figure 15. Observed Ratios of TIN to SRP for Cherry Creek (CC-10) and Cottonwood Creek (CT-2), 2000-2013; Note Different Scales

Table 1. Comparison of Volume-Weighted Average Nutrient Concentrations for Inflows, 2003-2009 and 2010-2013

Averaging Period	Volume-Weighted Average Inflow Concentration (ug/L) (Cottonwood Creek and Cherry Creek)		
	SRP	Nitrate	Ammonia
2003-2009	119	880	97
2010-2013	114	782	59

Inflow total suspended solids (TSS) concentrations are also relatively high (Figure 16). Median TSS concentrations for Cherry Creek and Cottonwood Creek are similar for 2003-2013, at 28 and 29 mg/L, respectively. Much higher TSS concentrations, however, can be observed during storm events on each of the tributaries. Both tributaries have shown an apparent reduction in non-storm event TSS concentrations since 2008, likely reflecting water-quality improvement projects in the watersheds.

**Figure 16. TSS Concentrations in Cottonwood Creek (CT-2) and Cherry Creek (CC-10). 2000-2013**

2.4 Meteorology

Meteorological data were compiled from four locations (Figure 17) to support the development of the conceptual understanding and compile inputs for the model. These included KAPA (Centennial Airport), CPW Met (Colorado Parks and Wildlife Met Station at Cherry Creek), KBKF (Buckley Air Force Base), and LRSS (Lowry Range Solar Station). KAPA data were used for all but solar radiation and air temperature. CPW Met data were used for solar radiation and air temperature. Unfortunately, wind data from CPW Met could not be used due to extensive data formatting and date-stamp issues. Missing data for air temperature were filled in from KAPA, and missing data for solar radiation were filled in from LRSS. Data from KBKF were used as a secondary backfill source for missing data which could not be filled from other sources.

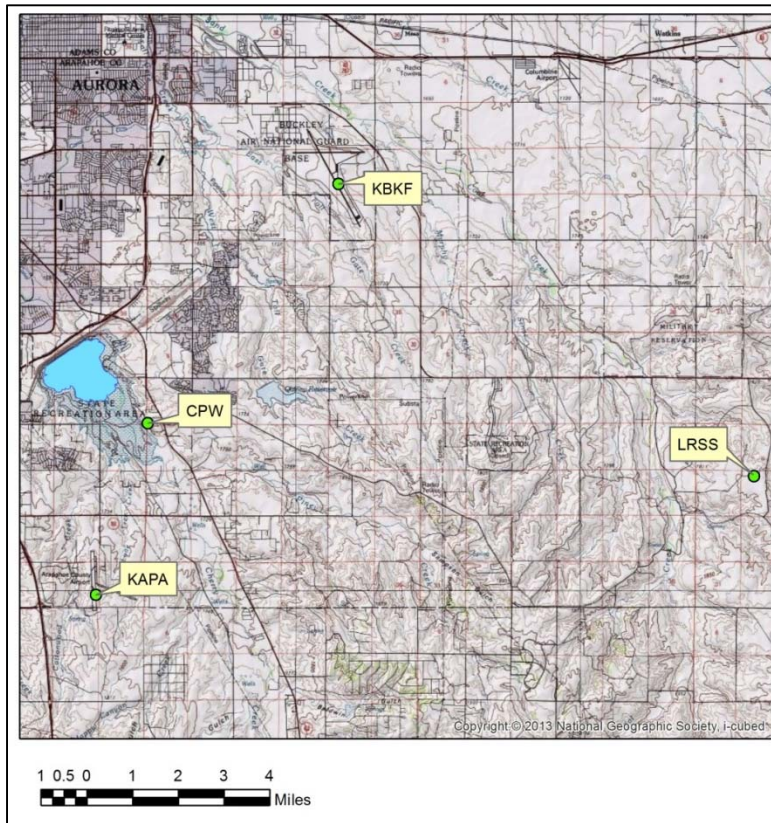


Figure 17. Locations of Met Stations Used to Compile Meteorological Inputs

Meteorological conditions at the reservoir are characterized by sunny and warm summers, relatively cool winters, low precipitation, and high winds. Peak summer air temperatures range from 96 °F (36 °C) to 107 °F (41.7 °C) for the simulation period of 2003-2013 (Figure 18). Within that period, the warmest summers were 2003, 2005, and 2012. The coolest summers were 2004 and 2009. Annual winter low temperatures range from 0.2 °F (-18 °C) to 12 °F (-11 °C). The coolest months in the simulation period were February of 2007 and February of 2012.

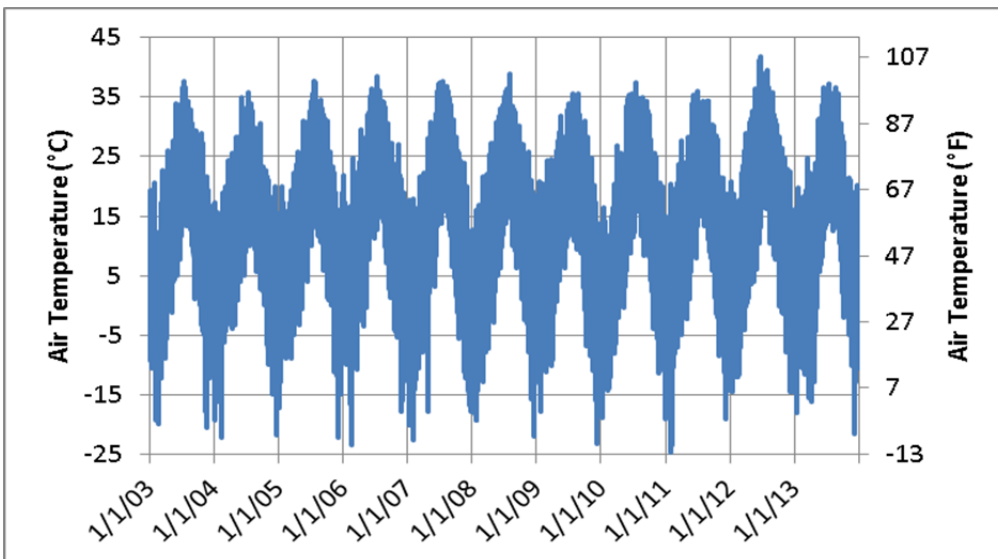


Figure 18. Hourly Air Temperature (Compiled from CPW and KAPA), 2003-2013

The average precipitation from 2003 through 2013 is ~17 inches per year (43 cm/yr), which is typical for the semi-arid, high plains. In general, the wettest months are August and April; the driest months are November through January (Figure 19). Total annual precipitation was lowest in 2008, 2010, 2011 and 2012. The wettest year was 2013, due to the major storm in September (Figure 19).

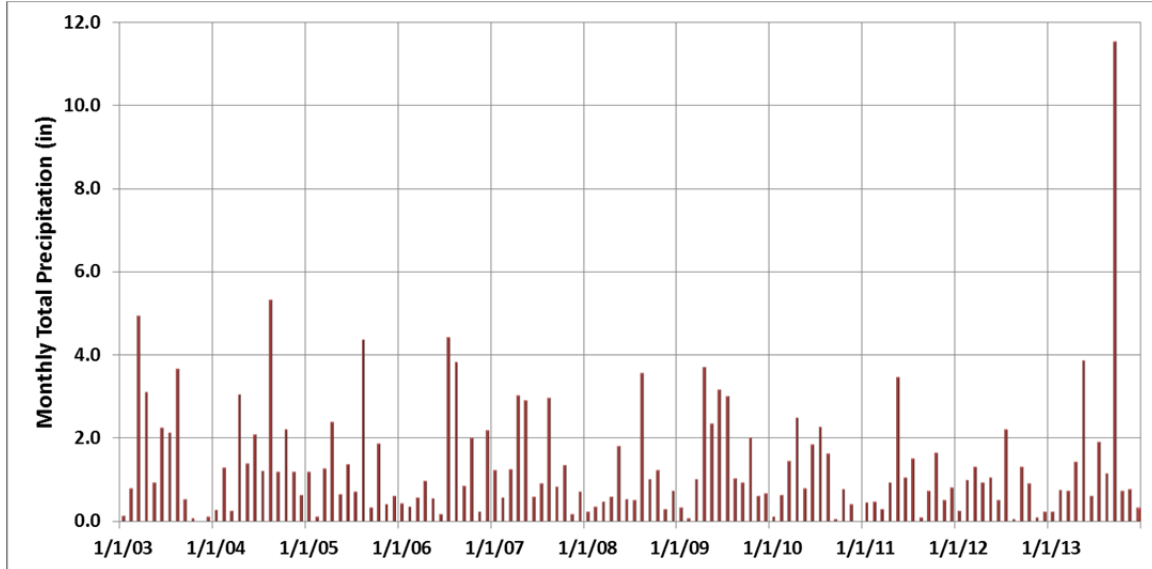


Figure 19. Monthly Precipitation, 2003-2013

Finally, average wind speeds (at the 10 m elevation of the wind data from KAPA) were approximately 9 mph (4 m/s). The wind comes most frequently from the south or north (Figure 20) and is characterized by occasional strong gusts, with calm conditions occurring during 10% of the record. The reservoir does not have much natural physical sheltering from the wind.

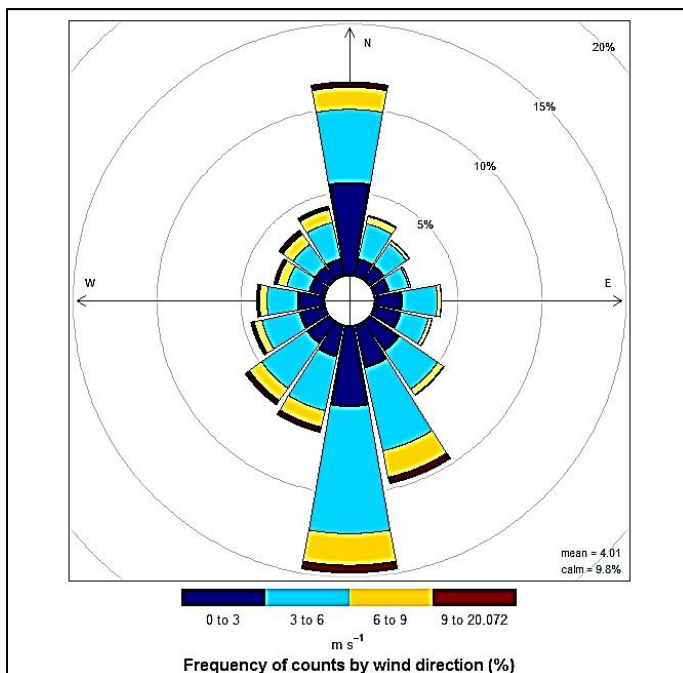


Figure 20. Wind Rose, 2003-2013, KAPA Data from 10 m

2.5 In-Reservoir Water Quality

Water-quality data from stations CCR1, CCR2 and CCR3 (Figure 4) were reviewed in detail. This section presents highlights focusing primarily on CCR2, the deepest sampling location. Data reflect a warm, relatively shallow, eutrophic, polymictic reservoir.

2.5.1 Temperature

Each year, water temperatures in the photic zone of the reservoir range 20-25+°C (Figure 21). Temperature profile data indicate the reservoir is frequently isothermal or nearly isothermal through the summer months (Figure 22). Peak surface temperature each summer ranges from ~23 °C (73 °F) to ~25 °C (77 °F). Thermistor data indicate that top to bottom temperatures in the reservoir vary only by 0 to ~4 °C from spring through fall (Figure 23). Temperatures at the deepest part of the reservoir reach relatively high peak temperatures, ranging from ~21 °C (70 °F) to ~23.5 °C (74 °F).

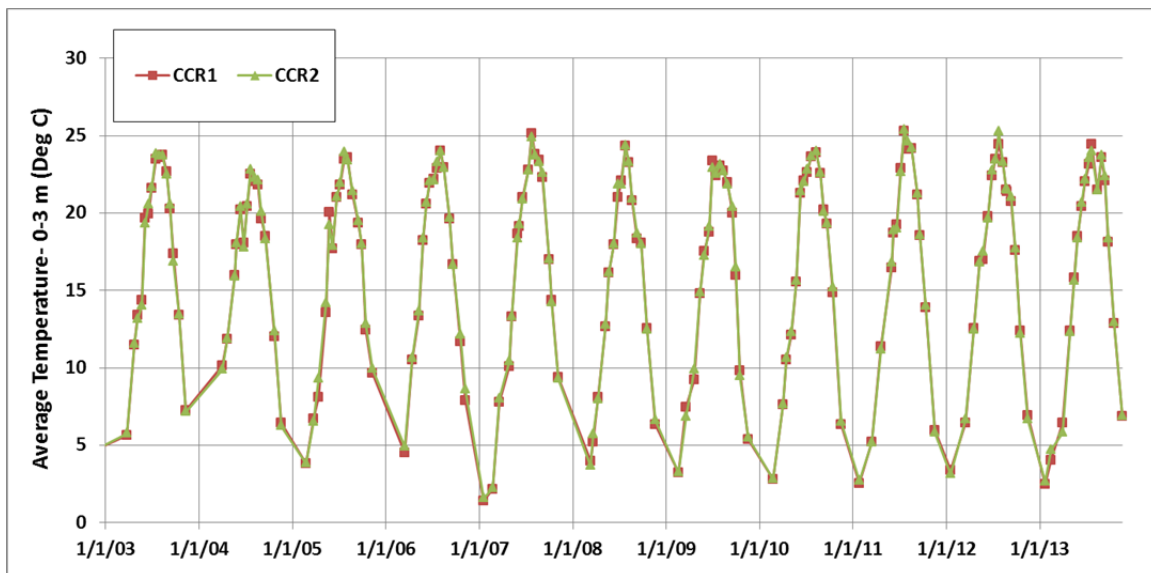


Figure 21. Water Temperature at CCR1 and CCR2, Photic Zone, 2003-2013

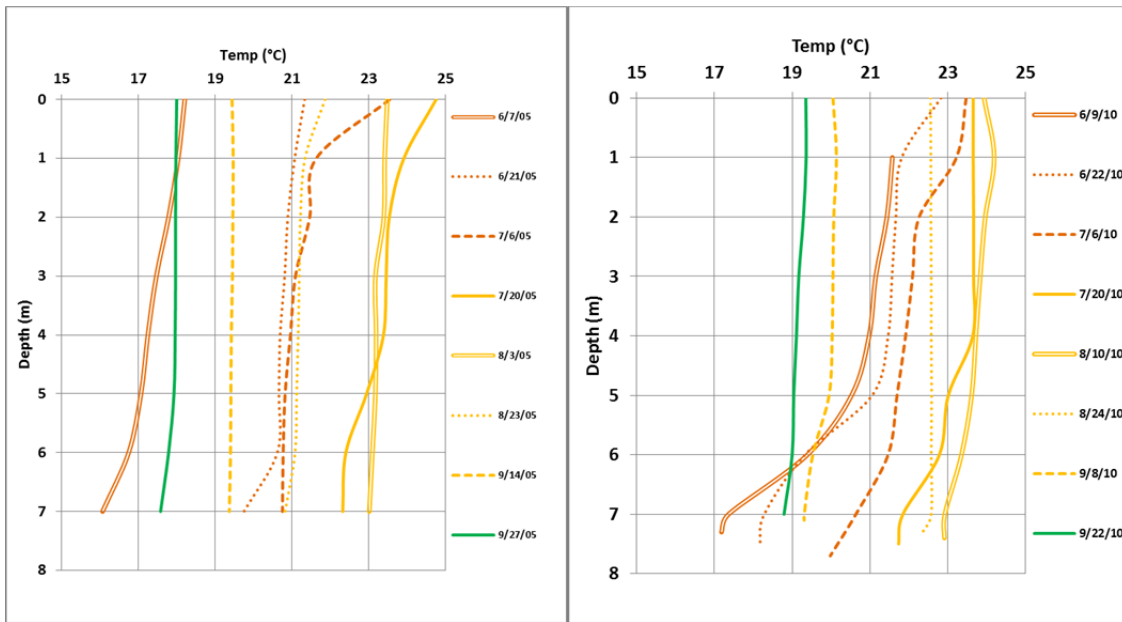


Figure 22. June through September Temperature Profiles at CCR2, 2005 and 2010

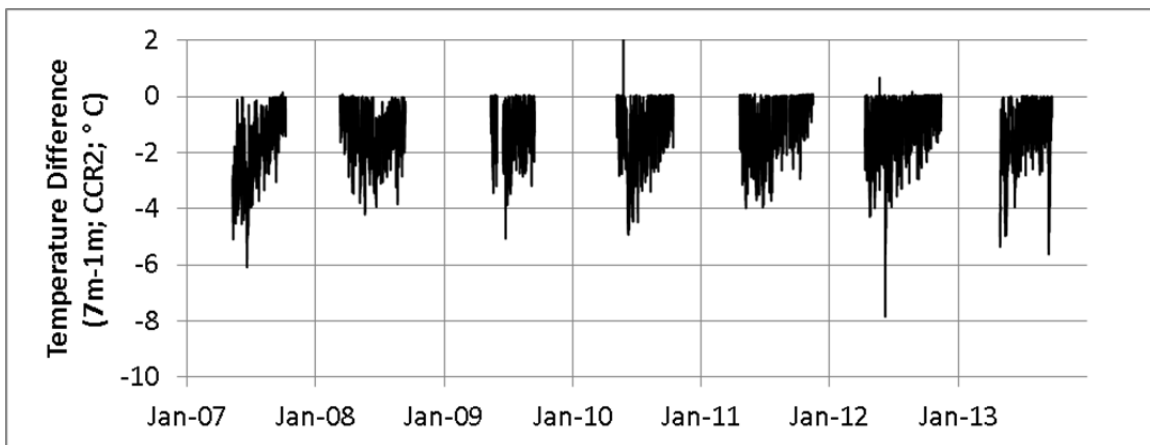


Figure 23. Thermistor-Measured Temperature Difference between 1 m and 7 m at CCR2, 2007-2013

2.5.2 Dissolved Oxygen

While the reservoir exhibits isothermal conditions periodically throughout the summer, there are typically vertical concentration gradients apparent in dissolved oxygen (DO) and nutrient data through the summer months. Dissolved oxygen data from 1 m and the bottom-most observation (usually within 1 m of the bottom³) are plotted from CCR2 and CCR3 in Figure 24.

³ Note that “Bottom” data at CCR2 and CCR3 prior to 2006 are often more than one meter above the bottom, resulting in higher DO values.

These data show anoxia or hypoxia at the bottom the reservoir at CCR2 each summer, and higher concentrations at the top. This gradient is driven by high sediment oxygen demand (SOD) at the bottom and reaeration and photosynthesis at the top. Since initiation of the destratification system, bottom DO concentrations have decreased slightly at CCR2 and increased at CCR3. The decrease at CCR2 likely reflects induced sediment oxygen demand. This is a phenomenon observed in other systems with oxygenation / circulation systems (e.g., Ashley, 1983, Soltero et al., 1994, Moore et al., 1996 and Gantzer et al., 2009), reflecting increased gradients and reductions in the diffusive boundary layer at the sediment water interface. Induced sediment demand occurs when the existing potential for DO consumption exceeds available DO. It is expected, as supported by sediment core data, that the SOD at CCR2 is higher than that at CCR3, possibly explaining the difference in response to the destratification system. Further, sediments at CCR3 are shallower than those at CCR2, and the effect of destratification mixing of oxygen from the surface may be greater at that depth.

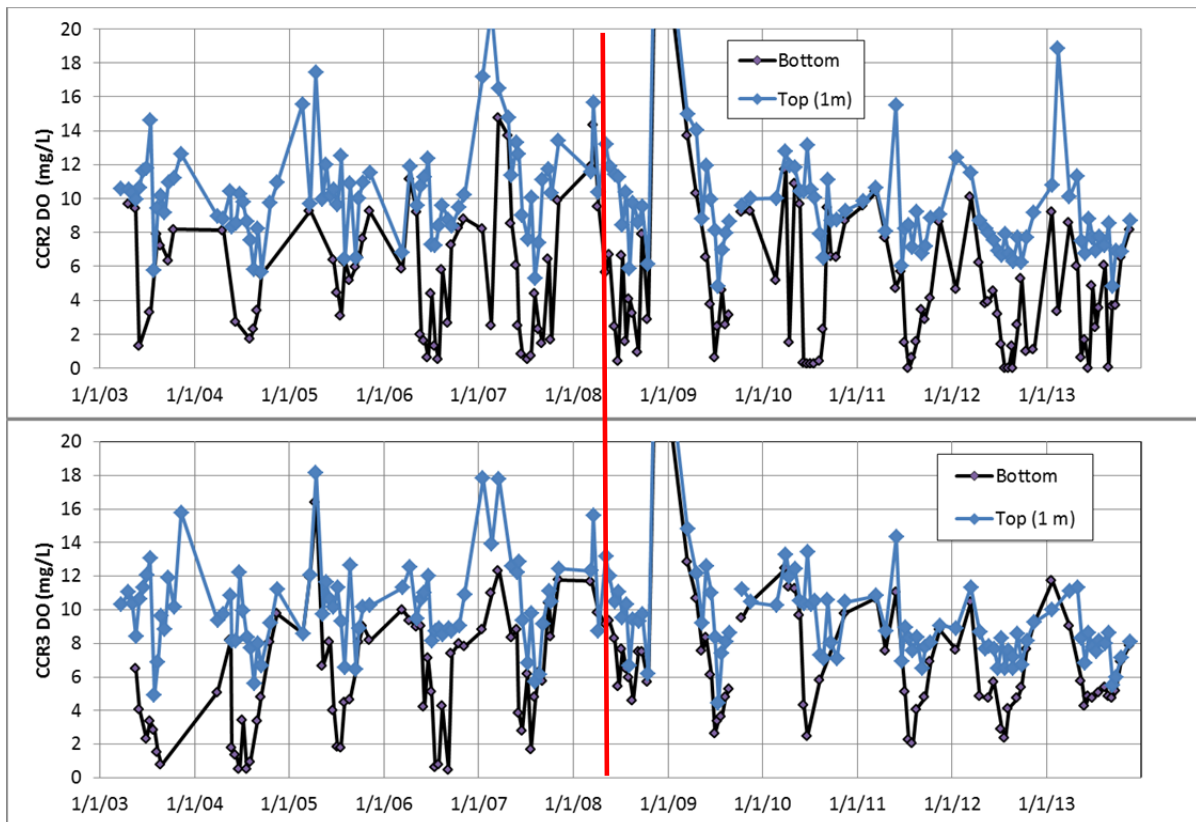


Figure 24. Dissolved Oxygen Concentration at 1 m and Near the Bottom of the Reservoir at CCR2 and CCR3; Red Line Indicates Start of Destratification System Operations

2.5.3 Nutrients

Top and bottom concentrations for nitrate and ammonia are shown in Figure 25. Concentrations of inorganic nitrogen species tend to be relatively low at the top of the reservoir, with an average of 12 ug/L for nitrate and 23 ug/L for ammonia. Recalling that the volume-weighted average inflow concentrations for nitrate and ammonia are 840 ug/L and 83 ug/L, respectively, it is apparent that concentrations at the top of the reservoir show a pattern of algal

uptake. At the bottom of the reservoir, nitrate concentrations tend to also be low (averaging 22 $\mu\text{g/L}$). Ammonia at the bottom, however, exhibits elevated concentrations (averaging 85 $\mu\text{g/L}$), indicative of decay of organic matter and ammonia release from sediments. Ammonia concentrations at the bottom can show multiple peaks in the summer, reflecting periodic mixing or partial vertical mixing.

The in-reservoir concentrations of inorganic nitrogen compared to inflowing concentrations indicate that, inorganic nitrogen enters the reservoir primarily as nitrate but is present within the reservoir primarily as ammonia. This reflects the dynamic nature of the reservoir. Inflowing nitrate is rapidly taken up by algae (and to a lesser extent lost to denitrification), and ammonia is released to the water column by decay of organic matter (both in the water column and in the sediments).

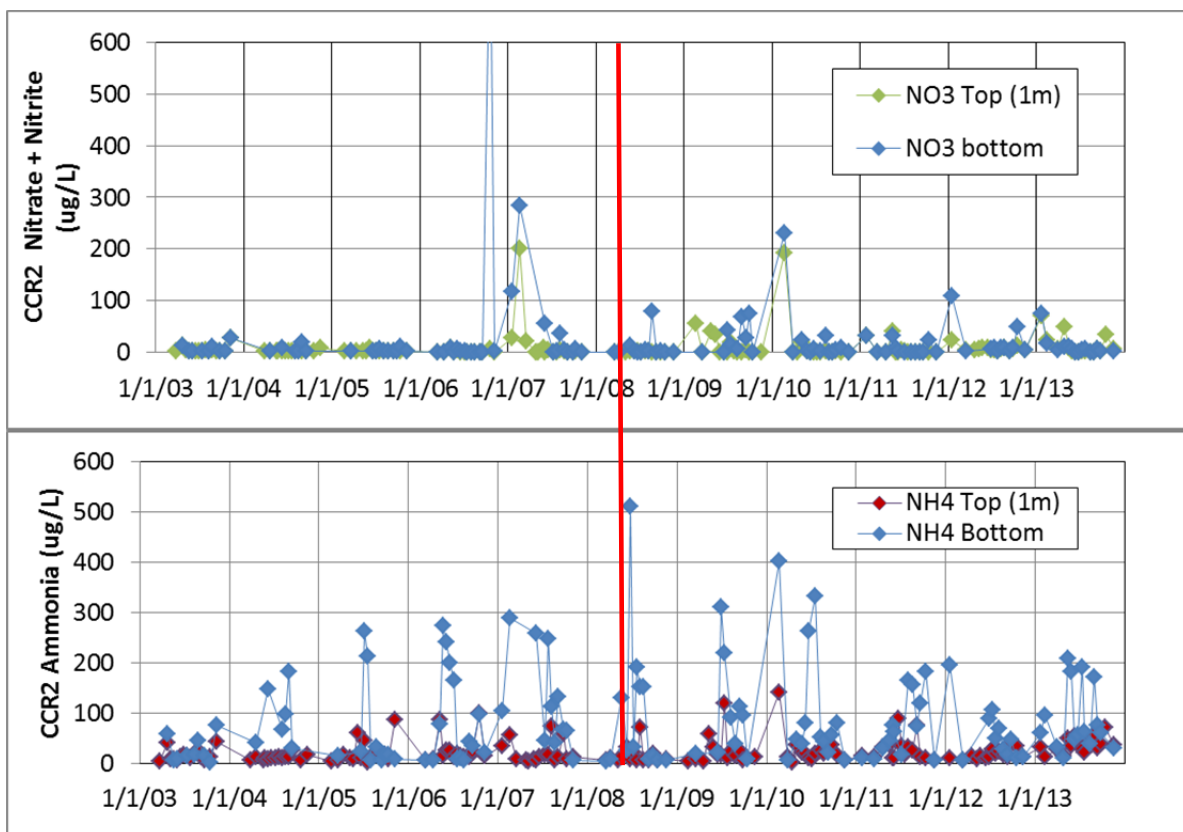


Figure 25. Nitrate and Ammonia Observations from the Top and Bottom of the Reservoir, 2003-2013; Red Line Indicates Start of Destratification System Operations

Observed concentrations of SRP at the top and the bottom of the reservoir indicate a seasonal pattern of low winter concentrations and summer peaks (Figure 26). There is a concentration gradient from the bottom to the top, indicative of nutrient release from sediments at the bottom and uptake from algae closer to the surface. Surface concentrations average 22 $\mu\text{g/L}$ and bottom concentrations average 50 $\mu\text{g/L}$. These in-reservoir concentrations are low relative to the average inflow volume-weighted average SRP concentration of 120 $\mu\text{g/L}$. Unlike, nitrate and ammonia however, concentrations near the surface of the reservoir exhibit a clear pattern of peak values in the summer. This is indicative of two things. First, there is some mixing and

diffusion from the bottom to the top of the reservoir, providing nutrients from sediment release to the surface throughout the summer months. Second there is excess SRP at the surface relative to inorganic nitrogen, indicating nitrogen limitation for algal growth, particularly in the summer months.

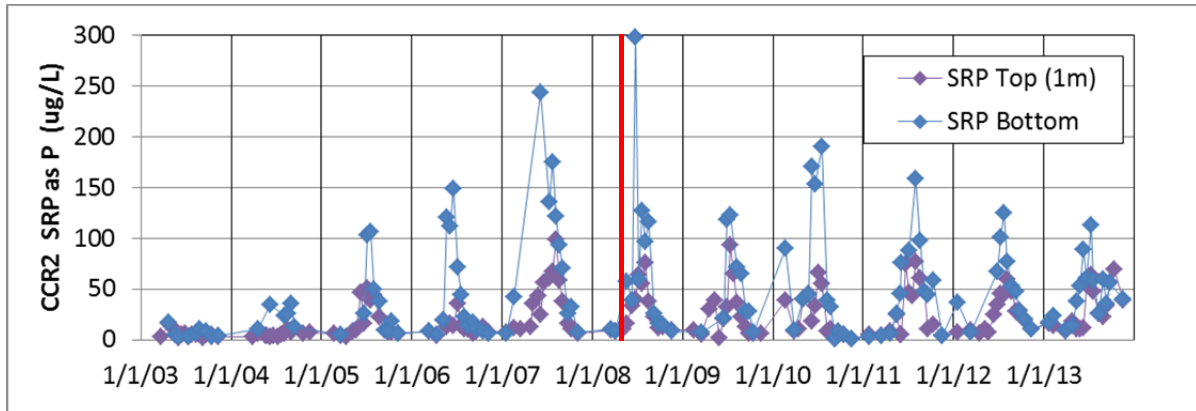


Figure 26. SRP Observations from the Top and Bottom of the Reservoir, 2003-2013; Red Line Indicates Start of Destratification System Operations

2.5.4 Chlorophyll a

The algal response in the reservoir, as indicated by chlorophyll *a*, is shown in samples from the photic zone at CCR2 in Figure 27. Chlorophyll *a* concentrations range from 1 ug/L to 57 ug/L, with an average for the 2003-2013 period of 20 ug/L. The summer chlorophyll *a* concentrations from 2004 through 2009 are somewhat lower than the other years. Interestingly, this corresponds to the period of time with increased inflow ratios of TIN:SRP (see Figure 15 and associated discussion). It is possible that higher inflow TIN:SRP ratios are beneficial, reducing the chlorophyll *a* response in the reservoir. The timing of inflows and mixing events as well as water temperature also appear to affect this response. There is also a pattern of lower summer chlorophyll *a* following greater spring/early-summer inflows (e.g., 2007, 2009, and 2015).

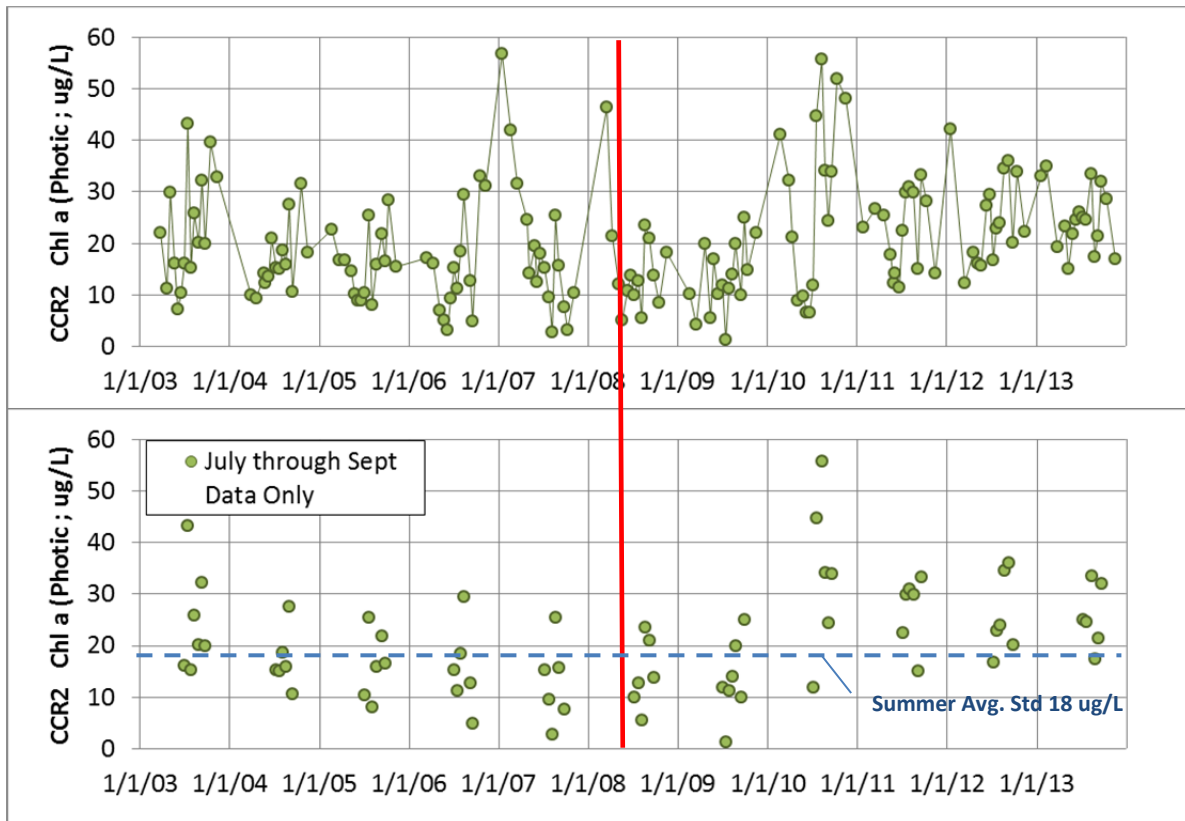


Figure 27. Observed Chlorophyll *a* Concentrations from CCR2 (2003-2013) and Comparison to Standard; Red Line Indicates Start of Destratification System Operations

In consideration of summer chlorophyll *a*, it is also important to understand that chlorophyll *a* concentrations do not necessarily indicate the amount of algae (biovolume or biomass) present in Cherry Creek Reservoir. For example, 2015 had the highest summer algal density and biovolume, but the second lowest summer chlorophyll *a* of the recent seven years (Figure 28). This indicates that different algal species in the reservoir have varying amounts of chlorophyll *a* for a given biovolume. Chlorophyll *a* content can also vary temporally for a particular species in response to varying light conditions and/or nutrient concentrations (Chapra, 1997).



Figure 28. Average Summer Chlorophyll *a*, Biovolume, and Algal Density, 2009-2015

2.5.5 Cyanobacteria

2.5.5.1 Effects of the Destratification System on Cyanobacteria

Previous monitoring reports have noted a significant (orders of magnitude) reduction in cyanobacteria population since 2009, attributing this to operation of the destratification system (e.g., GEI, 2014). Our analysis does not support that interpretation of the data.

The 2013 Monitoring Report (GEI, 2014) states:

“Prior to the operation of the destratification system, cyanobacteria represented between 40 and 80% of assemblage in terms of density (#/mL). During the first season of operation in 2008, green algae and cyanobacteria were still the dominant types of algae, with cyanobacteria dominating the summer assemblage. However, since 2009, the cyanobacteria population has been greatly reduced, representing between 1 and 7% of the algal

assemblage in terms of density (Figure 24). This shift in algal composition is notable as it provides some initial results that validate the effectiveness of the destratification system at achieving one of the primary objectives—reducing suitable habitat conditions for cyanobacteria.”*

* Figure 29 in this report.

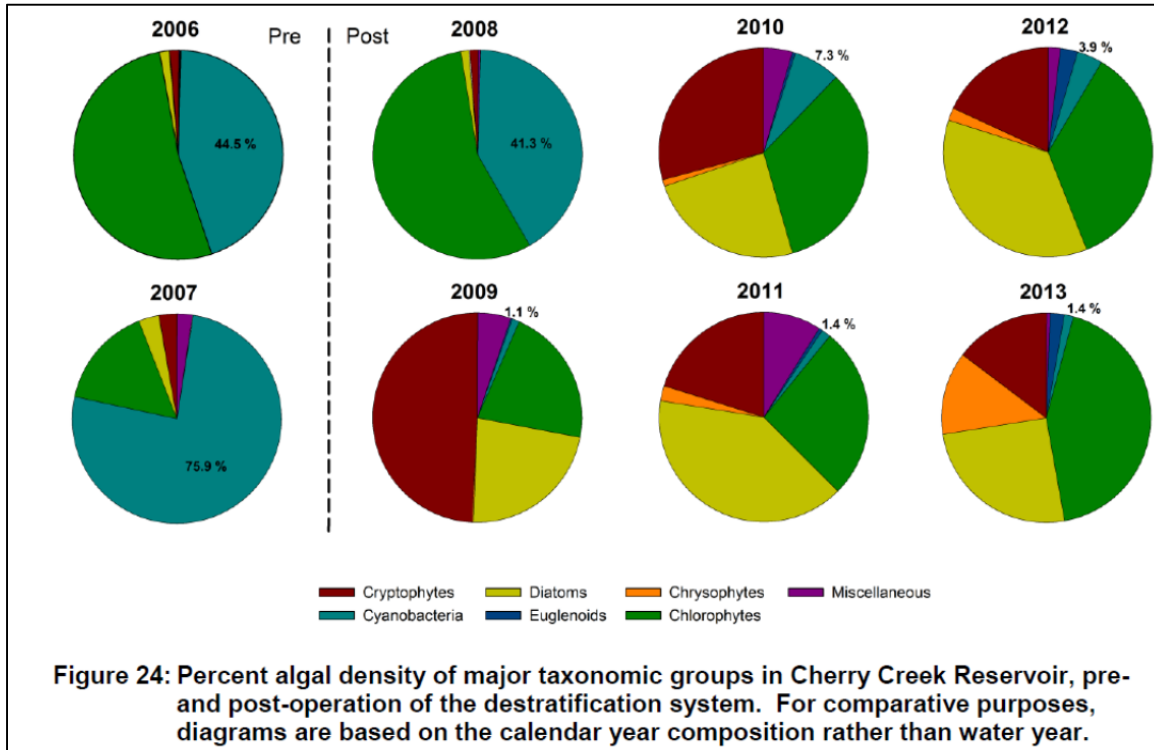


Figure 29. Figure 24 from the 2013 Monitoring Report (GEI, 2014); Data in these Pie Charts Reflect Relative % Density of Algal Species on a Calendar-Year Basis, Using Composite Samples of the Photic Zone (0-3 m)

The data presented in Figure 29 come from two different labs; and, the timing of the apparent dramatic change in cyanobacteria density corresponds exactly to the timing of the change from one lab to the other. From 2006 through 2008, the University of Colorado (CU) provided algal density by species in #/mL. Algal density data for the period 2009-2013 were provided by Aquatic Analysts. Although it seems that a dramatic improvement occurred starting in 2009 with a sharp drop in algal density, it is apparent that the dramatic shift in data occurred at the time of the change in labs (Figure 30). It is understood that there can be significant differences in results between phycologists, even when accepted methodologies are used (St. Amand, 2014). Aquatic Analysts uses a different counting methodology than the CU lab – one where smaller species (picoplankton) may not be counted and included in the density results (personal communication, C. Wolf [5/16/14]; M. May [6/27/14]). Because of this, conclusions cannot be drawn by comparing density data from the two labs.

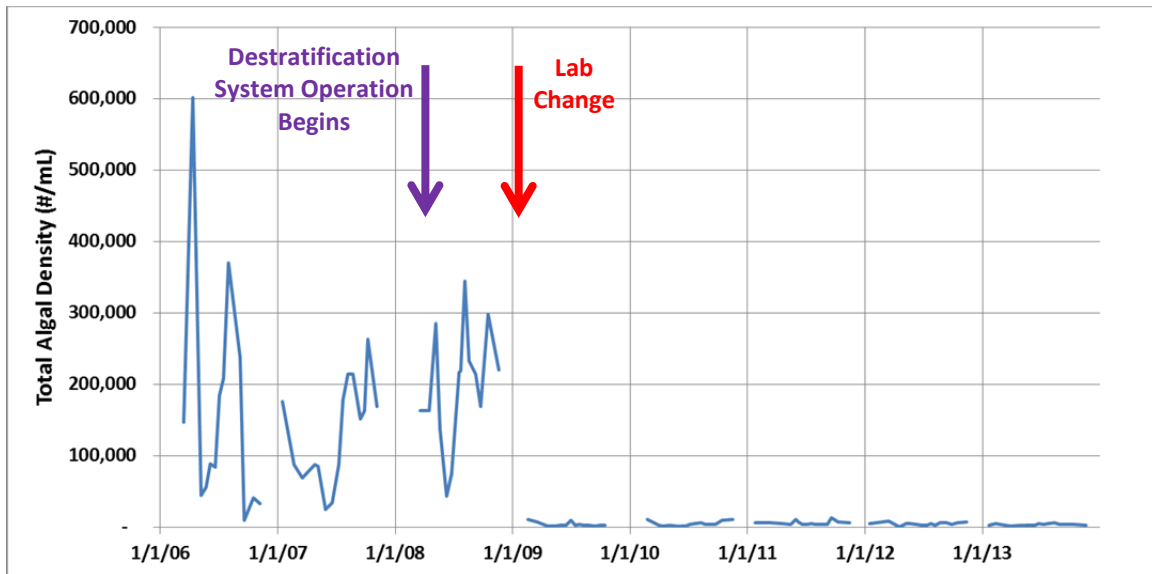


Figure 30. Algal Density Reported for 2006-2013. CU Data (2006-2008); Aquatic Analysts Data (2009-2013)

There is also some direct evidence that a dramatic shift in cyanobacteria may not have occurred starting in 2009. While the CU lab was not used for routine algal analysis after 2008, one algal sample was analyzed by the CU lab in July 2010 as part of a separate Water Quality Control Division (WQCD) study (May, 2014). The cyanobacteria density in that 2010 sample was in the same range as that observed in the pre-destratification system period by the same lab (Figure 31).

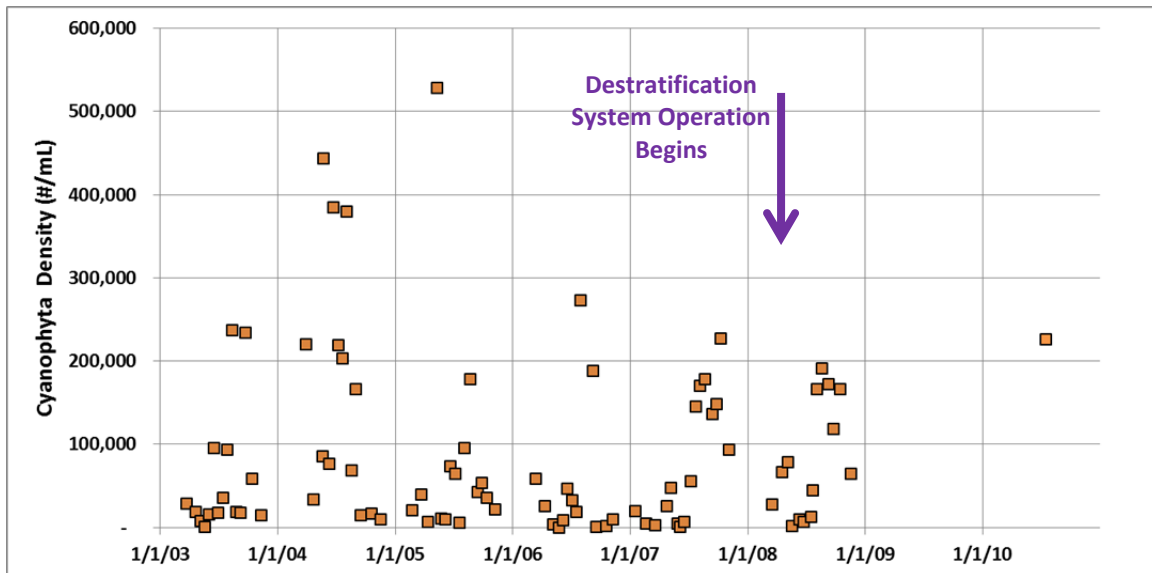


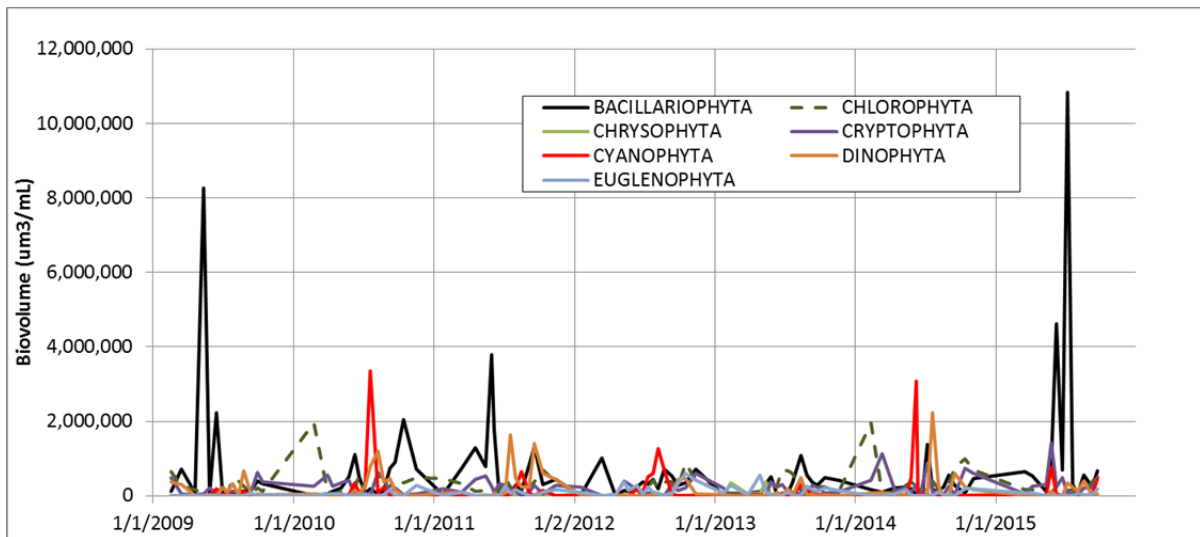
Figure 31. Cyanophyta Density (2003-2010). All CU Data. Data in July 2010 from a Separate WQCD Study (May, 2014)

The single result in 2010 alone, however, is not adequate evidence to confidently draw the opposite conclusion that there has been no change in cyanobacteria abundance associate with the destratification system operation. In short, based on data alone, there remains uncertainty

about whether the destratification system has affected cyanobacteria in the reservoir; but it should be noted that there is no definitive evidence in the observed dataset that it has.

2.5.5.2 *Patterns in Cyanobacteria Occurrence*

Focusing on algal data from 2009 through 2015, for which there are density and biovolume data from the same lab⁴, a general understanding of cyanobacteria bloom occurrence patterns and drivers can be gleaned. Cyanobacteria appear to some extent in all years in the data from Cherry Creek Reservoir. Density and biovolume data from 2009-2015 are presented in Figure 32. Overall, cyanobacteria (cyanophyta) dominate the algal species, in terms of density and/or biovolume, only for short periods of time in spring or summer of some years (Figure 32). Still, such blooms have the potential to produce toxins and other nuisance concerns.



⁴ In addition to apparent differences in counting techniques between the two labs, the CU lab (2003-2008) did not generate biovolume data.

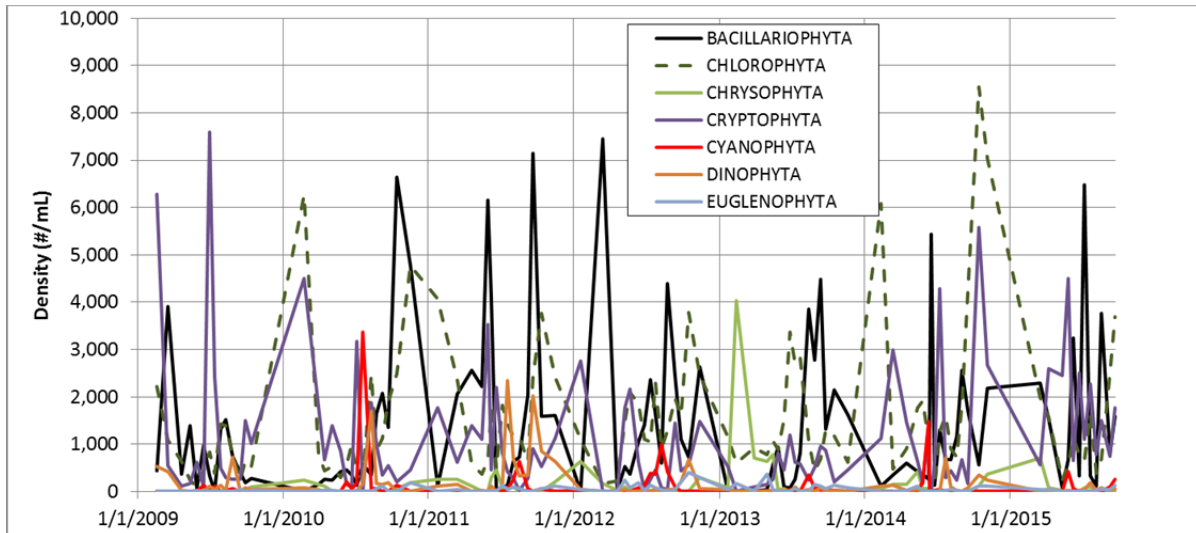


Figure 32. Biovolume and Density of Major Taxonomic Groups of Algae in Cherry Creek Reservoir, 2009-2015

Cyanobacteria blooms in May/June or September tend to be primarily *Anabaena flos-aquae*, while July and August blooms tend to be *Aphanizomenon flos-aquae*. Both of these types of cyanobacteria are capable of nitrogen fixation. This seasonal pattern is expected to reflect temperature preferences of these species in the reservoir.

The data indicate that no single water-quality condition triggers cyanobacteria blooms in the reservoir, but instead a combination of factors is needed. Further, data suggest that common conditions need to persist for roughly two weeks prior to a bloom. Those conditions identified in this analysis are:

- **Calm Conditions** – There tends to be minimal inflow and often thermally-stratified conditions in the period leading up to a bloom. Inflows preceding the major blooms tend to be less than ~50 acre-ft per day (AF/d) for at least two weeks before major blooms.
- **Seasonally-Warm Water Temperatures** – Major *Aphanizomenon* blooms appear to occur in calm surface water between ~23 and ~26 °C in the reservoir. Major *Anabaena* blooms seem to occur in calm conditions between ~18 and ~21 °C, though the range for *Anabaena* is more uncertain given limited occurrences in the observed dataset. Warm temperatures at the surface are tied to meteorological conditions, but can also develop more rapidly under calm, thermally-stratified conditions.
- **Nitrogen Limitation in the Photic Zone** – Another consistent condition that precedes major cyanobacteria blooms in the reservoir is nitrogen limitation in the photic zone. This makes sense given the ability of some cyanobacteria to fix atmospheric nitrogen, giving them an advantage under such conditions.
 - Dissolved phosphorus levels tend to be elevated (>~40 ug/L) in the photic zone and total inorganic nitrogen (TIN; ammonia plus nitrate) tends to be lower than dissolved phosphorus (Figure 33).

- This is more apparent in the TIN-to-dissolved phosphorus ratio in the photic zone (Figure 34). Before each major bloom, this ratio drops to <1 (often less than 0.5). This was also seen for the smaller bloom in 2013.

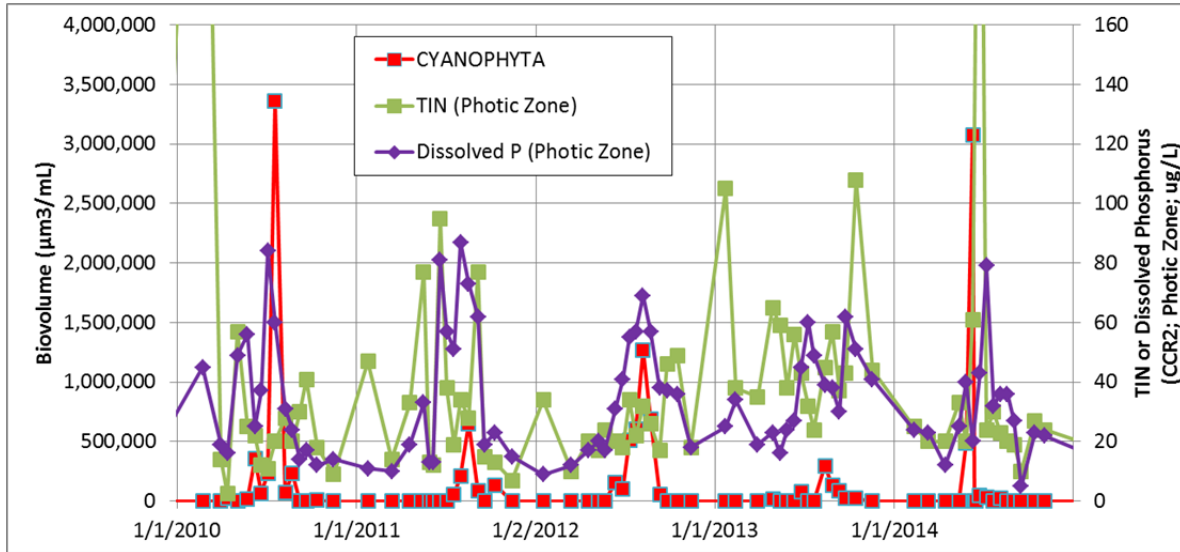


Figure 33. TIN and Dissolved Phosphorus Concentrations in the Photic Zone with Cyanobacteria Biovolume, 2010-2014

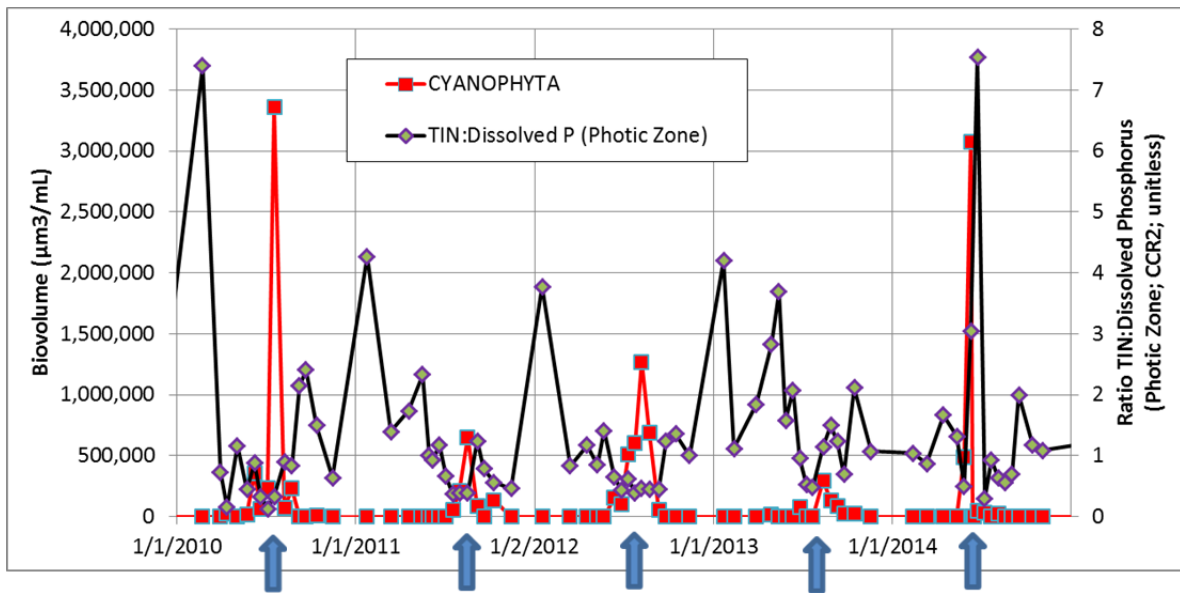


Figure 34. TIN:Dissolved Phosphorus Ratio and Cyanobacteria Biovolume, 2010-2014
(Blue arrows indicate low TIN:Dissolved P Ratios in the Photic zone before and during cyanobacteria blooms.)

Conditions precipitating a crash in the major cyanobacteria blooms correspond to loss of the trigger conditions listed above. Such a crash can occur due to increased inflow, loss of stratification (and associated cooling at the surface), increased TIN, and an increase in the TIN:dissolved phosphorus ratio. All of these changes result in loss of advantages for the cyanobacteria over other algal groups.

2.5.6 Zooplankton

In the recent record⁵, zooplankton data have been collected since 2011. These are composites of tows from CCR1, CCR2, and CCR3. For eight of the 11 years of the model simulation period (2003-2013), no zooplankton data are available. Zooplankton data from 2011-2015 are presented in Figure 35.

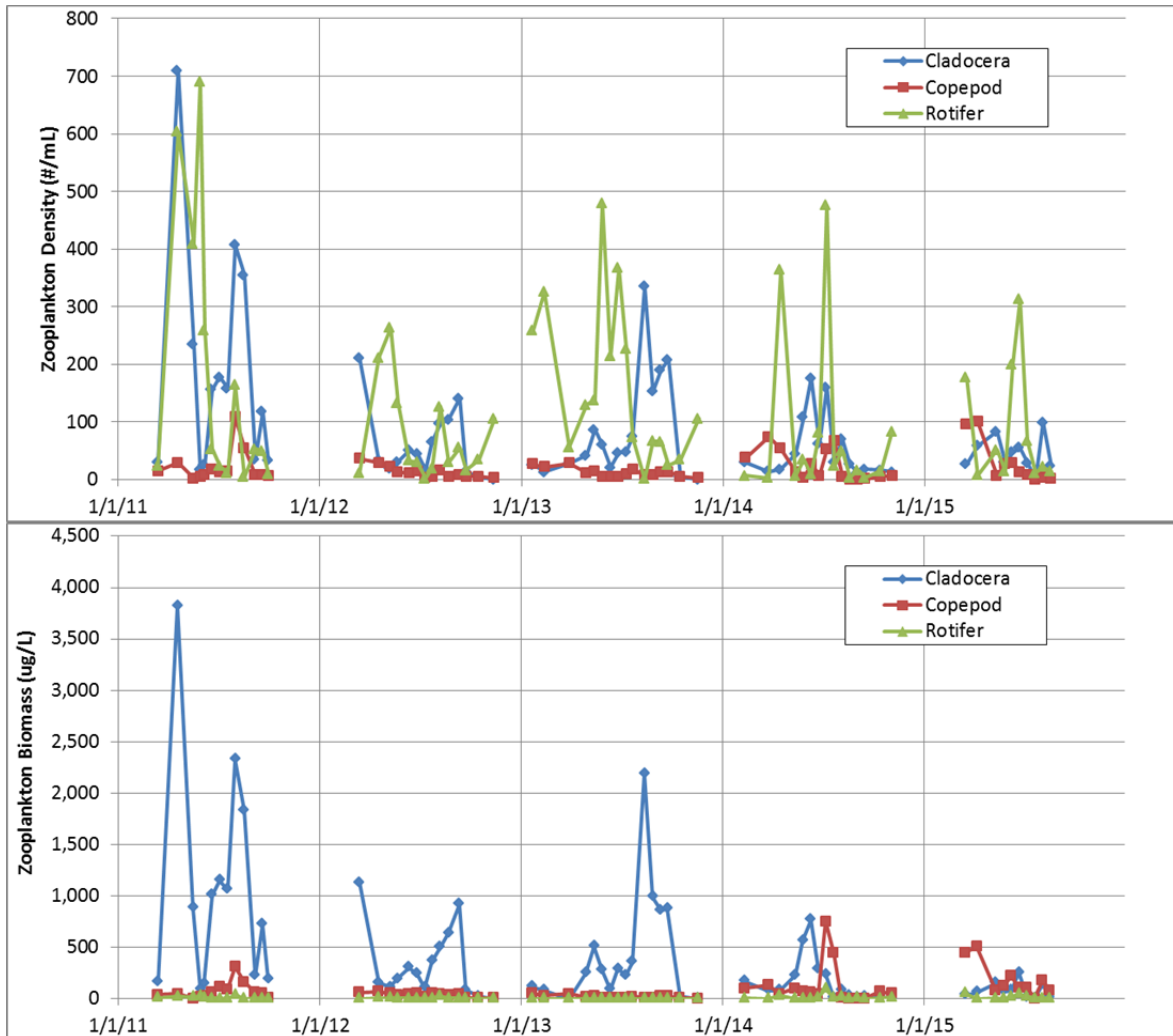


Figure 35. Cherry Creek Reservoir Zooplankton Density and Biomass, 2011-2015

Lewis et al. (2004) concluded that zooplankton played an insignificant role in managing algae in Cherry Creek Reservoir. Lewis et al. (2004) indicated that the dominant zooplankton for their study in Cherry Creek was a cyclopoid, *Diacyclops thomasi*, which is more likely to feed on protozoan than phytoplankton, citing Dobberfuhl et al. (1997).

⁵ Zooplankton data were also collected from 1996 through 2001, available only in terms of counts per liter.

Time-varying density and biomass of zooplankton and algae (biovolume) were compared to look for indications of more recent zooplankton influence on algae. A predator-prey relationship seems to exist at times in some years (Figure 36). Generally, zooplankton and algal densities follow similar relative patterns of increases and decreases, with some exceptions. Typically, a predator-prey concentration pattern shows predator peaks occurring after (lagging) prey concentration peaks. That lag is not consistently apparent in the observed dataset, but it may be absent due to issues of sampling frequency relative to the rate at which populations change.

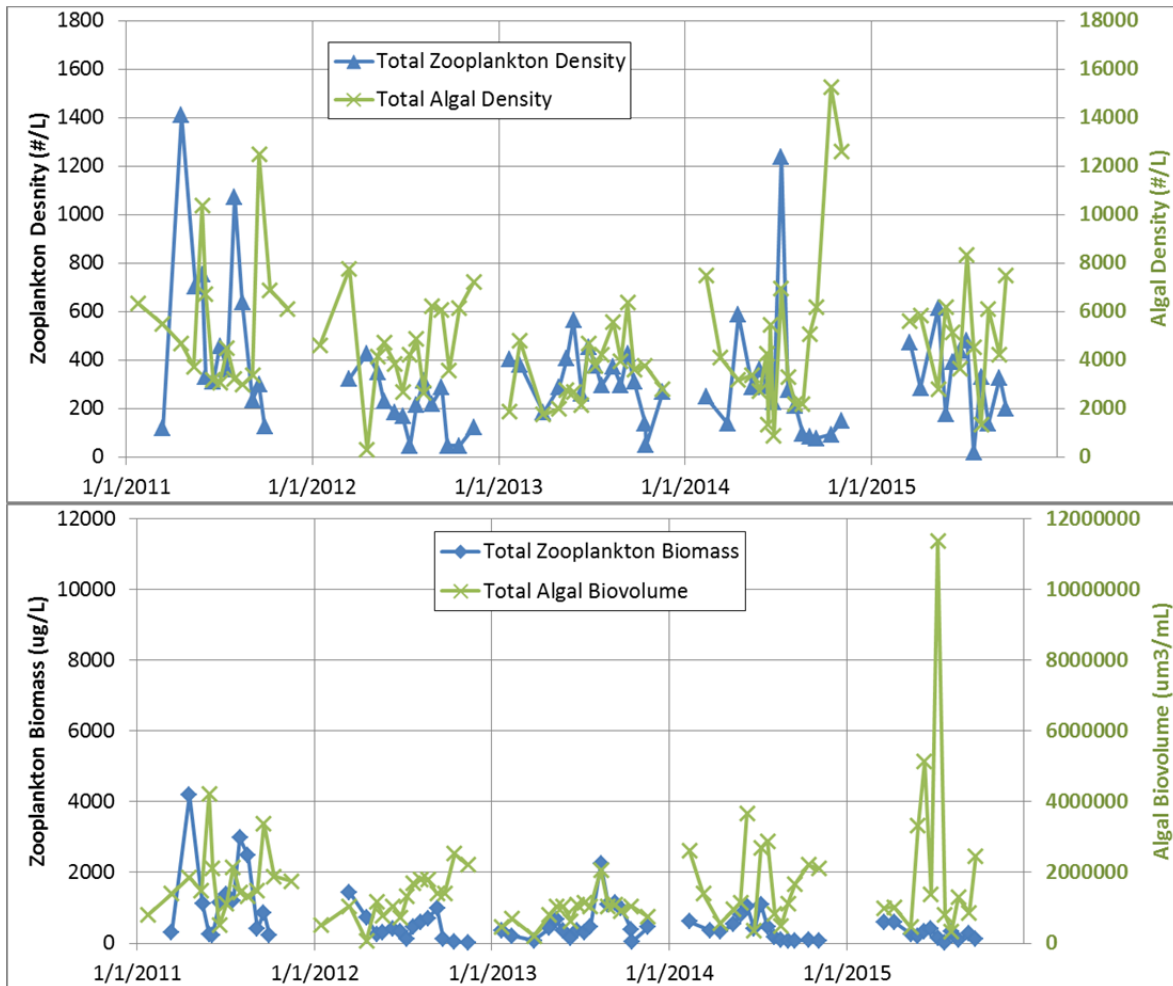


Figure 36. Comparison of Total Zooplankton and Total Algae, Densities, Biomass, and Biovolume

Johnson (2014; Attachment A) reviewed zooplankton, water-quality, and fish data from Cherry Creek Reservoir and found the following regarding zooplankton:

- Zooplankton species assemblages in Cherry Creek Reservoir are comparable to other Colorado reservoirs. The *Daphnia* assemblage is more diverse, but not unexpected.
- Excluding 2011, *Daphnia* density during April through May was about 3.5 daphnids/L, which seems low compared to *Daphnia* observed in less productive Colorado reservoirs, such as Granby and Blue Mesa. *Daphnia* populations in Cherry Creek Reservoir may be limited by predators (e.g., shad).

- The invasive tropical cladoceran *Daphnia lumholtzi* was found in Cherry Creek Reservoir in 2011 and 2012 (but not in 2013). However, their high thermal optimum (>26°C) and rarity during periods when age-0 fish are small suggests that their impact to the food web in Cherry Creek Reservoir will be very limited.
- Drawing definitive conclusions linking zooplankton data to algae concentrations or fish populations and the effect of the destratification system is limited by lack of zooplankton data from 2003-2010 and lack of fish abundance estimates (discussed further in Section 2.6).

2.5.7 Clarity

Due to high algal concentrations, as well as high overall TSS (averaging 15 mg/L in the photic zone, per data available from 2011-2013), the reservoir exhibits low clarity (Figure 37). This can affect algal growth patterns, indicating low light transmission to deeper parts of the reservoir. The average clarity as measured by Secchi depth is 0.9 m. Clarity ranged from 0.4 m to 2.9 m; both measured in 2009.

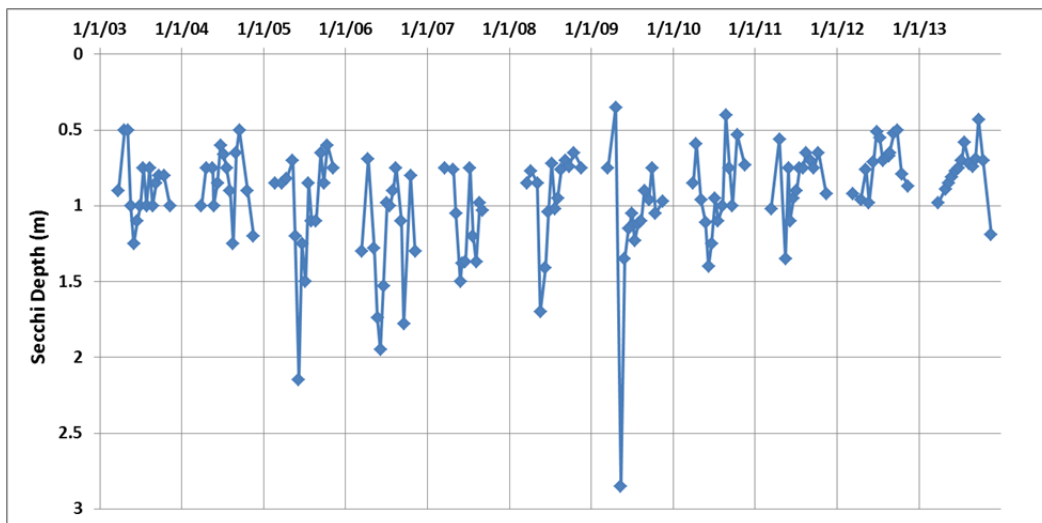


Figure 37. Secchi Depth at CCR2

2.5.8 pH and Conductivity

There is an overall trend of decreasing pH and increasing conductivity in the reservoir. pH has been decreasing and specific conductivity has been increasing roughly since 2009 (Figure 38). Seasonality previously observed in conductivity in the reservoir is no longer apparent, though large precipitation events (e.g., September 2013 and spring/summer 2015) have clear dilution effects on conductivity.

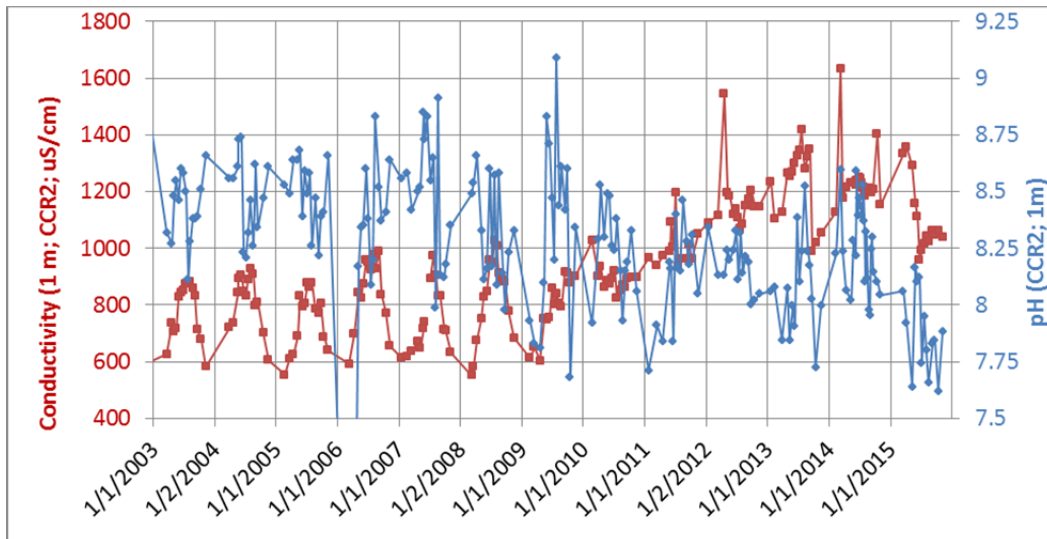


Figure 38. In-Reservoir pH and Conductivity at 1 m at CCR2, 2003-2015

The in-reservoir pattern for pH and conductivity appears to be driven by inflow water quality since the same patterns are apparent in the inflows (Figure 39). This suggests either a change in sources or a change in distribution of sources. While temporal trend patterns match, the conductivity in both of these tributaries is higher than in-reservoir values, and the pH is lower. Direct adverse impacts of these changes on the reservoir are not apparent at this time; however, the source of these changes should be identified in the watershed. Such an understanding may identify associated contaminants of concern and potentially offer a solution to reverse the trends, as needed.

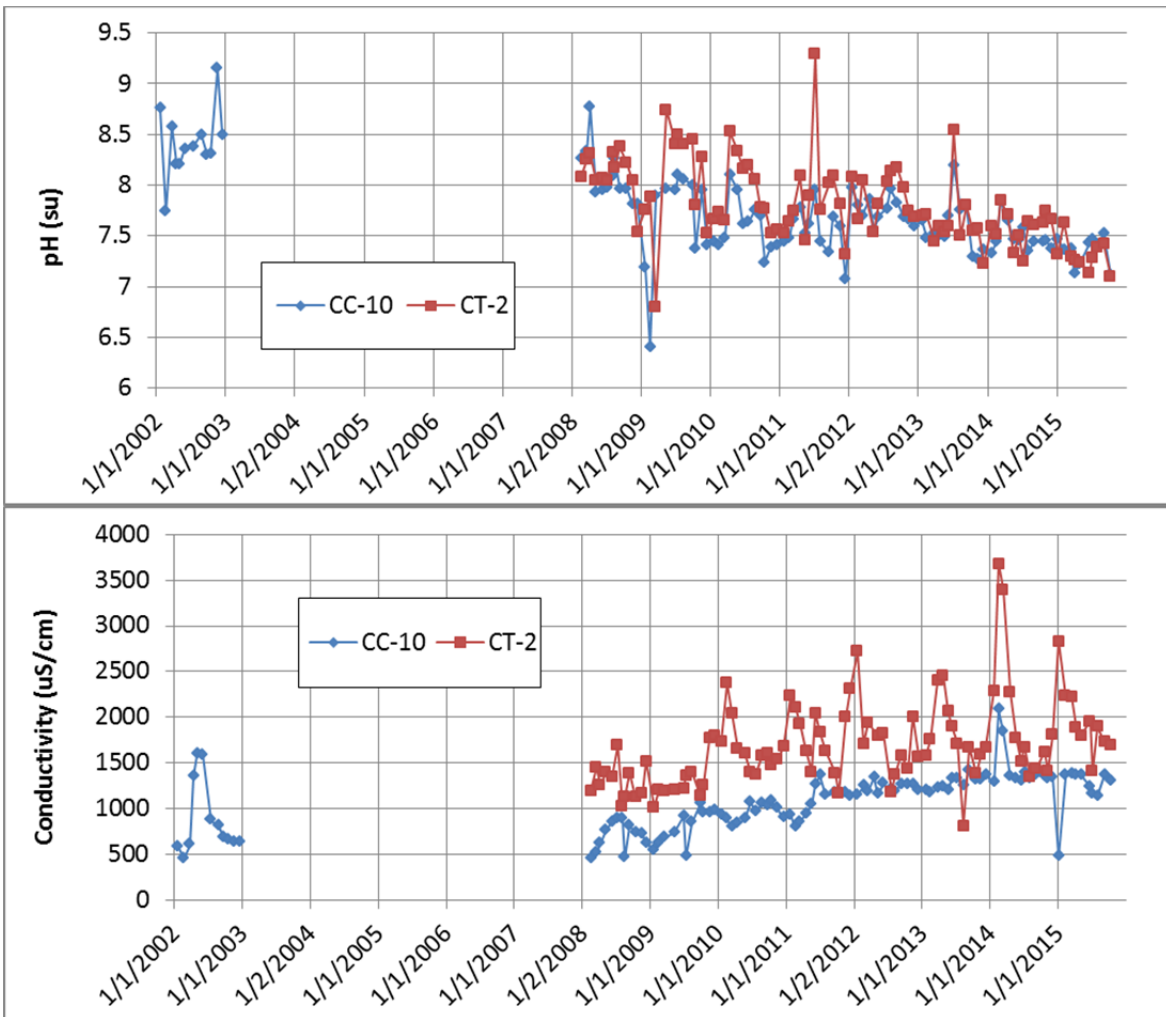


Figure 39. Inflow pH and Conductivity, 2002-2015

2.6 Fish

Cherry Creek Reservoir is a high-quality walleye fishery and the Authority is interested in information that is useful for managing, maintaining and protecting this important feature of the reservoir. The reservoir is also one of the top producers of walleye eggs in the State (CCBWQA, 2013). In 2012, there was a fish kill in the reservoir between August 14 and August 23. The cause of the fish kill is expected to be a combination of high water temperatures and low dissolved oxygen creating poor conditions, also known as a “temperature-oxygen squeeze”. Of the 548 dead fish collected by Colorado Parks and Wildlife, 97% were gizzard shad and 3% were walleye. There were no other such fish kills observed in the reservoir in the period between 2003 and 2013 (Wolf, personal communication, 2015).

Understanding fluctuations in fish populations is important from a recreational fishery perspective and also as it relates to interpretation of zooplankton, phytoplankton, and general water-quality response. A particular question of interest is “Does the destratification system impact the food web, and if so, how?”. To assess the health of the fishery in Cherry Creek Reservoir over time, Dr. Brett Johnson compiled and reviewed available food web data (Johnson, 2014; Attachment A). These data include zooplankton, phytoplankton and fish survey information as well as water temperature, and dissolved oxygen. Site-specific data, as well as information from the scientific literature were considered. The following are highlights of findings of that study:

Walleye

- Over the period examined, the walleye population appears to have been quite strong.
 - Growth was good;
 - Body condition was very good;
 - Medium and large size fish were always present; and
 - Recruitment was consistent.
- As of 2013, there was no evidence that the installation of the destratification system has negatively impacted growth, condition, or size structure of the walleye population.
- It appears that fishery management practices have been effective in sustaining walleye populations.
- Cherry Creek Reservoir is warmer than is optimal for walleye in most summers. Because the reservoir is often nearly isothermal (regardless of operation of the destratification system), there is no thermal refuge in the main body of the reservoir when surface temperatures exceed preferred temperature (22-24°C).
- Sufficient dissolved oxygen for walleye is typically available in the upper half of the water column, based on review of the periodic sampling results.
- It was not possible to evaluate the relative importance of stocking and wild recruitment in the reservoir walleye because stocking has occurred in almost every year of record. While the status-quo management of the walleye population seems effective, if the

population is self-sustaining, then walleye fry not stocked into Cherry Creek Reservoir could be used to supply other waters. Alternative year stocking and strontium isotope analysis of otoliths could determine if stocked fish contribute to walleye year class strength.

Gizzard Shad

- Gizzard shad have the potential to be a keystone species in Cherry Creek Reservoir. They are likely an important food source for walleye, but they also have the ability to limit walleye recruitment, and worsen water quality by depleting zooplankton grazers and recycling sediment nutrients.
- To better understand the effects of gizzard shad on the system, regular monitoring of their abundance and size structure is needed. Fish aging work in addition to standardized electrofishing surveys of shad size and abundance in fall and spring are recommended to evaluate overwinter survival.

3 Model Development

The mechanistic⁶, hydrodynamic and water-quality modeling software CE-QUAL-W2 v3.71 (Cole and Wells, 2011) was selected for development of the hydrodynamic and water-quality model of the reservoir. This modeling software was selected in consideration of the modeling objectives, available data, ability to simulate water-quality dynamics expected to be important in Cherry Creek. Further, it is a tool in the public domain that is currently maintained, widely-accepted and applied, can be operated in a Windows environment, and is coded in FORTRAN with the flexibility of an open source code. CE-QUAL-W2 (W2) is a two-dimensional model. As such, it assumes lateral homogeneity, but simulates variation longitudinally and vertically to the resolution specified. Based on similarity in water quality at two sampling stations parallel to the Cherry Creek Dam, CCR1 and CCR2 (see map Figure 4), a laterally-averaged representation seems supported for Cherry Creek Reservoir (e.g., temperature [Figure 21] and chlorophyll a [Figure 40]). The U.S. Army Corps of Engineers originally developed the model software, and it is

⁶ A mechanistic model consists of mathematical equations describing the physical, chemical, and biological relationships in a reservoir. Mechanistic models are based on fundamental laws and hypotheses about controlling processes, and as such, can be used to help understand why one variable impacts another. In addition, it allows for the capability to make predictions under a different set of circumstances (e.g., an alternative management scenario, climate change, etc.). This is much more difficult when empirical models are used – which are based on relationships developed using historical data (e.g., regression equations). Empirical relationships are derived using statistical analyses, often without consideration of the controlling mechanisms, and are thus limited by the data used to derive the relationships (McCutcheon, 1990).

currently supported and updated by Portland State University. Detailed documentation of the software and associated technical manuals are available at <http://www.ce.pdx.edu/w2/>.

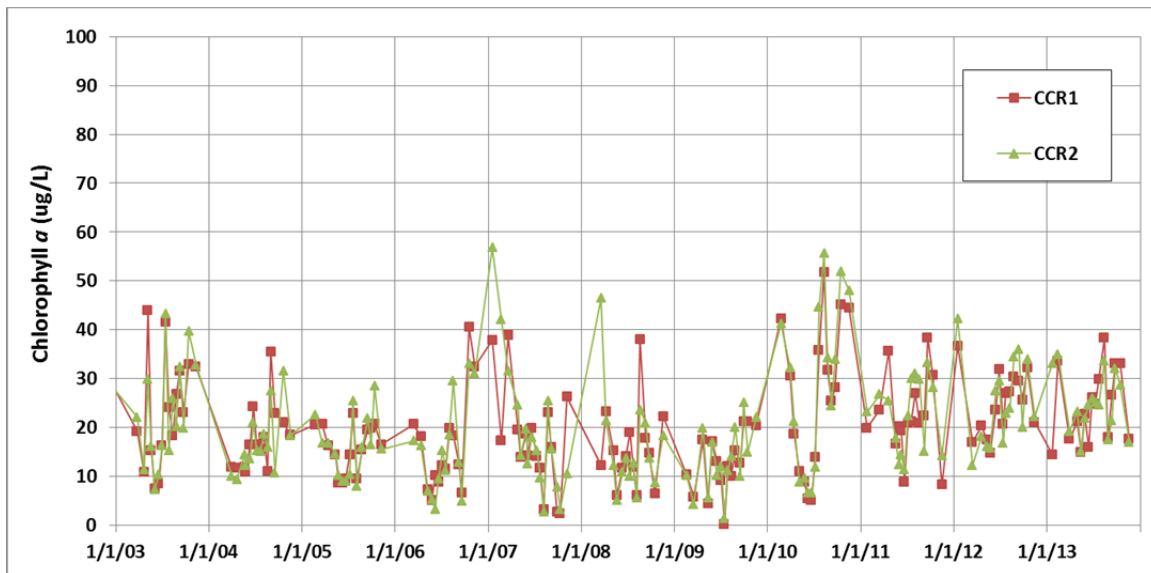


Figure 40. Chlorophyll a at CCR1 and CCR2, Photic Zone, 2003-2013

3.1 Bathymetry

Developing the bathymetric representation of the reservoir in W2 requires designation of segments and layers. Segments were oriented perpendicular to the direction of flow of the original thalweg of Cherry Creek. This resulted in segments laid out parallel to the dam. Spacing of segments considered capturing the variations in the bathymetric structure and the destratification system, as well as the location of in-reservoir sampling data. Ultimately, an even segment spacing of 200 m was set, for a total of 12 active segments, as shown in Figure 41.

Model layer spacing was defined considering observed vertical variability in water-quality response and the need to simulate aerator placement. Based on profile data such as that shown in Figure 42, a vertical discretization of 0.5 m was selected. This resulted in 19 active layers in the model (Figure 43).

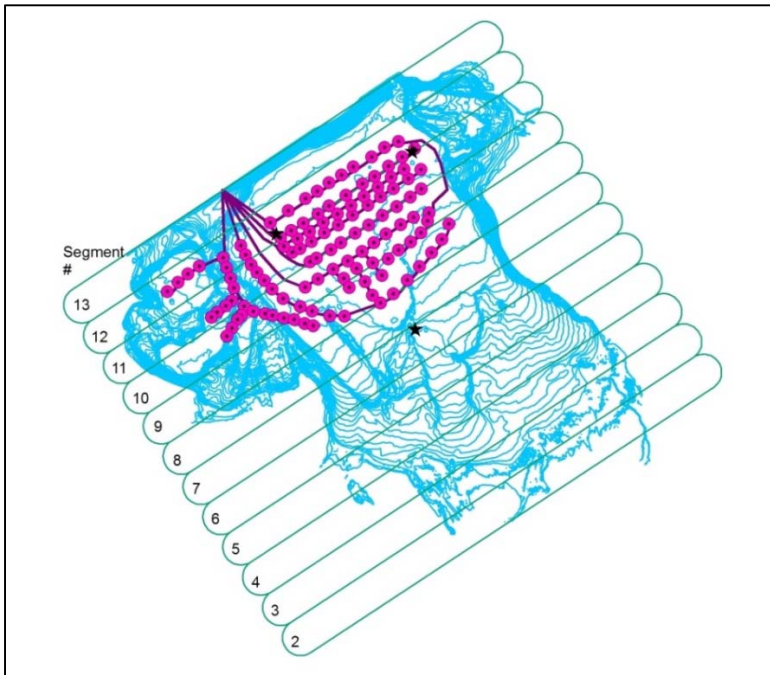


Figure 41. Model Segment Layout Shown with Bathymetric Contours, Destratification System (Pink Circles), and Sampling Locations (Three Black Stars)

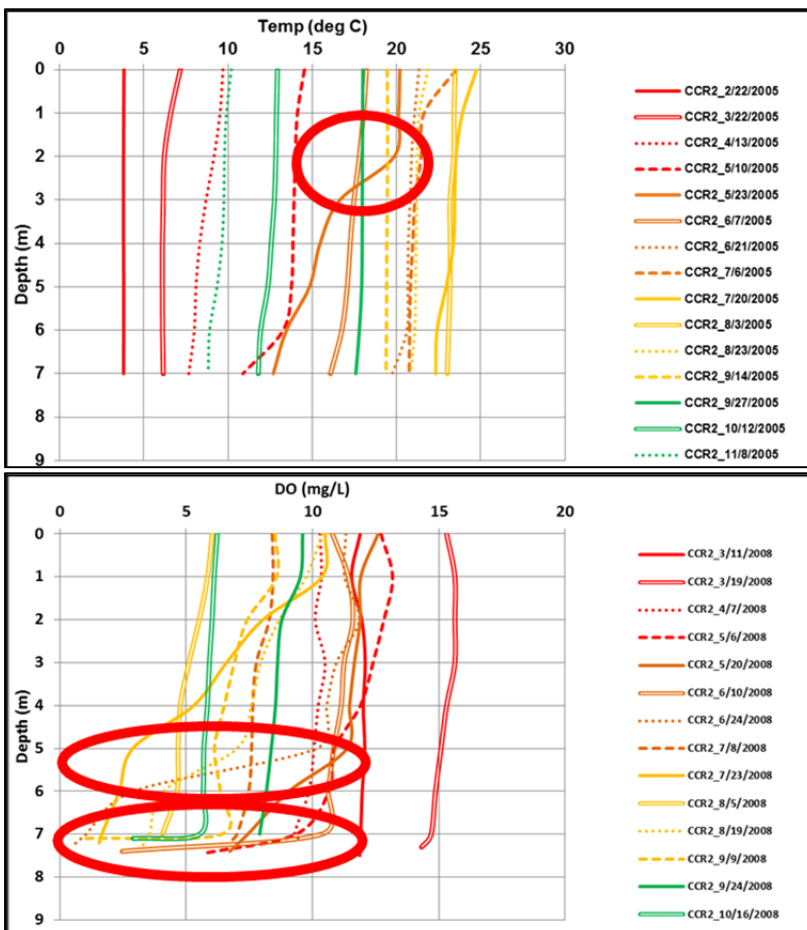


Figure 42. Example of Profile Data Considerations in Selecting Vertical Discretization of Model Layers

A view of the model profile without vertical exaggeration is presented in Figure 44 to support visualization of the reservoir, and a plan view of the model is shown in Figure 45. Cross-sections developed from the 1-ft bathymetric contours were used to develop the grid and widths for each cell⁷. An example section-view of a segment (segment 12) is shown in Figure 45.

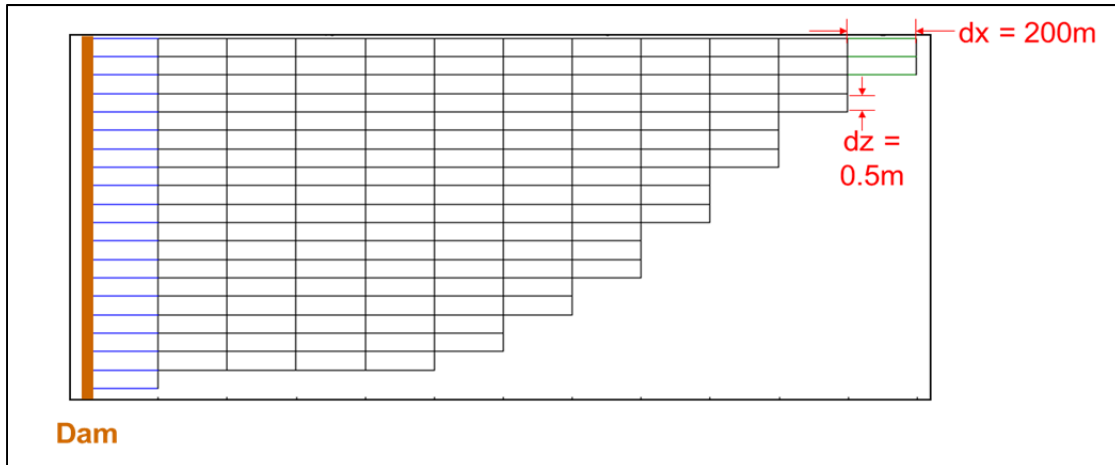


Figure 43. Profile View of Model Grid

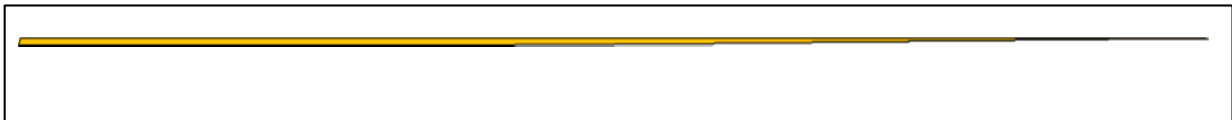


Figure 44. Model Profile without Exaggerated Vertical Scale

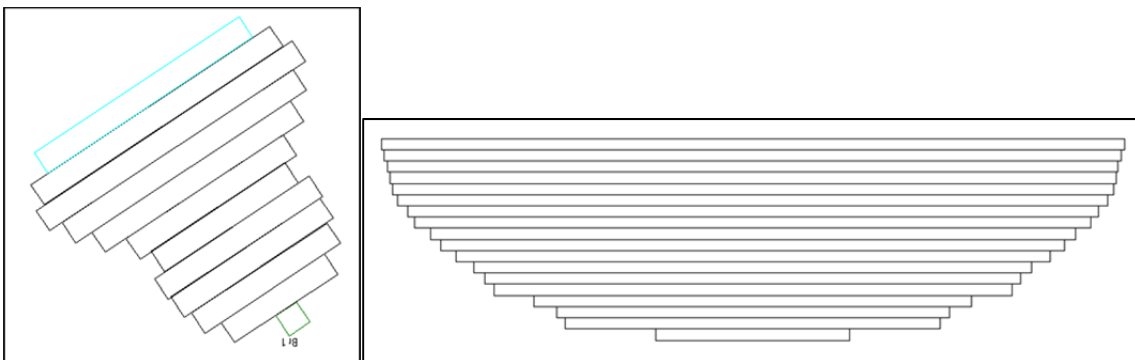


Figure 45. Plan View of Model Grid (Left) and Section View of Segment 12 (Right)

⁷ Model bathymetry was calculated from these contours by measuring widths perpendicular to the principal direction of flow at each contour depth along 24 transects equally-distributed at 100 meter intervals over the reservoir. The average width at each depth in each of the 12 active model segments was calculated, and the vertical discretization of the model bathymetry was set at 0.5 meter resolution using linear interpolation between measured contours to calculate center-line widths. Where necessary, adjustments were made to ensure bottom widths were greater than or equal to 10 meters, and so that the width of each cell was at least 10% of the width of the cell directly above it, as recommended for optimal model performance.

The resulting elevation-to-volume and are elevation-to-surface area relationships were compared to those based on the 1-ft contour data. The bathymetry in the model matches the observed bathymetry well. A comparison of model and contour-based elevation-to-volume relationship is presented in Figure 46, with an indication of the operating range of the 2003-2013 period. The mean absolute error (MAE) is 0.28% (49 AF; 60,400 m³), and the root mean squared error (RMSE) is 0.37% (66 AF; 81,400 m³).

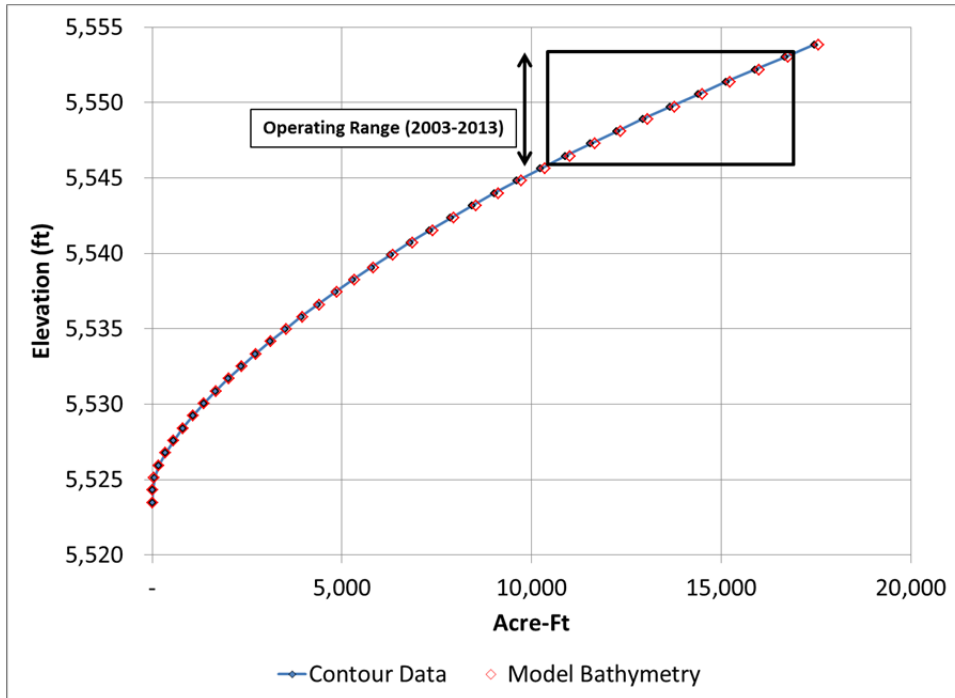


Figure 46. Comparison of Model Bathymetry and Contour Data Elevation - Volume Relationship

A comparison of model- and contour-based surface area-to-volume relationship is presented in Figure 47, with an indication of the operating range of the 2003-2013 period. The MAE is 0.49% of the total area (4.8 acres; 19,400 m²), and the RMSE is 0.60% of the total area (6.0 acres; 24,300 m²).

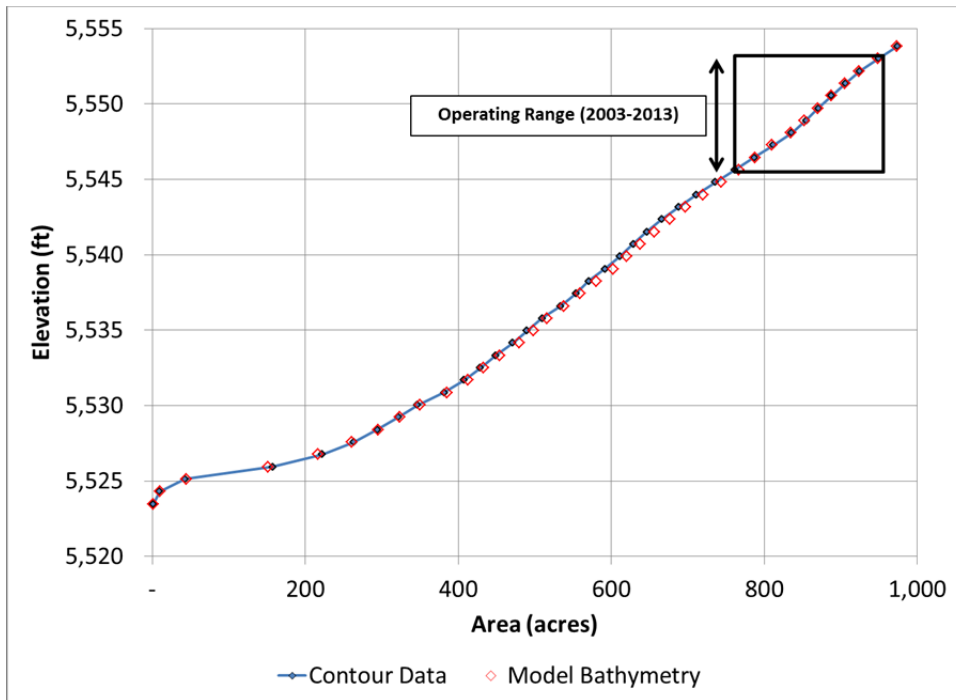


Figure 47. Comparison of Model Bathymetry and Contour Data Elevation - Volume Relationship

3.2 Water Balance

Daily flow rates developed for the water balance were applied in the model to approximate actual flow patterns as described below and as shown on Figure 48:

Inflows:

- **Cherry Creek** inflows were assigned as the branch inflow, entering the model at the first active segment. Cherry Creek inflows are set to flow in according to relative density.
- **Cottonwood Creek** inflows were assigned as a tributary inflow, entering the model at the second active segment and set to flow in according to relative thermal density.
- **Groundwater** inflows were set to enter the model in the second segment also. This is based on the location a greatest seepage identified by Lewis et al. (2005) through seepage meter measurements and sediment conductivity and water content observations. The groundwater inflows are set to flow in according to relative density.
- **Un-gaged Surface Water** inflows were assigned as tributary inflows into the eighth active segment, recognizing that some of this inflow enters the reservoir via un-gaged channelized flows adjacent to this segment. These flows are also set to flow in according to relative density.
- **Precipitation** enters the model distributed across the reservoir surface in proportion to the surface area of the segments.

Outflows:

- **Dam Releases** are simulated as releases from a point-type structure in the last active segment, defined in the model by elevation of the outlet within the reservoir. The outlet is set up to use the selective withdrawal algorithm in the W2 code. This algorithm calculates a time-varying withdrawal zone for each outlet based on outflow, outlet geometry, and upstream density gradients.
- **Evaporation** is set to be removed from the top layer of the reservoir, distributed in proportion to the surface area of the segments.
- **Outflow Seepage** is designated in the model as an outflow from the final active segment and seepage is specified to come from the bottom layer of that segment.

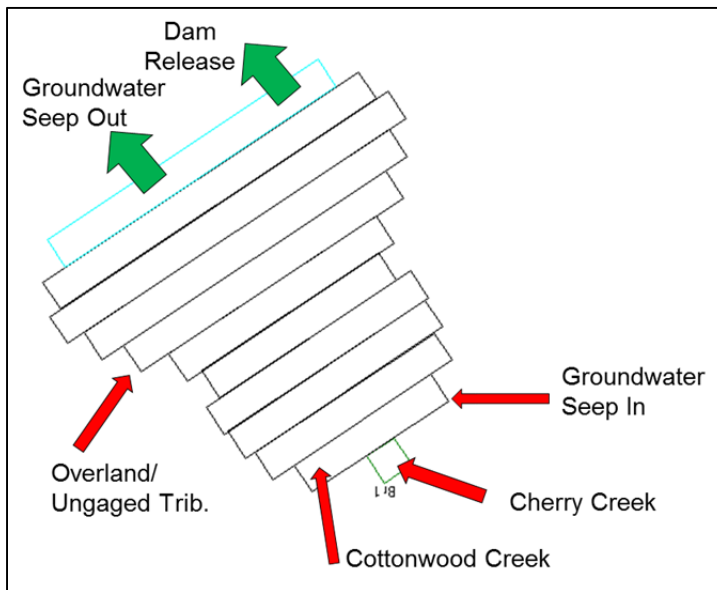


Figure 48. Location of Inflows and Outflows Applied in Model

3.3 *Algae and Zooplankton*

Algal species biovolume and density data were reviewed for seasonal progression patterns to develop inputs for algal groups. There are some patterns in the data, but there is considerable variability from year to year. From the data, five algal groups were assigned in the model:

1. **Group 1: Winter Algae.** This group includes algae often observed to occur through winter months including cold water conditions. These include chlorophyta, cryptophyta, and bacillariophyta (diatoms).
2. **Group 2: Spring and Early Summer Algae.** The data show spring and fall occurrence and sometimes dominance of bacillariophyta, including *Fragilaria crotonensis*. Also observed in these conditions at times are cryptophyta, euglenoids, chrysophytes, and dinophyta.
3. **Group 3: Spring / Fall Nitrogen-Fixing Cyanobacteria.** Major *Anabaena* blooms have been observed to occur in calm conditions at temperatures less than ~20 °C. This group

has been assigned the capability of nitrogen fixation in the model. This group has also been assigned lower settling rates to reflect buoyancy advantages.

4. **Group 4: Summer, Nitrogen-Fixing Cyanobacteria.** Major *Aphanizomenon* blooms appear to occur in calm surface water between ~ 23 and ~ 26 °C in the reservoir. This group has been assigned the capability of nitrogen fixation in the model. This group has also been assigned lower settling rates to reflect buoyancy advantages.
5. **Group 5: Summer Algae.** Under warmer conditions at the top of the reservoir, a wide range of non-nitrogen-fixing algal types have been observed, including dinophyta, cryptophyta, chrysophyta, euglenophyta, and sometimes chlorophyta.

Maximum growth rates specified in the model for these five algal groups are presented as a function of water temperature in Figure 49. This figure also presents the maximum growth rate settings for zooplankton. Both zooplankton groups in the model feed on particulate organic matter, but only the first zooplankton group feeds on phytoplankton as well. The second group acts as a predator for the first zooplankton group. Through calibration, relatively low growth rates, with strong predator-pressure were set. This suggests a relatively small role for zooplankton in algal control though it does play a role in timing of seasonal shifts between algal groups in the model.

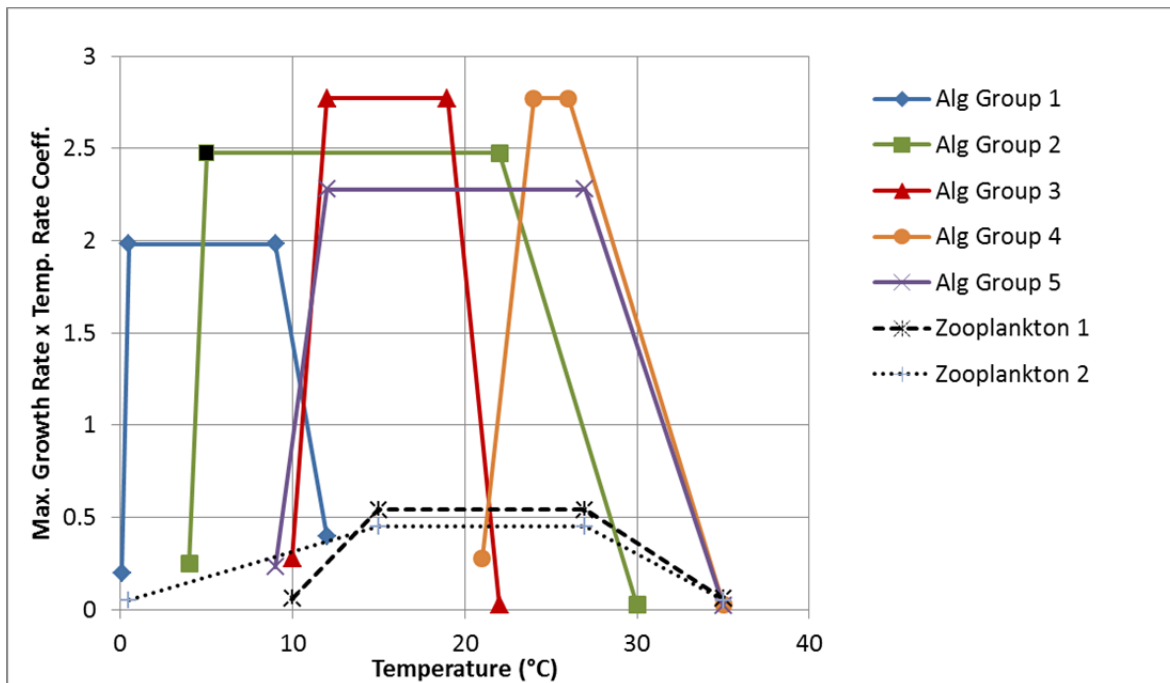


Figure 49. Maximum Growth Rate as a Function of Water Temperature for Algal and Zooplankton Groups in the Model

3.4 Sediment

Sediment oxygen demand and internal loading are simulated applying both the zero-order and first-order sediment modules in W2. The zero-order sediment module simulates anaerobic oxygen demand and associated anaerobic internal loading. The first-order sediment module simulates aerobic decay of detritus at the sediment-water interface, consuming oxygen and

providing nutrients to the water column (i.e., aerobic internal loading). These are explained in detail in the W2 documentation (Cole and Wells, 2011). It was decided to apply both sediment modules, recognizing the highly productive nature of the reservoir and the variable dissolved oxygen concentrations at the bottom, even during warm summer months.

3.5 Destratification System

The destratification system is represented in the model using the W2 Aeratec controls. This module allows the user to apply a multiplier to the vertical mixing coefficient on a segment-by-segment basis, over the layers of interest (Cole and Wells, 2011). CE-QUAL-W2 also allows for the direct addition of oxygen to the water. In the model, aerators were designated in the second active layer above the bottom (corresponding to 0.5 to 1 m above the bottom, reflecting the ~0.6 to 0.75 m height of the aerator heads). Mixing was designated from the aerator heads to the surface of the reservoir, recognizing that bubbles from this system are routinely observed at the surface. The aerators were designated in four segments, patterning their actual location in the reservoir (Figure 50). The aerator vertical mixing factor was calibrated using the continuous thermistor data collected at each meter at CCR2 since 2007. Aerator mixing was systematically increased until it began to increase error in simulation of continuous temperature observations and continuous temperature differences from top to bottom. Aerator mixing was also assessed against simulated water-quality response to assure that the temperature-based calibration of mixing also provided good water-quality response.

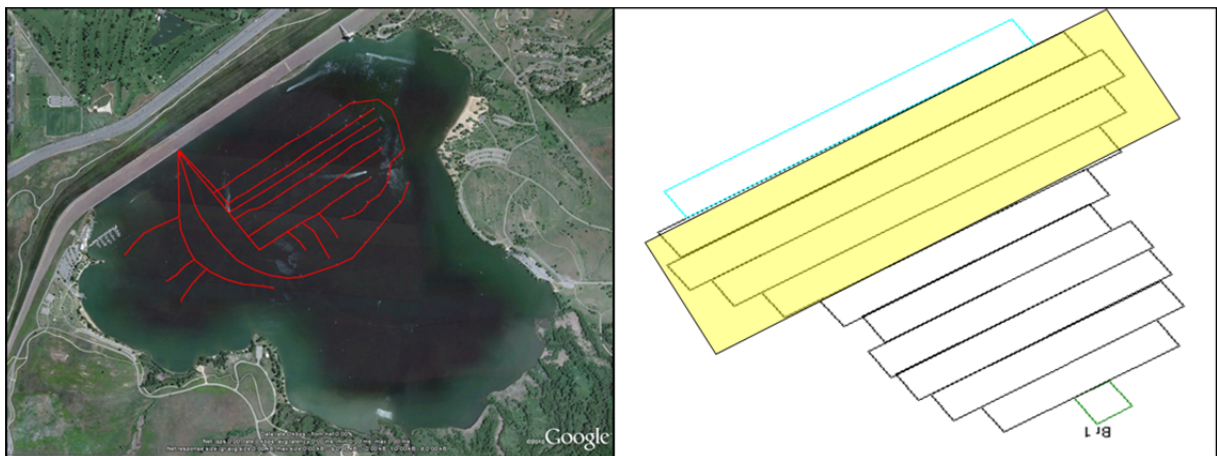


Figure 50. Actual Location of Aerators on Reservoir Footprint (Left) and Model Segments Designated to Contain Aerator Heads (Right)

Because the aerator bubbles have a relatively short contact time with the water before reaching the surface (due to the relatively shallow nature of the reservoir), and because the aerators supply air and not oxygen, limited direct oxygen loading is expected. Addition of oxygen by aerator bubbles was assigned by first estimating the maximum possible oxygen load from the aerators. The aerators provide 200 to 250 cubic feet of air per minute (or 8,155 cubic meters per day). Assuming a density of air of 0.93 kg/m^3 at an altitude of 5,500 ft at 90°C , this corresponds to 7,584 kg of air per day. Assuming 23% oxygen, this equates to 1,744 kg oxygen per day. Since the aerators are distributed over four reservoir segments, this is the equivalent

of a maximum potential of 436 kg of oxygen per day per segment, assuming an even distribution. A total of 200 kg of oxygen per day per segment was used in the modeling. This is a little less than half the maximum potential. The effect of this directly-added oxygen is minimal in the modeled response, as was simulation of the maximum potential load in a test run.

3.6 Model Code Adjustments

To better simulate the observed algal response, two adjustments were made to the W2 code:

1. Nitrogen Fixation Recoding

Data from Cherry Creek Reservoir indicate periods of nitrogen limitation and the presence of nitrogen-fixing cyanobacteria (Aquatic Solutions and Water & Waste, 1989; Jones, 1998; Lewis, 2004; and Hydros, 2014). The W2 model simulates nitrogen fixation; however, the model only allows nitrogen fixers to obtain nitrogen from the atmosphere. In reality, nitrogen-fixing algae revert to direct ammonia and/or nitrate uptake when these forms of nitrogen become available in the water column again (Bergman et al., 1999, pg. 4). This pattern is reflected in the observed data from Cherry Creek Reservoir also (Hydros, 2016). The model code was adjusted so that nitrogen fixing algae better reflect this behavior. Thresholds for total inorganic nitrogen (TIN) concentrations and TIN-to-PO₄ ratios at which cyanobacteria begin (and stop) fixing nitrogen were added. This approach is similar to that applied in the EPA ecosystem modeling tool Aquatox (Clough, 2014). These adjustments allowed for better simulation of cyanobacteria timing and effect.

2. Fish Kill Effects

The fish kill in August of 2012 is expected to have resulted in an increased organic matter load to the bottom of the reservoir (in the form of dead fish). This organic matter would also be expected to not be buried as quickly as algal detritus. In the absence of accounting for effects of the fish kill, the model under-simulates subsequent nutrient concentrations and corresponding algal biomass, particularly in the spring of 2013. Based on this, the model code was adjusted to allow for an increase in organic matter concentration in the 1st-order sediment module following the fish kill. Further, sediment burial rates were also decreased somewhat, starting after the fish kill in 2012. The burial rate effect was limited to 300 days after the fish kill event.

To estimate the increase in organic matter delivered to the bottom the reservoir, it was assumed that 90% of the fish settled to the bottom of the reservoir (Johnson, personal communication, 2015). Based on the number of fish collected at the surface, this was assumed to be roughly 5,000 fish. It was assumed that the average weight of each fish was 0.2 kg/fish, resulting in ~1,000 kg of settled dead fish. Assuming 850 acres of bottom surface (3.4E6 m²), this corresponds to 0.29 g of organic matter per square meter. Assuming that half of this organic matter was carbon and applying the Redfield ratio (C:N:P = 106:16:1), the following increases in sediment composition concentrations were applied: carbon +0.14 g/m², nitrogen +0.02 g/m², phosphorus +0.001 g/m², and organic matter +0.161 g/m².

4 Model Calibration

The calibration of the Cherry Creek Reservoir Model is described in this section. Calibration was performed by adjusting conceptually-relevant coefficients within reasonable ranges. Reasonable ranges of coefficient settings were defined by model guidance documents and literature. The process was iterative and not prescriptive. The calibration focused on the observed record from January 2003 through December 2013.

The ultimate calibration metric for this model, based on the site-specific standard driver for this work, was the summer chlorophyll *a* concentrations. Simulating chlorophyll *a*, however, required reasonable simulation of water temperature, nutrient concentrations, sediment dynamics, and oxygen. Therefore, these are also considered calibration targets for this effort. The focus, in review of simulation results through calibrations, was on simulating concentration ranges, seasonal patterns, spatial patterns, and year-to-year differences by visual review of graphical comparisons of observed and simulated results. The goal of this approach was to reflect water-quality mechanisms at work in the reservoir instead of simply focusing on minimizing residual error statistics. In addition to visual review of patterns, calibration summary statistics were calculated and are presented.

Numerical calibration targets were set for surface water elevation, temperature, dissolved oxygen, nutrients, and chlorophyll *a*. The values of these targets match those used by the group that supports and manages CE-QUAL-W2 model development at Portland State University (Wells, et al., 2008). These targets are:

- For water level: an mean absolute error (MAE) within 10 cm;
- For temperature: an MAE within 1 °C;
- For dissolved oxygen: an MAE within 2 mg/L; and
- For nutrients and algae concentrations: an MAE within 10-20% of the range of field data.

The following subsections present the calibration assumptions and results for water levels, temperature, nutrients, dissolved oxygen, and algae / chlorophyll *a*. This section is supported by Attachments B and C, which include simulated and observed temperature results (profile and thermistor) and simulated and observed dissolved oxygen results (profile).

4.1 Surface Water Elevation

Applying the water balance described in Section 3.2, simulated surface water elevations were compared to the observed record. The model matched observations well and met the numerical calibration target of $MAE \leq 10$ cm. The simulated MAE was 0.1 ft (4 cm). The RMSE and average error were also 0.1 ft (4 cm). Simulated and observed daily water levels are shown in Figure 51.

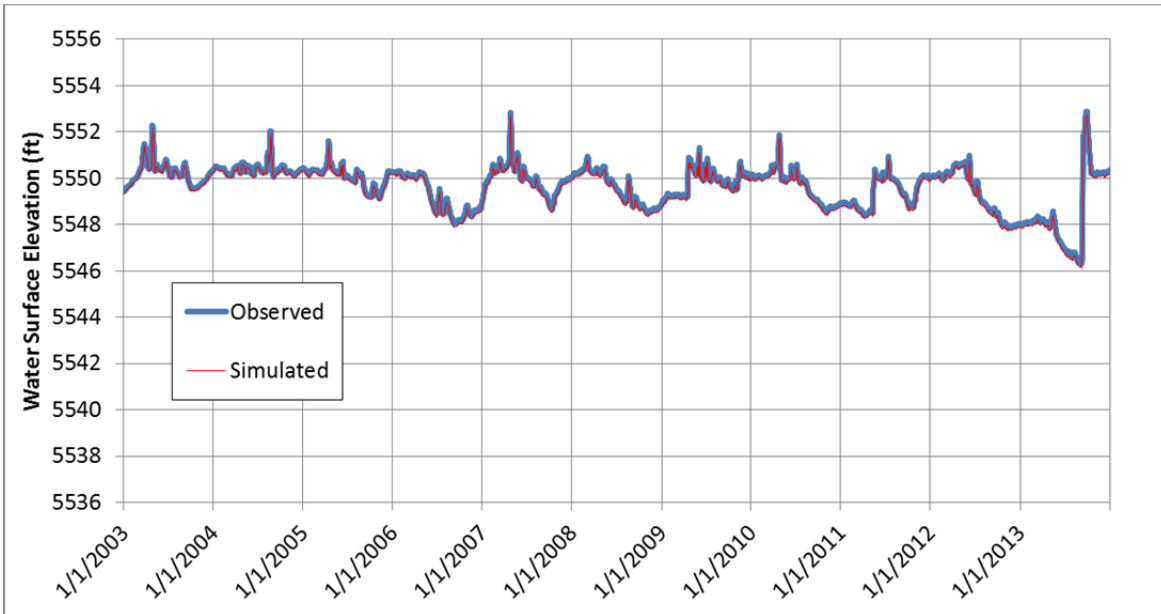


Figure 51. Comparison of Simulated and Observed Daily Water Levels, 2003-2013

The model simulates “water age”, indicating how long water in a given cell has been in the reservoir. This output is generally comparable to residence time. Simulated water age in Segment 12 (the segment corresponding to CCR1 and CCR2) at 1 m and at the bottom are shown in Figure 52. Note that water age starts at zero across the reservoir at the start of each simulation, though a steady pattern is reached in the second year. Water age at the top of the reservoir is not very different from that at the bottom, indicating that short-circuiting underflows or overflows are very limited in this part of the reservoir. The exception is simulated overflow in some winter months and some brief underflow during non-winter storm events. The average water age simulated by the model at CCR2 from 2004-2013 is 247 days. In this figure, major reservoir inflows and associated outflows reducing residence time are apparent in the first half of 2007 and 2009, as well as in September of 2013.

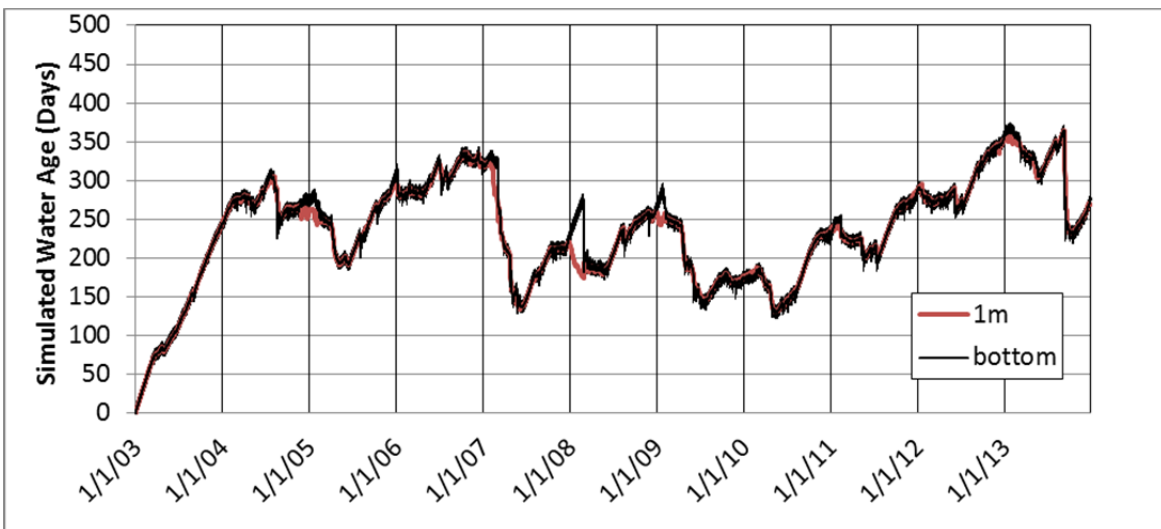


Figure 52. Simulated Water Age at 1 m and at the Bottom at CCR2, 2003-2013

4.2 Temperature

Accurate simulation of water temperature in the reservoir is critical to water-quality modeling. Temperature is one indication of the simulation of mixing within the reservoir. Temperature is also an integral part of simulating various reaction, growth, and decay rates within the model. In addition, calibration of water temperature is dependent on the water-quality simulation, particularly in a eutrophic system like Cherry Creek Reservoir. The water-quality simulation, which includes simulation of total suspended solids, affects the transmission of light through the reservoir, which in turn, affects the temperature response with depth. Therefore, the temperature calibration was completed iteratively with the water-quality simulation.

In this relatively shallow system with residence time on the order of 250 days, accurate simulation of water temperature required good data for meteorological drivers. Air temperature, wind, and solar radiation were the most critical meteorological inputs. Data from the local meteorological stations (Figure 17) were tested in the model, and the compilation described in Section 3.4 was identified as the best combination of information. Air temperature and solar radiation data from the CPW Met station were particularly valuable in improving calibration response. Based on this, it is recommended that the Authority coordinate with CPW to check and improve data collection and data management protocols for the CPW meteorological station. Alternatively, a meteorological station could be installed at the dam (or on the reservoir or other proximal location), monitoring, at a minimum, air temperature, solar radiation, wind speed, and wind direction. These data would be valuable for future modeling and model refinements.

The thermal simulation was less sensitive to inflow water temperatures from the tributaries, as compared to meteorological inputs, though not completely insensitive, particularly during larger storm events. The 2003-2013 dataset does not include continuous temperature data for the inflows, so inputs were developed by applying seasonal multiple regressions of air temperature, solar radiation, and flow rate to the available monthly temperature observations. Recently-installed thermistors in the inflow tributaries should help refine thermal inputs for future modeling, particularly during storm events.

The 328 observed reservoir temperature profiles from CCR2 and CCR3, collected between 2003 and 2013, were reviewed relative to simulation results to guide the calibration. Additionally, the thermistor data from CCR2 were compared to simulation results. The thermistors have collected continuous temperature data at 1 m intervals since 2007. Thermistors are deployed in March, April, or May of each year and retrieved in September, October, or early November. The thermistor dataset was particularly useful for refining calibration in this dynamic system. Comparison of the simulated and observed temperature differenced from the top to bottom, as measured at CCR2 by the 1 m and 7 m thermistors, were also a useful review for calibration.

In addition, the in-reservoir thermistor data were helpful in calibration of increased vertical mixing due to the destratification system. Following calibration of the pre-destratification system period (2003-2007), simulated destratification system mixing was increased progressively from zero until it no longer improved (and started to deteriorate) the calibration

of thermistor response at CCR2 for 2008-2013. Specifically, this optimization of calibration focused on matching the thermistor-measured temperature difference between 1 m and 7 m at CCR2. Based on this approach, a 20% increase in vertical mixing was set for the destratification system when operating.

Overall, the thermal calibration is very good. The model successfully simulates the overall seasonal patterns and magnitudes of observed water temperatures. This includes simulation of periods of brief stratification and isothermal conditions. Three example CCR2 calibration profiles over a range of temperatures are presented in Figure 53. The full set of calibrated and observed profiles from 2003-2013 for CCR2 and CCR3 are presented in Attachment B.

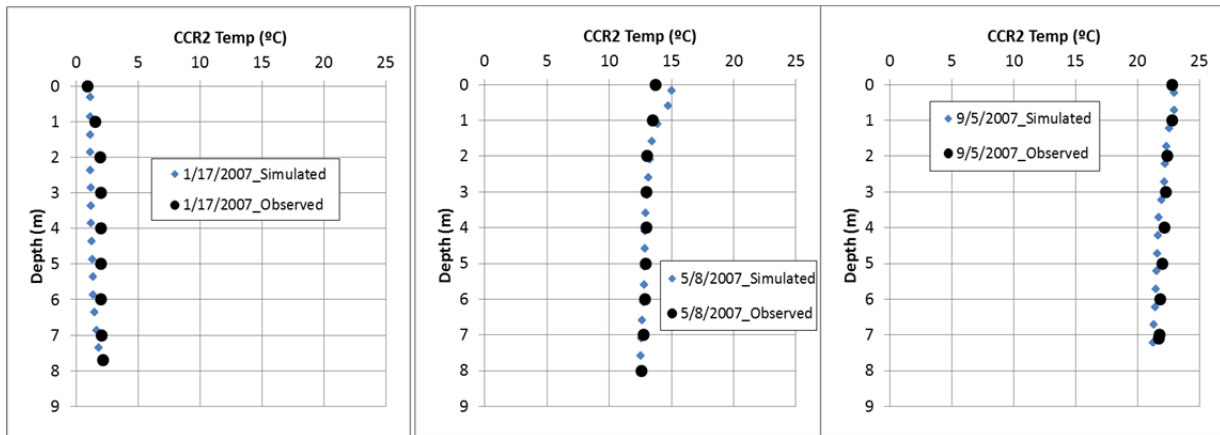


Figure 53. Example Calibration Profiles at CCR2 from 2007

Residuals for each profile were calculated and compiled to evaluate simulation error. In general, residuals tended to be slightly greater in May or June, when water temperatures were increasing most rapidly. The MAE, RMSE, and average error for the temperature profiles are presented in Table 2. All of these metrics were less than the MAE calibration target maximum of 1 °C. Results indicate similar statistics at CCR2 and CCR3. Further, results were the same (to the tenth of a degree) for the period before and after the start of the destratification system (2008).

Table 2. Summary Calibration Statistics for Temperature Profiles, 2003-2013

Metric	CCR2	CCR3
Profiles - Average MAE	0.5 °C	0.5 °C
Profiles - Average RMSE	0.6 °C	0.6 °C
Profiles - Average Error	-0.1 °C	0.1 °C

Observed thermistor data plotted against simulated temperatures also show good matches of seasonal patterns, magnitude, and diurnal range from the top to the bottom in all years. As an example, the hourly simulated and observed temperatures at 1 m and 7m at CCR2 in 2008 are shown in Figure 54 and Figure 55, respectively.

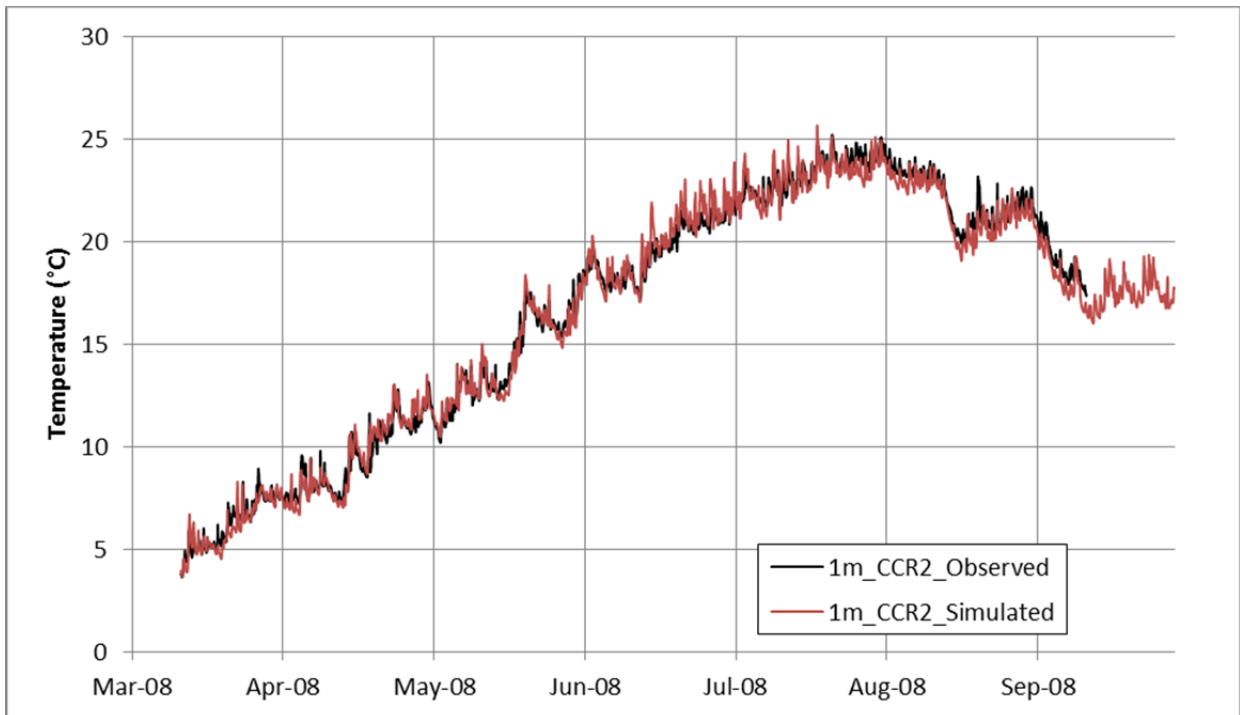


Figure 54. Observed and Simulated Hourly Temperatures at 1 m at CCR2, 2008

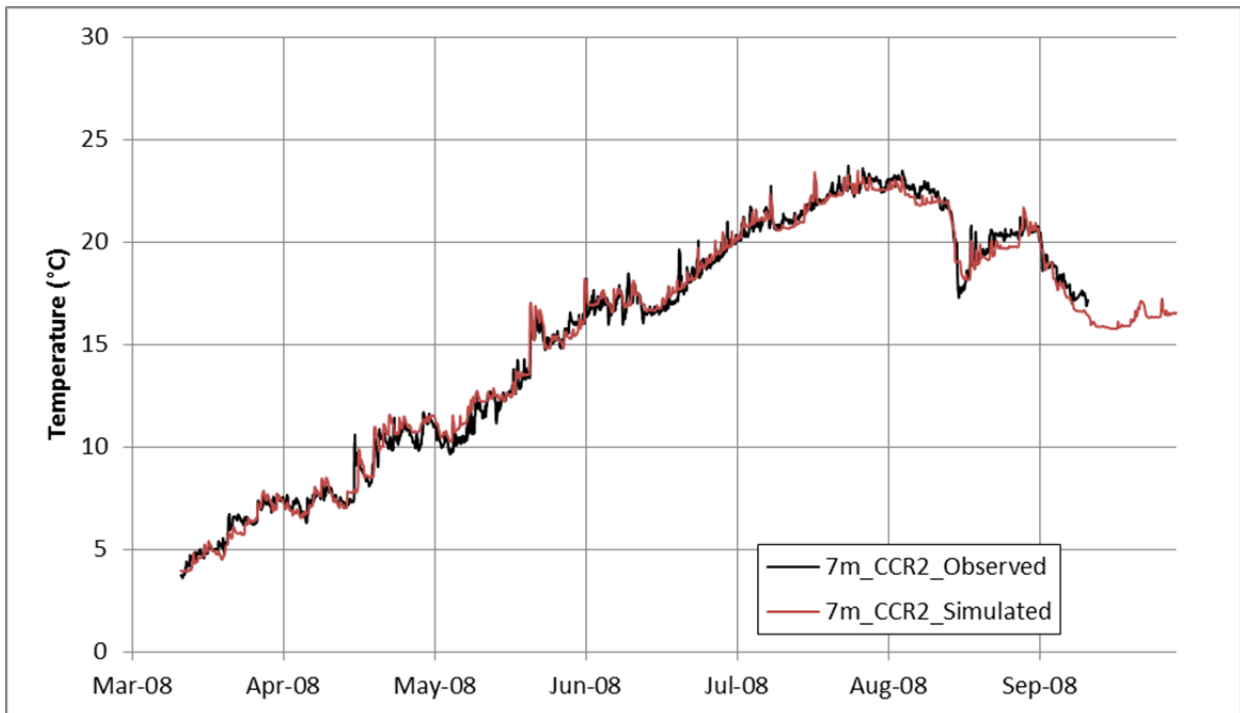


Figure 55. Observed and Simulated Hourly Temperatures at 7 m at CCR2, 2008

In addition, top-to-bottom temperature differences are well simulated by the model. An example of the observed and simulated 1m to 7m temperature difference is provided in Figure 56. The complete set of observed and simulated data for the CCR2 thermistors is provided in Attachment B.

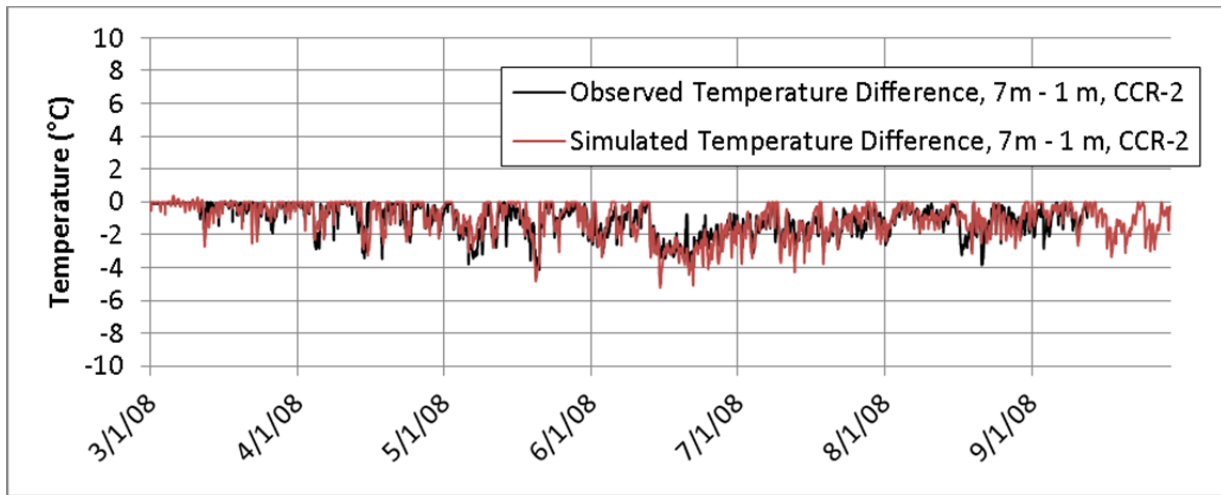


Figure 56. Observed and Simulated Hourly Temperature Differences between 7 m and 1 m at CCR2, 2008

Calibration summary statistics for continuous thermistor data are summarized in Table 3. All of these measures of residuals are less than the calibration target maximum of 1° C, providing good confidence in the thermal simulation.

Table 3. Summary Calibration Statistics for Thermistors at CCR2, 2007-2013

Metric	CCR2		
	MAE	RMSE	Average Error
Thermistors - Average MAE / RMSE / Average Error	0.6°C	0.7°C	-0.2°C
Temp. Diff. (1m to 7m) – MAE /RMSE/ Average Error	0.5°C	0.8°C	+0.1°C

4.3 Nutrients

The model simulates ammonia, nitrate, and orthophosphate as state variables. Simulation of these nutrient concentrations in the reservoir was most sensitive to algal settings, anaerobic (0-order) sediment release rates of ammonia and orthophosphate⁸ (PO₄), and sediment burial rates affecting aerobic sediment release rates of ammonia and PO₄.

Overall, the refined model meets calibration goals in simulation of the major processes of nutrient uptake, nutrient release from sediments, and the resulting nutrient difference from bottom to top. Calibration summary statistics for nitrate, ammonia, and PO₄ are presented in

⁸ For the purposes of modeling, observations of SRP were considered to represent orthophosphate for inputs and review of results. Throughout the calibration section observations of SRP are referred to as orthophosphate or PO₄.

Table 4. These include average error, MAE, and RMSE for CCR1, CCR2 and CCR3. All MAE results meet the numerical target of $\leq 20\%$ of the observed range of results (Table 5). The following subsections compare the time-series simulation results to observations.

Table 4. Average Error, MAE, and RMSE Calibration Statistics for Nutrients, 2003-2013

	CCR1			CCR2						CCR3		
	Photic (0-3m)			Photic (0-3m)			Bottom			Photic (0-3m)		
	Avg. Error	MAE	RMSE	Avg. Error	MAE	RMSE	Avg. Error	MAE	RMSE	Avg. Error	MAE	RMSE
Nitrate and Nitrite as N (ug/L)	8	15	34	6	16	37	8	22	48	9	19	45
Phosphate as P (ug/L)	2	19	29	3	19	28	-14	34	51	2	20	29
Total Ammonia as N (ug/L)	-10	21	32	-6	19	29	-23	58	88	-10	18	28

Table 5. MAE as a Percent of Observed Range for CCR1, CCR2, and CCR3 for Nutrients, 2003-2013

	MAE as % of Observed Range				Overall	Goal
	CCR1	CCR2		CCR3		
	Photic (0-3m)	Photic (0-3m)	Bottom	Photic (0-3m)		
Nitrate and Nitrite as N	12%	8%	3%	3%	6%	$\leq 20\%$
Phosphate as P	19%	19%	11%	20%	17%	$\leq 20\%$
Total Ammonia as N	14%	14%	11%	12%	13%	$\leq 20\%$

The reservoir exhibits significant cycling of nutrients between the water column and the sediments. Aerobic and anaerobic decay of organic matter in the sediments releases ammonia and PO₄. Algae take up nutrients and eventually settle to the sediment surface decaying in the water column while settling or at the sediment-water-interface. Due to sporadic mixing from the bottom to the top in summer months, these products of algal decay are reintroduced to the surface of Cherry Creek Reservoir at times throughout the growing season. Such rapidly-changing dynamics can be a challenge to capture in numerical modeling; however, the calibrated Cherry Creek model is simulating these major nutrient cycling mechanisms. As with any generic purpose modeling software, there are simplifying assumptions in CE-QUAL-W2 v.3.72. Some of these simplifying assumptions may explain some remaining variation in simulated and observed nutrient responses. These are not suggested as critical model refinement needs; the calibrated model is a useful tool for the Authority as is. Instead these are listed here (and explained further in Attachment E) to support an informed review of results:

- Constant sediment burial rates,
- Stoichiometry of algae (no luxury uptake of PO₄), and
- Overly simplistic options to simulate sorption of orthophosphate to iron and inorganic suspended solids.

4.3.1 Total Ammonia

Observed and simulated ammonia concentrations at the top and bottom of the reservoir at CCR2 are presented in Figure 57. Results are presented on the same vertical scales to highlight

the difference between top and bottom concentration ranges. The model effectively simulates uptake of ammonia by algae in the photic zone as well as ammonia release from the sediments. The general magnitudes, seasonal patterns, and relative concentration gradients from the bottom to the top of the reservoir are reflected in the simulation results.

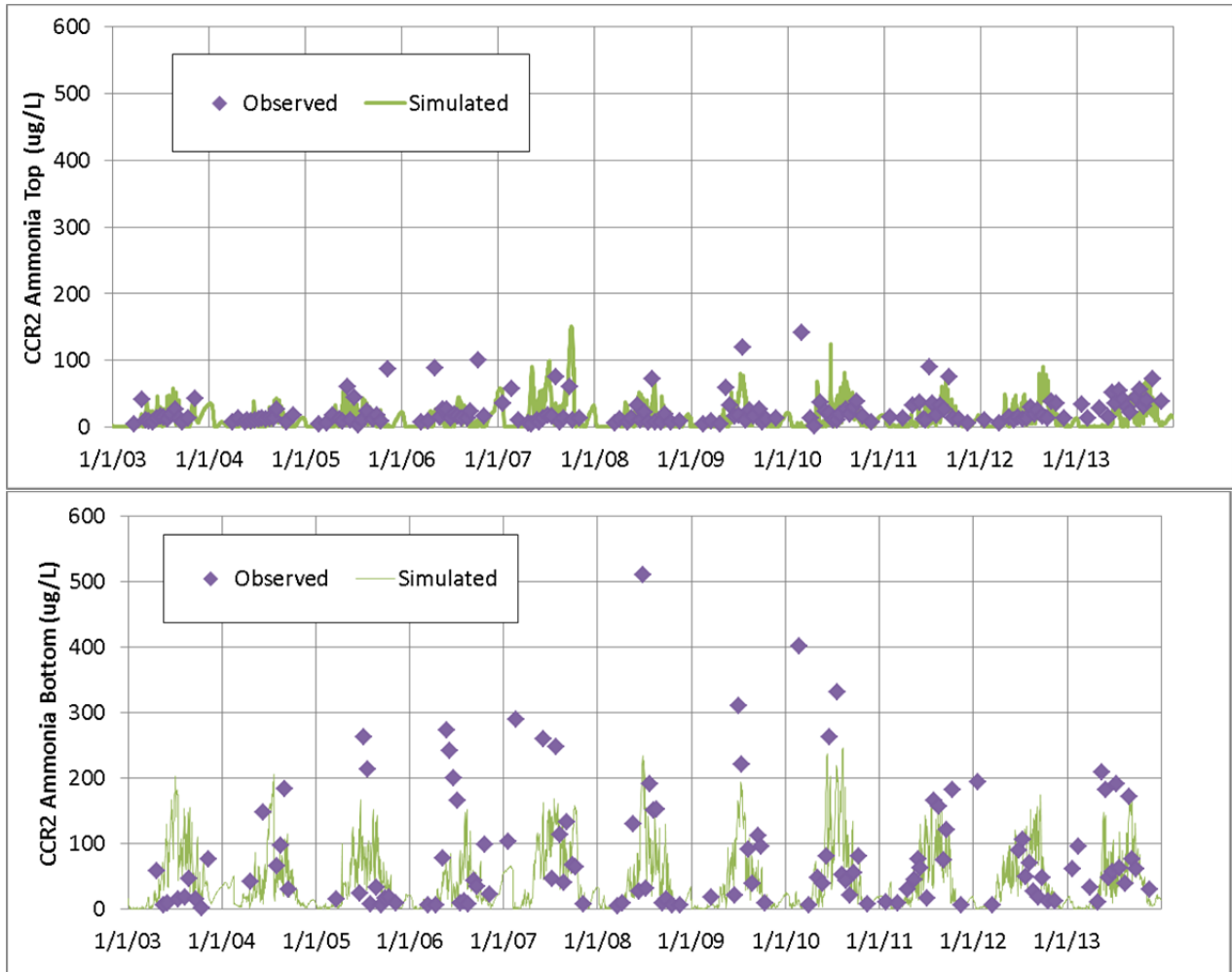


Figure 57. Simulated and Observed Ammonia Concentrations at CCR2 (Top and Bottom), 2003-2013

4.3.2 Nitrate

Observed and simulated nitrate concentrations at the top and bottom of the reservoir at CCR2 are presented in Figure 58. Results are presented on the same vertical scales to highlight the difference between top and bottom concentration ranges. The model effectively simulates uptake of nitrate by algae in the photic zone. The model shows increased nitrate concentrations in winter months, in accordance with winter data available in some years. Nitrate is not released from the sediments, and nitrification produces very little nitrate in the simulation. As a reminder for reference, the inflow nitrate volume-weighted average concentration was 840 $\mu\text{g/L}$ through this period. As such, consistent with observations, the model simulates high levels of nitrate uptake relative to inflow concentrations and the lack of a strong concentration gradient from top to bottom.

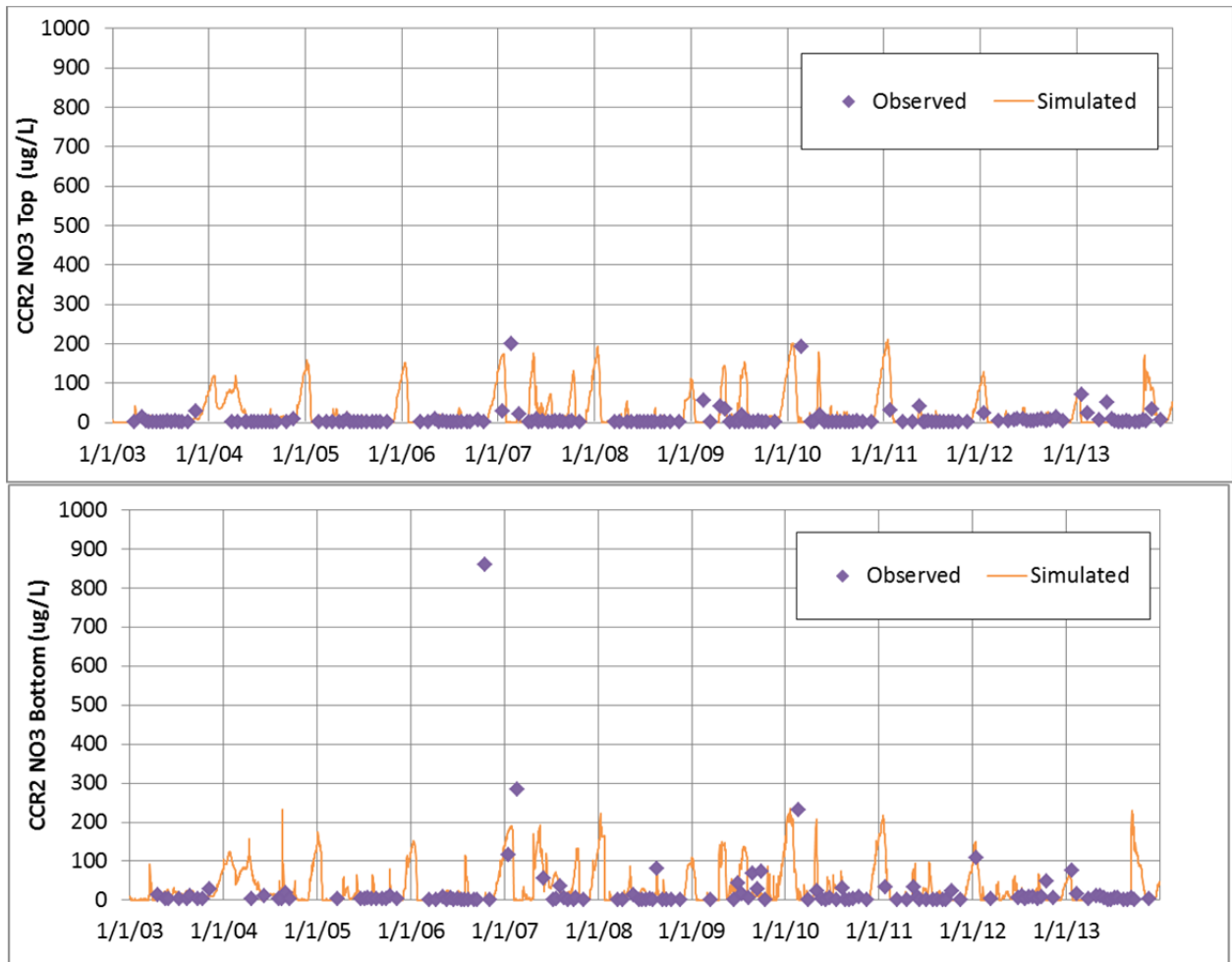


Figure 58. Simulated and Observed Nitrate Concentrations at CCR2 (Top and Bottom), 2003-2013

4.3.3 Orthophosphate

Observed and simulated orthophosphate (PO₄) concentrations at the top and bottom of the reservoir at CCR2 are presented in Figure 59. The model simulates seasonal excess PO₄ at the top of the reservoir, sediment releases of PO₄, and the concentration gradient of increasing PO₄ concentrations with depth. Peak PO₄ concentrations at the top and bottom of the reservoir are under-simulated in some years. This may reflect failure to capture inflow loading from all storm events and/or over-simulation of vertical mixing and algal uptake rates at times. Further, in late summer and early fall of some years, the model over-simulates PO₄ concentrations in the reservoir. The lack of luxury uptake or sorption-settling behavior in the model may help to explain this (see Attachment E).

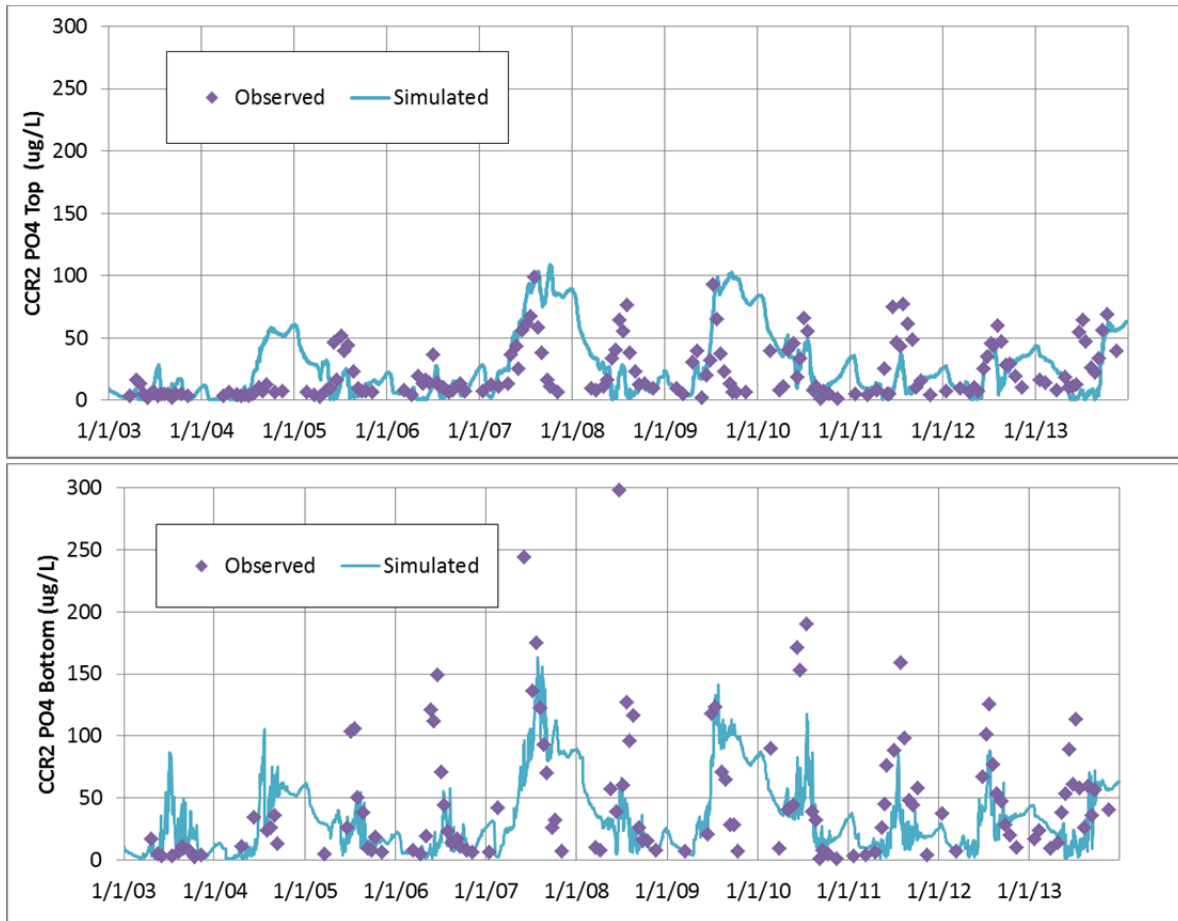


Figure 59. Simulated and Observed Orthophosphate Concentrations at CCR2 (Top and Bottom), 2003-2013

4.4 Dissolved Oxygen

In Cherry Creek Reservoir, dissolved oxygen is primarily controlled by aerobic and anaerobic SOD, organic matter decay in the water column, and reaeration from the surface. The dissolved oxygen response, therefore, reflects the dynamic nature of mixing and algal activity in the reservoir. Calibration of dissolved oxygen was sensitive to anaerobic (0-order) SOD rates, the 1st-order sediment burial and decay rates, and the amount of algal biomass simulated.

Review and attempted simulation of DO observations generated some questions about the raw DO data provided. First, there is an apparent shift in the observed DO values after 2010. Specifically, observed dissolved oxygen concentrations at the top are consistently lower, by a few mg/L, than the earlier period (2003 -2010) (Figure 60). In contrast, the model simulates fairly consistent, seasonally-varying DO concentrations at the top through the entire period (2003-2013). Other data were reviewed for relevant changes that could correspond to this temporal pattern in the observed DO dataset, but none were found. Specifically, there was no change in wind, relative chlorophyll *a* concentrations, or nutrient loading that matched this pattern.

There were also cases of unexpected large differences in observed super-saturation of DO between CCR1 and CCR2 that are not explained by differences in chlorophyll *a*. For example, on October 16, 2008, DO at the top of the reservoir at CCR1 was 12.5 mg/L with a chlorophyll *a* concentration of 6.3 ug/L. The same-day sample at CCR2 was 6.5 mg/L DO with a chlorophyll *a* concentration of 9 ug/L. These profiles and another example from 2005 are shown in Figure 61. This does not represent a complete QAQC review of all observed DO profiles relative to observed chlorophyll *a* data. Instead, this is a note of perceived uncertainty in the observed dissolved oxygen dataset.

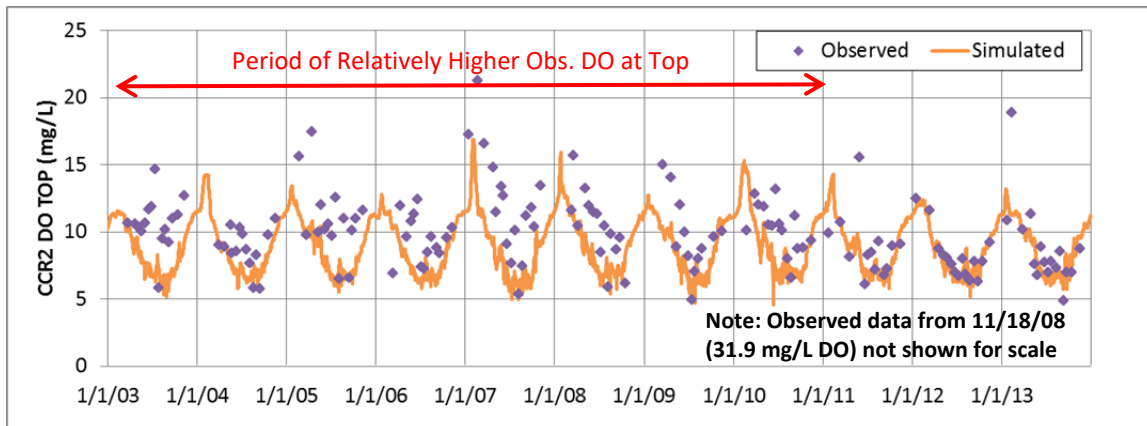


Figure 60. Observed and Simulated Dissolved Oxygen at the Top, CCR2, 2003-2013

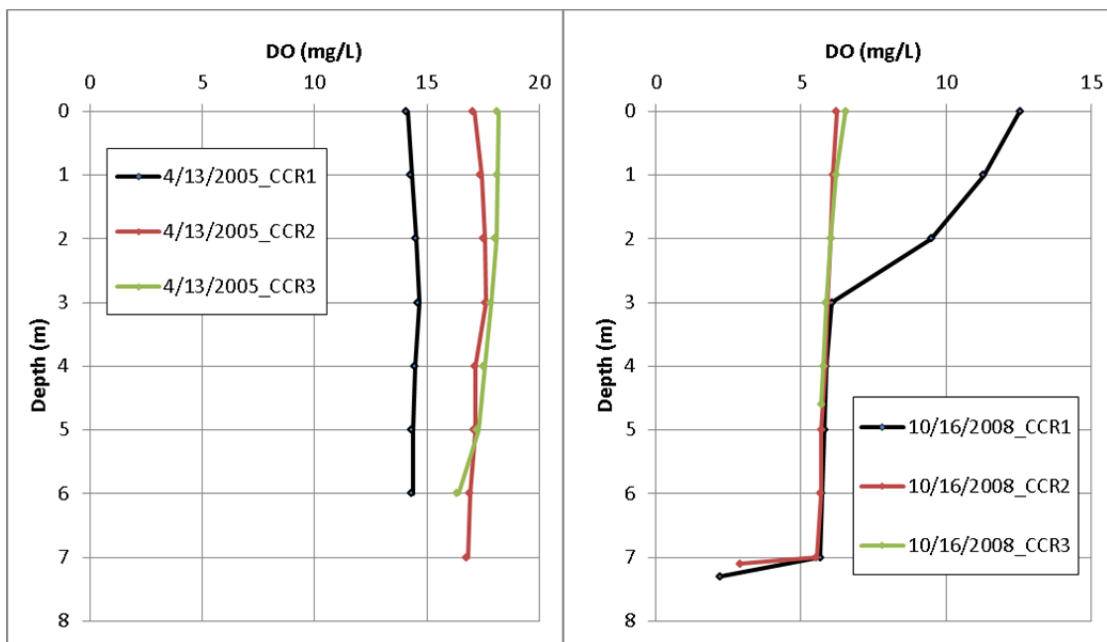


Figure 61. Observed DO Profiles at CCR1, CCR2, and CCR3 on April 13, 2005 and October 16, 2008

Despite this possible uncertainty in the observed dataset, the data were used without adjustment or censoring for calibration. The complete set of observed and simulated DO profiles is presented in Attachment C. Simulated bottom DO concentration data are plotted against the deepest observed DO data at CCR2 in Figure 62. The model simulates highly variable

DO concentrations at the bottom the reservoir, reflecting intermittent mixing due to intermittent isothermal or near isothermal conditions and associated wind and destratification-system-driven mixing. The model also simulates an increase in dissolved oxygen at the bottom at CCR3 starting in 2008 (Figure 63), matching relative observations during destratification system operations. The increased mixing, bringing oxygenated water to the bottom, is responsible for this increase, in the model and in the field. As noted in Section 3.5, the observed data suggest possible apparent induced sediment oxygen demand at CCR2. This effect is not clearly reflected in the simulation results, as the model does not simulate reductions to the diffusive boundary layer. A future refinement could consider modifying the code or testing the new sediment diagenesis version to improve simulation of apparent induced increases to SOD. The current calibrated model, however, reasonably simulates patterns and ranges of DO at the bottom of the reservoir.

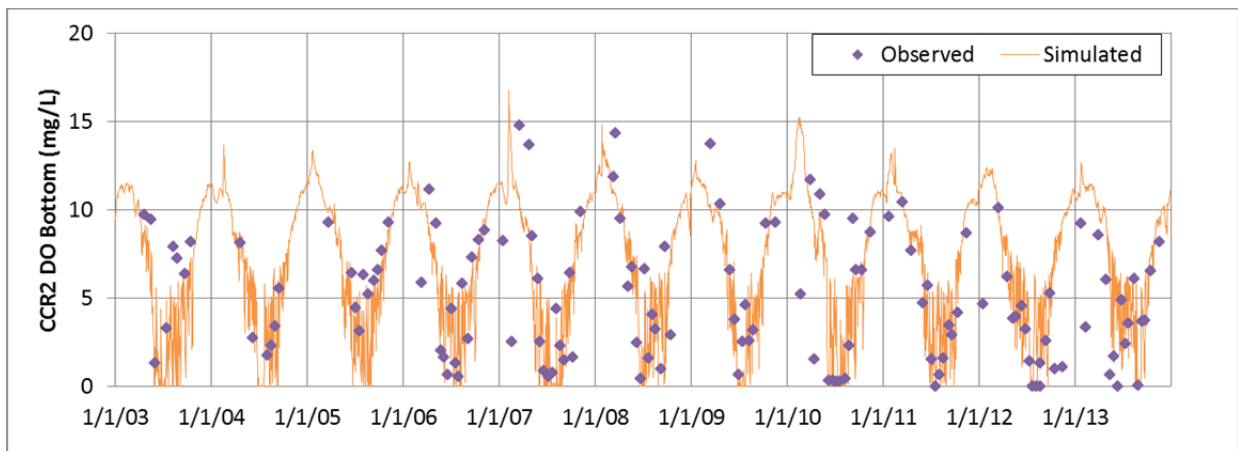


Figure 62. Observed and Simulated Dissolved Oxygen at the Bottom, CCR2, 2003-2013

(Note: Not all observations were within 0.5 m of the bottom. Data from 2003-2006 are typically greater than 0.5 m from the bottom.)

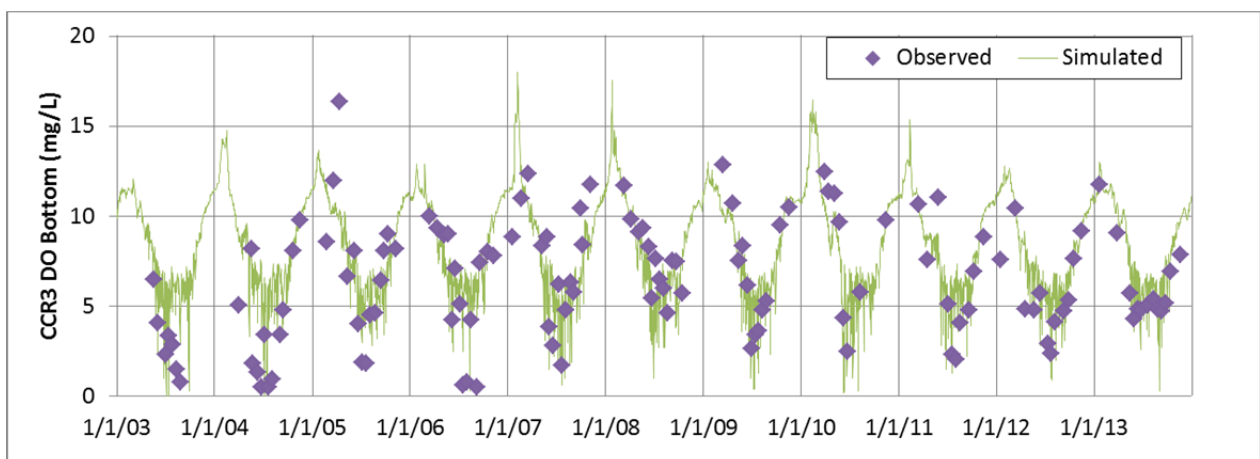


Figure 63. Observed and Simulated Dissolved Oxygen at the Bottom, CCR3, 2003-2013

(Note: Not all observations were within 0.5 m of the bottom. With the exception of several months in 2007, 2008, and 2010, most of these observed data are from roughly 1 m above the bottom.)

The simulated data were also reviewed to evaluate the simulation of the DO gradient from the top of the reservoir to the bottom. As shown in Figure 64, the model simulates a gradient similar to the observed patterns.

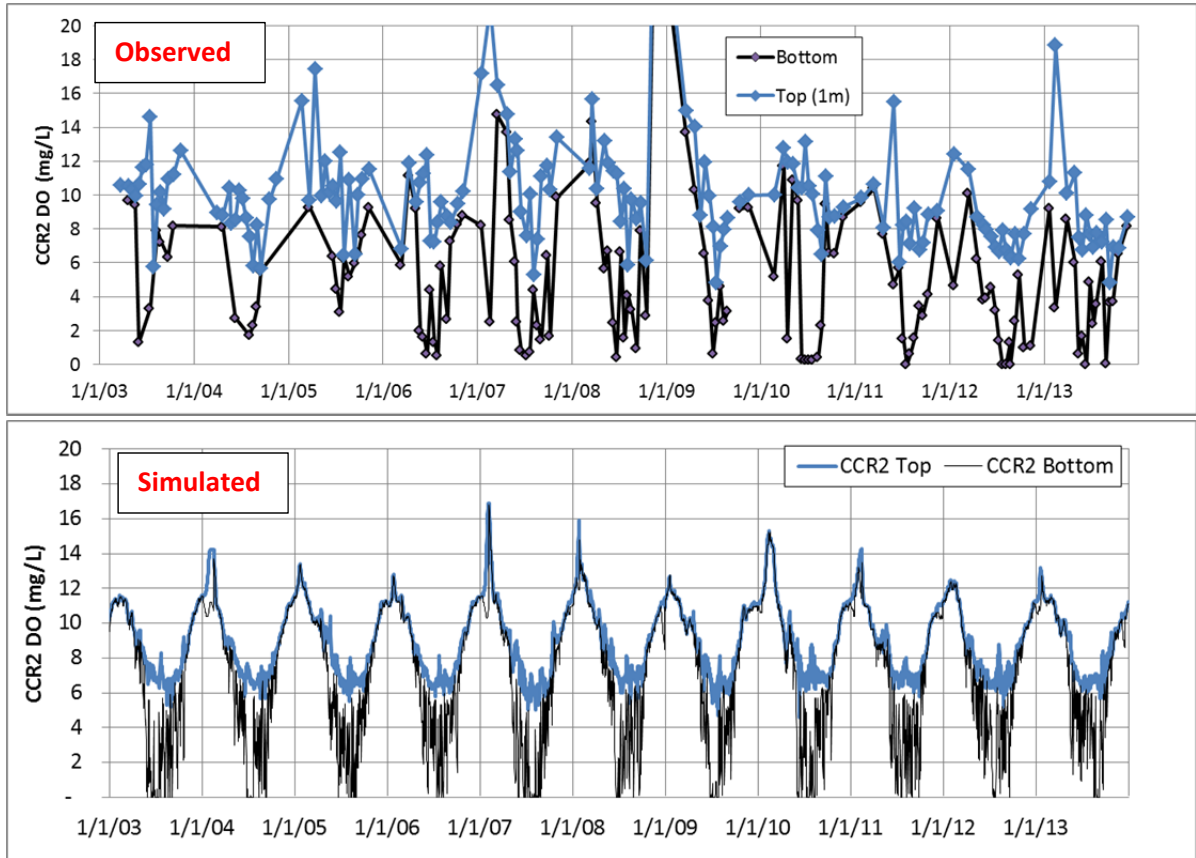


Figure 64. Observed and Simulated Dissolved Oxygen Gradient from Top to Bottom, CCR2, 2003-2013

(Note: Not all “bottom” observations in the upper figure were within 0.5 m of the bottom. Data from 2003-2006 are typically greater than 0.5 m from the bottom.)

Overall, dissolved oxygen is a key area of remaining uncertainty in the model; however, the model produces a reasonable simulation of concentration patterns and ranges as well as the general difference from top to bottom. The model also meets the numerical calibration target criteria of MAE ≤ 2 mg/L at each location (Table 6).

Table 6. Summary Calibration Statistics for Dissolved Oxygen Profiles, 2003-2013

Metric	CCR2	CCR3
Profiles - Average MAE	1.4 mg/L DO	1.3 mg/L DO
Profiles - Average RMSE	1.5 mg/L DO	1.5 mg/L DO
Profiles - Average Error	0.3 mg/L DO	0.2 mg/L DO

To help ground truth the model, it is recommended that the Authority install continuous DO probes at 1 m below the surface and at 0.5 m above the bottom of the reservoir at CCR2.

Alternatively, an in-reservoir buoy-based profiler could be placed in the reservoir for daily profile collection. These data would help determine how dynamic the actual DO response is in the deepest parts of the reservoir and provide more information to help assess potential apparent induced SOD.

4.5 Algae

Simulation of summer chlorophyll *a* in the reservoir was the primary calibration goal for model development due to the site-specific standard. This is consistent with the objectives of model development as described in the Introduction (Section 2). Simulation of algal response in the reservoir was highly sensitive to a wide range of algal settings, including algal growth rates, mortality, settling, temperature rate multipliers, and stoichiometry. The nitrogen-fixing algal groups were also sensitive to the TIN and TIN-to-PO₄ ratio triggers for nitrogen fixation behavior. Additionally, algal growth was sensitive to sediment burial rates and ammonia and PO₄ release rates from the 0-order sediment module. Adjustments to reflect the 2012 fish kill (described in Section 4.6) were also important for the simulation of chlorophyll *a* in 2013.

Simulated chlorophyll *a* concentrations are plotted with observed data for CCR2 in Figure 65. The model reasonably simulates general patterns and concentration ranges, though the timing and magnitude of peaks do not always match, as reflected in point-by-point statistics. As discussed in Section 4.3, algal biomass and chlorophyll *a* concentrations in the reservoir do not correlate well. This reflects varying chlorophyll *a* content by algal type as well as varying chlorophyll *a* content within an algal type in response to environmental conditions. The model uses constant chlorophyll *a*-to-carbon ratios within an algal group over time. In spite of this limitation, the model is capturing seasonal patterns and ranges.

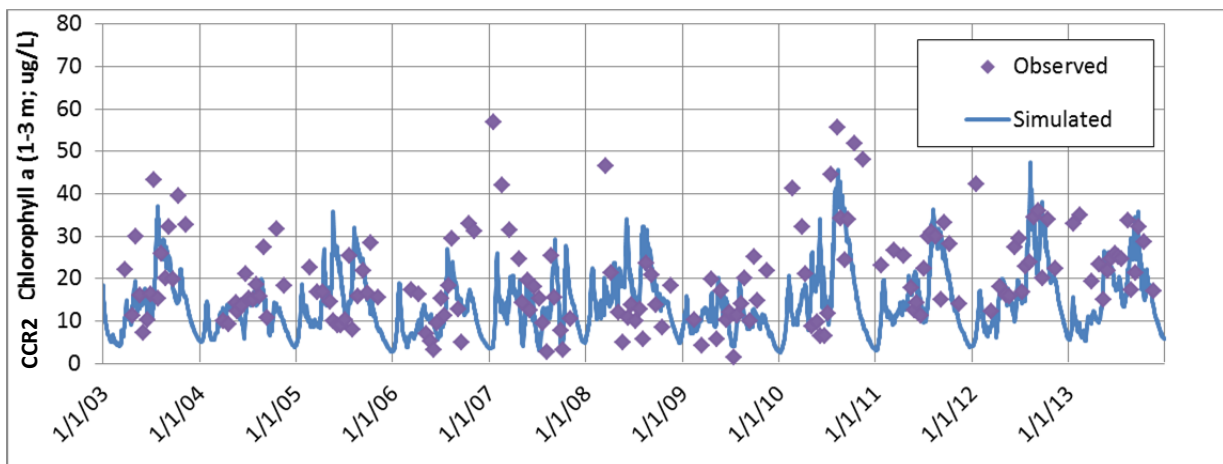


Figure 65. Simulated and Observed Chlorophyll *a* Concentrations in the Photic Zone, 2003-2013

Because the chlorophyll *a*-to-carbon ratios are calibrated and not observed inputs, the simulated mass of algal growth (a state variable) was ground-truthed by comparison to algal biovolume data. Algal biomass is what the model simulates. Biomass is translated to chlorophyll *a* in the model by user-specified, fixed algal biomass: chlorophyll *a* ratios. Observed

algal biovolume data is more directly comparable to the algal biomass simulated by the model than algal counts (due to size variation) or chlorophyll *a* (due to variation by algae and condition-response). Assuming a dry weight density of 1.27 g/cm³ and a 90% water content, biomass estimates were generated from the biovolume data, where available from 2009-2013. These observed biomass estimates compare well with simulated biomass (Figure 66), giving confidence that the model is producing a reasonable simulation of the amount of algae in addition to chlorophyll *a*.

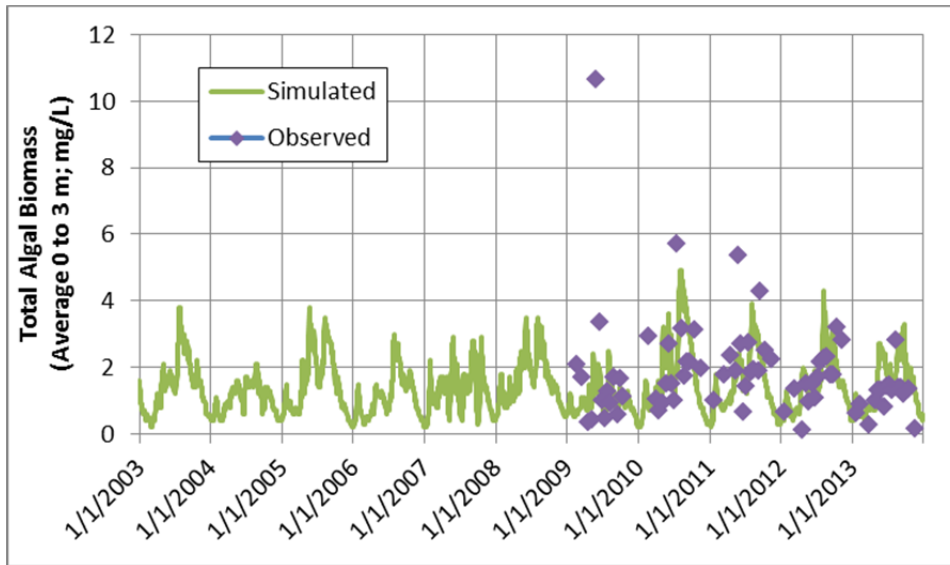


Figure 66. Comparison of Simulated and Observed Algal Biomass

Calibration summary statistics for the entire simulation period for chlorophyll *a* are presented in Table 7. The average error is less than 4 ug/L, and the MAE at each location is less than 20% of the observed range, in accordance with the numerical calibration targets.

Table 7. Summary Calibration Statistics for Chlorophyll *a* Concentrations in the Photic Zone, 2003-2013, All Months

Metric	CCR1	CCR2	CCR3
Average Error	-2.9 ug/L	-3.3 ug/L	-1.8 ug/L
MAE	8.4 ug/L	9.1 ug/L	7.9 ug/L
RMSE	11 ug/L	12 ug/L	11 ug/L
MAE as % of Observed Range	16%	16%	13%
Goal	≤ 20%		

Simulated summer (July through September) average chlorophyll *a* concentrations are compared to observed concentrations in Figure 67. These show a good pattern and magnitude match for all simulated years. Summary calibration statistics for the summer average chlorophyll *a* concentrations are presented in Table 8. All error statistics are less than 4 ug/L for

the summer average prediction. Further, predictions for all individual years were within 5 ug/L of observed averages.

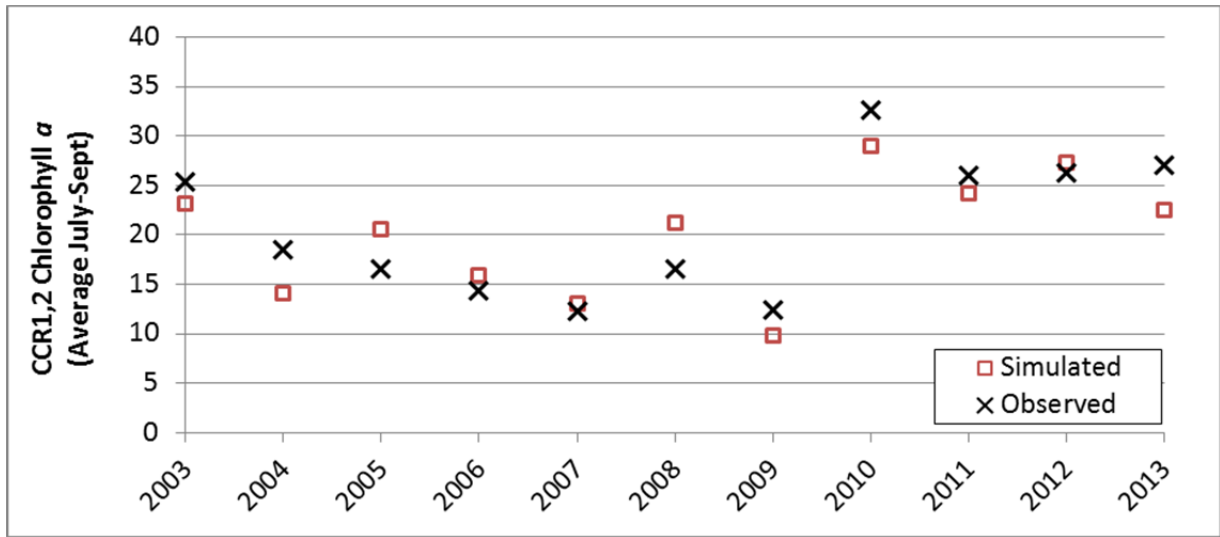


Figure 67. Simulated and Observed Summer Average Chlorophyll a Concentrations in the Photic Zone, 2003-2013, July – September, CCR1 and CCR2

Table 8. Summary Calibration Statistics for Summer Average Chlorophyll a Concentrations in the Photic Zone, 2003-2013, July – September, CCR1 and CCR2

Metric	Summer Average Chlorophyll a
Average Error	-0.7 ug/L
MAE	2.8 ug/L
RMSE	3.1 ug/L

Simulation of the timing of summer cyanobacteria blooms (nitrogen-fixing Algal Group 4) was also evaluated relative to observations. As shown in Figure 68, the model is performing well capturing the timing and relative magnitude of these blooms. Bloom peak timing is simulated to occur between the observations bracketing the observed peak. This provides confidence in the simulation of factors that lead to these blooms (water temperature and nitrogen limitation) as well as the setting of corresponding triggers for bloom development.

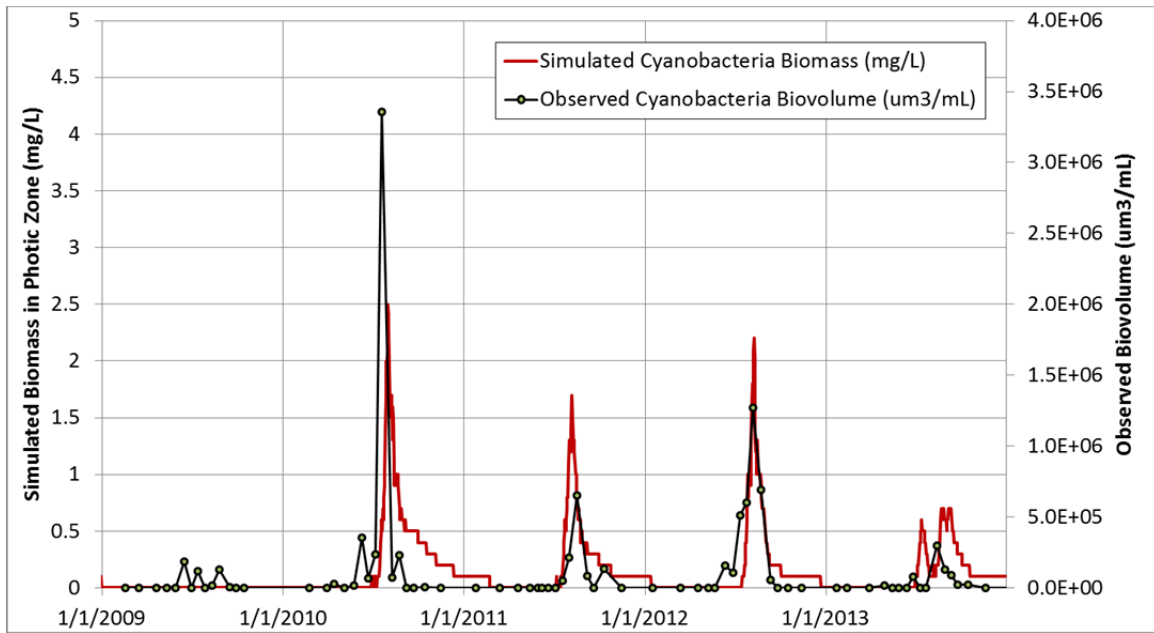


Figure 68. Comparison of Observed and Simulated Cyanobacteria Peak Timing, 2009-2013
(The data presentation is limited to 2009 through 2013 because data prior to 2009 did not include biovolume, and counts included picoplankton, which obscures bloom timing apparent in biovolume data.)

While not a specific calibration target, simulated zooplankton biomass was compared to observations (available starting in 2011) as a further simulation check. As noted in Section 2.5.6, zooplankton counts in the reservoir include species that are not representing the model, such as those that feed primarily on protozoa (the model represents those that feed primarily on algae [simulated zooplankton group 1] and those that feed primarily on other zooplankton (zooplankton group 2). Therefore, the model is expected to under-simulate total observed zooplankton biomass somewhat. Observed and simulated results were compared for general pattern matches and ranges to indicate whether the simulation was reasonable. As shown in Figure 69, the model performed well in simulating total zooplankton biomass, particularly in 2012 and 2013. The model under-simulates the higher values observed in 2011, which are notably higher than observations from 2012 through 2015 (Figure 35, Section 2.3.6). Overall, the general agreement between observed and simulated zooplankton biomass gives confidence that the role of zooplankton is being reasonably simulated.

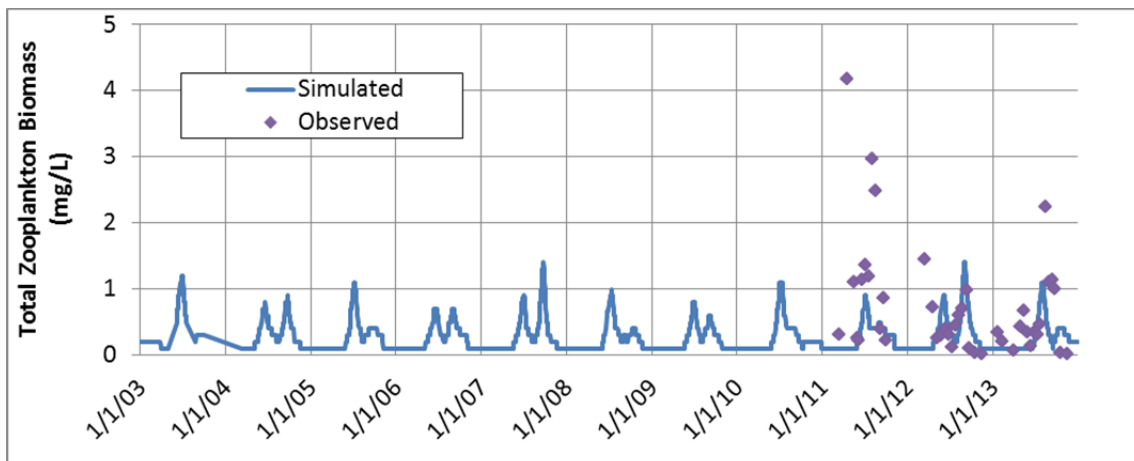


Figure 69. Comparison of Observed and Simulated Zooplankton Biomass

5 Sensitivity Analysis

A sensitivity analysis was conducted on the calibrated model. The following subsections describe the approach taken and results.

5.1 Approach

A sensitivity analysis tests the effects on simulation results of varying select settings or model inputs. Sensitivity analyses can help identify areas of greatest uncertainty and possibly direct additional data collection to reduce that uncertainty. The sensitivity analysis was generally scoped to include variation of five parameters, to be informed by the process of model development and calibration.

Through development of the calibrated model, numerous model runs were conducted, varying a wide range of settings relevant to the Cherry Creek Reservoir. Through this process, an understanding of the most sensitive model settings, in terms of summer chlorophyll *a* response, was developed. From that work, a relatively long list of sensitive settings was identified, including:

- Algal Settings for Groups 2 and 5 (growth rates, settling, temperature ranges, stoichiometry, light saturation intensity);
- Algal Settings for Groups 3 and 4 (growth rates, mortality, settling, temperature ranges, stoichiometry, half-saturation nitrogen, inorganic nitrogen and nitrogen-to-phosphorus ratio thresholds for nitrogen fixation, light saturation intensity);
- Sediment Burial and Decay Rates;
- SOD and Ammonia / PO4 Release Rates; and
- Particulate Organic Matter Settling Rates.

Also, through the calibration effort, areas of greater uncertainty and recommendations for additional data collection were identified (summarized in Section 7).

Therefore, much of a sensitivity analysis was completed through the calibration process. This was discussed at the June 22, 2015 meeting with the peer reviewer Dr. Wells, and appropriate additional model runs were proposed for the sensitivity analysis task. These model runs focus on understanding the relative roles of major forcing functions in the model, including wind, destratification system (called “aerators” in run names) mixing, internal loading, and nutrient loading from major tributaries. Some of these forcing functions can be managed, and some cannot (e.g., wind). As such, these do not represent realistic management scenarios, but they were defined to help support selection of management model runs. A total of seven model runs were performed, as listed in Table 9.

Table 9. Sensitivity Analysis Runs

Group	Run #	Run Description
Mixing	1	No Aerators
	2	Aerator Mixing x10
	3	No Wind
Inflow Nutrient Loading	4	Cherry Creek - Halve Concentration Nitrate, Ammonia, Orthophosphate
	5	Cottonwood Creek - Halve Concentration Nitrate, Ammonia, Orthophosphate
Internal Loading	6	Turn off 0-Order (Anaerobic) Sediment Processes
	7	Turn off 1 st -Order (Aerobic) Sediment Processes

5.2 Results

Model simulations were conducted and reviewed relative to the calibration simulation (termed *Baseline* in these comparisons). Results were assessed for temperature, nutrients, dissolved oxygen, and algal response. Graphical output of results is presented in Attachment D.

5.2.1 Destratification System Mixing Effects

The first set of sensitivity runs focused on extremes of destratification system mixing. As discussed in Sections 4 and 5, data and modeling indicate Cherry Creek destratification system operations have some small effects on temperature and dissolved oxygen concentrations at the bottom of the reservoir. Two destratification system runs were conducted:

- **No Aerators:** The aerator module (AERATEC) was turned off.
- **Aerator Mix x10:** The vertical mixing factor for the destratification system was increased to be ten times that simulated in the calibration run for the period 2008-2013. No change was made to the amount of oxygen loaded to the water column.

Review of water temperature results shows that destratification system mixing, through the range of no aerator mixing to ten times the current destratification-system mixing, has a relatively small effect on average daily water temperature at the surface of the reservoir. Increased mixing primarily serves to decrease the diurnal temperature range at the top of the reservoir and minimize peak temperature at times when brief periods of thermal stratification sets up in the baseline conditions, as shown in Figure 70 for 2009. This relatively limited effect of high levels of additional mixing on surface temperatures is indicative of the large amount of mixing that occurs under natural conditions due to wind.



Figure 70. Hourly Simulated Water Temperature at 1 m for Aerator Mixing Simulations, CCR2, 2009

There is more potential for effect of destratification system mixing on temperature at the bottom of the reservoir. As shown in the example for 2009 (Figure 71), increased destratification system mixing results in higher temperatures at the bottom of the reservoir. The effect at ten times the current level of mixing is to create continuous isothermal conditions from top to bottom in the reservoir while the aerators are operating (Figure 72). In the other direction, no mixing (No Aerators) results in greater top-to-bottom temperature differences, though only slightly greater when compare to the Baseline run including the current destratification system.

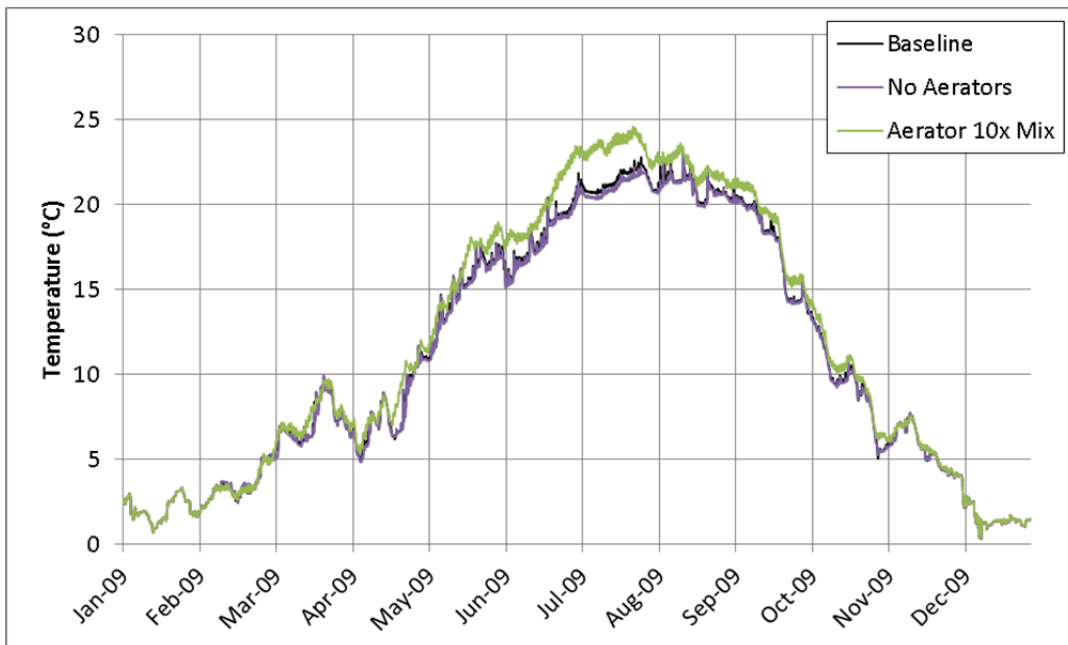


Figure 71. Hourly Simulated Water Temperature at the Bottom for Aerator Mixing Simulations, CCR2, 2009

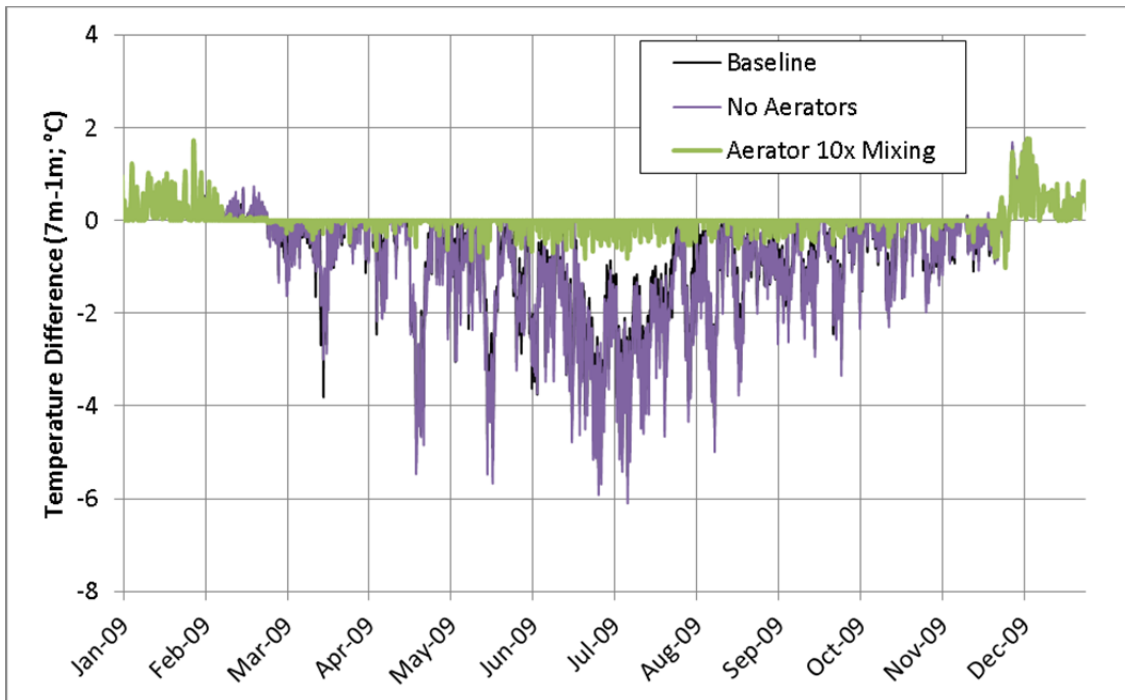


Figure 72. Hourly Simulated Difference in Water Temperature from 1 m to 7 m for Aerator Mixing Simulations, CCR2, 2009

Increased destratification system mixing results in circulation of more DO from the surface to the bottom of the reservoir. With the 10x mixing simulation, the model indicates that dissolved oxygen concentrations at the bottom of the reservoir can be maintained above ~5 mg/L in summer months (Figure 73). In contrast, the No Aerators simulation shows slightly lower DO concentrations at the bottom of the reservoir, relative to simulation of current conditions. Neither scenario results in large changes in DO at the top of reservoir.

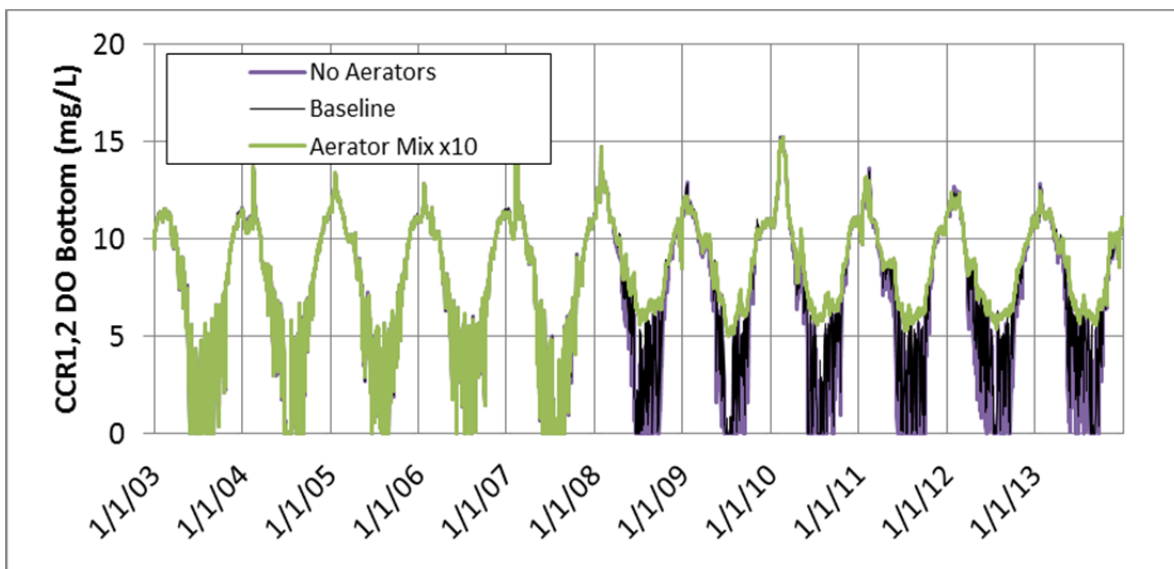


Figure 73. Simulated DO at the Bottom of the Reservoir (CCR1,2), Aerator Mixing Simulations, 2003-2013

The increased DO at the bottom with greater destratification system mixing results in decreased anaerobic loading of ammonia and PO₄. The decreases in loading are apparent in nutrient concentrations at the bottom relative to the No Aerator simulation (e.g., Figure 74). Note that these lower concentrations also reflect the additional mixing, further reducing buildup of nutrients at the bottom of the reservoir. Nutrient concentrations at the top of the reservoir show smaller changes, as compared to effects at the bottom. Remaining ammonia and PO₄ concentrations reflect loading from external inflow and aerobic internal loading.

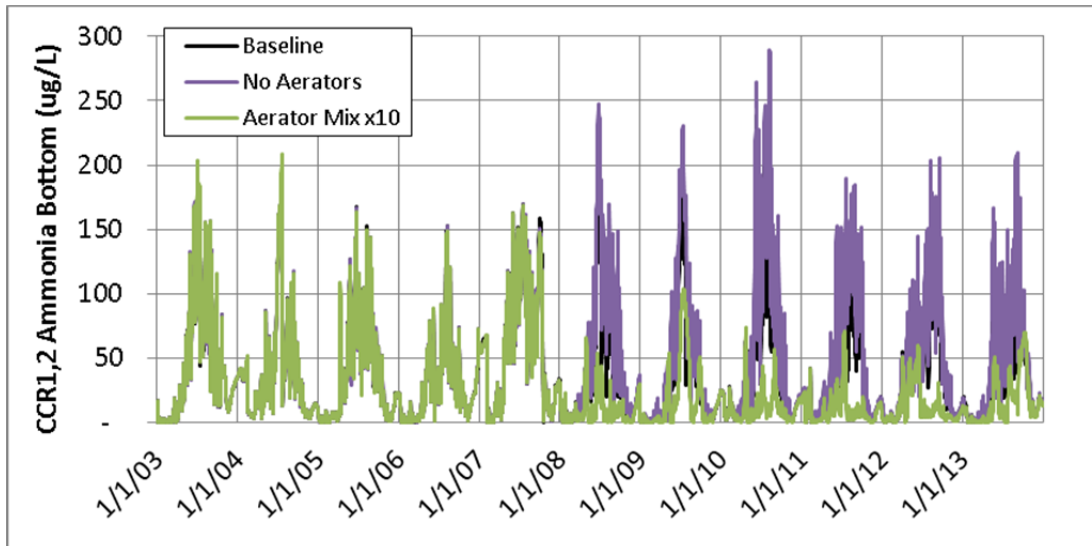


Figure 74. Simulated Total Ammonia at the Bottom of the Reservoir (CCR1,2), Aerator Mixing Simulations, 2003-2013

The resulting decrease in internal anaerobic nutrient loading associated with destratification system mixing results in a simulated decrease in chlorophyll *a* concentrations in the reservoir. Specifically, the simulation indicates that current destratification system operation reduced summer average chlorophyll *a* by an average of 2.7 ug/L from 2008-2013, ranging from less than 0.8 to 4.7 ug/L in individual years; though this result should be interpreted cautiously⁹.

The Aerator Mix x10 simulation, compared to No Aerator, results in an average decrease in simulated summer chlorophyll *a* of 10 ug/L, ranging from 5 to 16 ug/L. The simulation indicates,

⁹ The simulated magnitude of reductions in summer chlorophyll *a* concentrations relative to the No Aerator simulation should be interpreted cautiously. As noted in preceding discussions, the model does not simulate the apparent induced SOD effects of mixing (e.g., reducing the diffusive boundary layer). Depending on the magnitude of any induced SOD at the moderate mixing (Baseline) level, anaerobic loading may not be reduced to the extent simulated. As a result, actual reductions in chlorophyll *a* concentrations may be even less. This effect is not a concern for interpreting the Aerator Mix x10 simulation results, however, because the amount of mixing of DO from the top to the bottom for that simulation is expected to be adequate to compensate for any induced SOD.

however, that the reservoir would not have met the 18 ug/L chlorophyll *a* standard in each individual year (e.g., 2010), even with ten times the current amount of mixing from the destratification system.

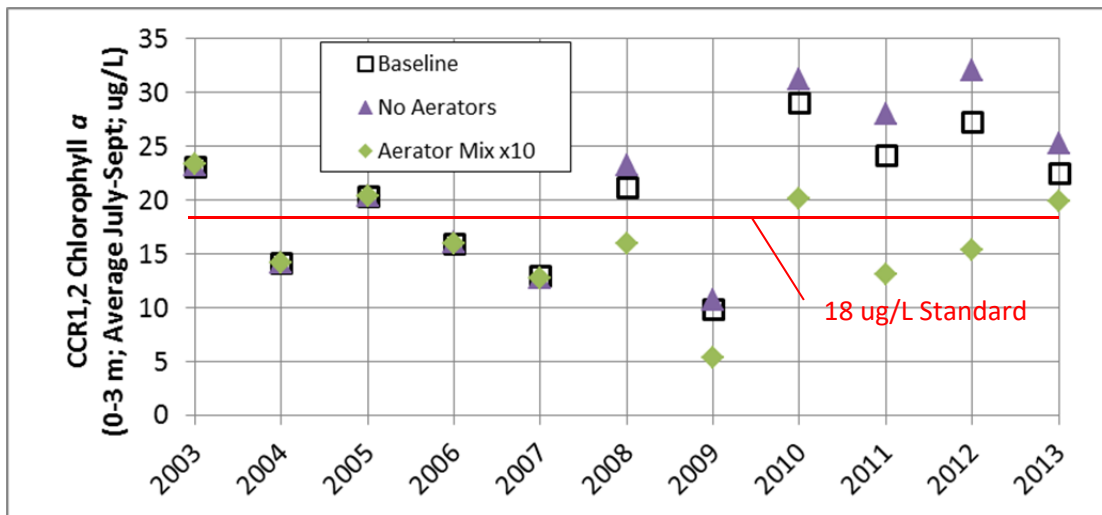


Figure 75. Simulated Average Summer (July-September) Chlorophyll *a* (CCR1,2), Aerator Mixing Simulations, 2003-2013

5.2.2 Wind Mixing Effects

The second set of sensitivity analysis runs focused on identifying the role of the wind in the water-quality response of Cherry Creek Reservoir. Through the calibration process, model sensitivity to wind was apparent, particularly on the thermal response, when different meteorological inputs were tested and when wind sheltering coefficients were tested. To evaluate the effects of wind, a model run was conducted setting the wind to zero to evaluate the role of wind on mixing (Run Name: No Wind). There are two key considerations to note about this zero wind simulation before reviewing results:

- Effect of No Wind on Aerator Simulation:** Because the destratification system must be defined in the model by a multiplier increasing vertical mixing, reducing wind to zero effectively also sharply reduces destratification system mixing (2008-2013). Therefore, destratification system mixing was also set to zero for this simulation. As such, results for 2008-2013 should be interpreted as the combined effects of no wind and no aerators. Therefore, the Baseline run for comparison to the No Wind simulation is the No Aerators simulation.
- Evaporative Volume Not Affected:** Setting wind to zero does not reduce evaporation losses in this simulation because of the way evaporation was input into the model (Section 4.2). Therefore, there are not changes to the water surface elevation to consider in the water-quality response. Changes to the heat-exchange effects of wind on evaporative cooling, however, are simulated.

Review of water temperature results shows that wind has a major effect on water temperature and mixing in Cherry Creek. The No Wind simulation exhibits much higher temperatures at the

surface (Figure 76) and much lower temperatures at the bottom (Figure 77), as compared to the Baseline simulation. In fact, in the absence of wind the reservoir consistently remains stratified throughout the summer (Figure 78). As a result, in the absence of wind, the reservoir behaves like a classic dimictic water body, with turnover occurring in the spring and fall.

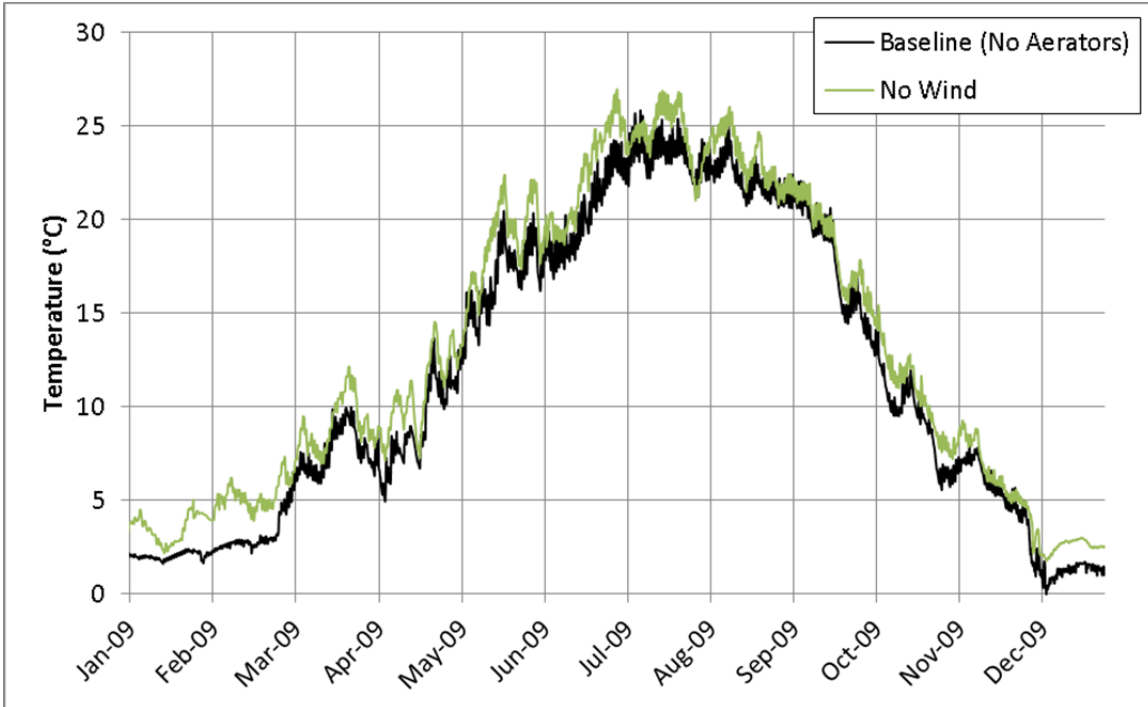


Figure 76. Hourly Simulated Water Temperature at 1 m for the No Wind and Baseline Simulations, CCR2, 2009

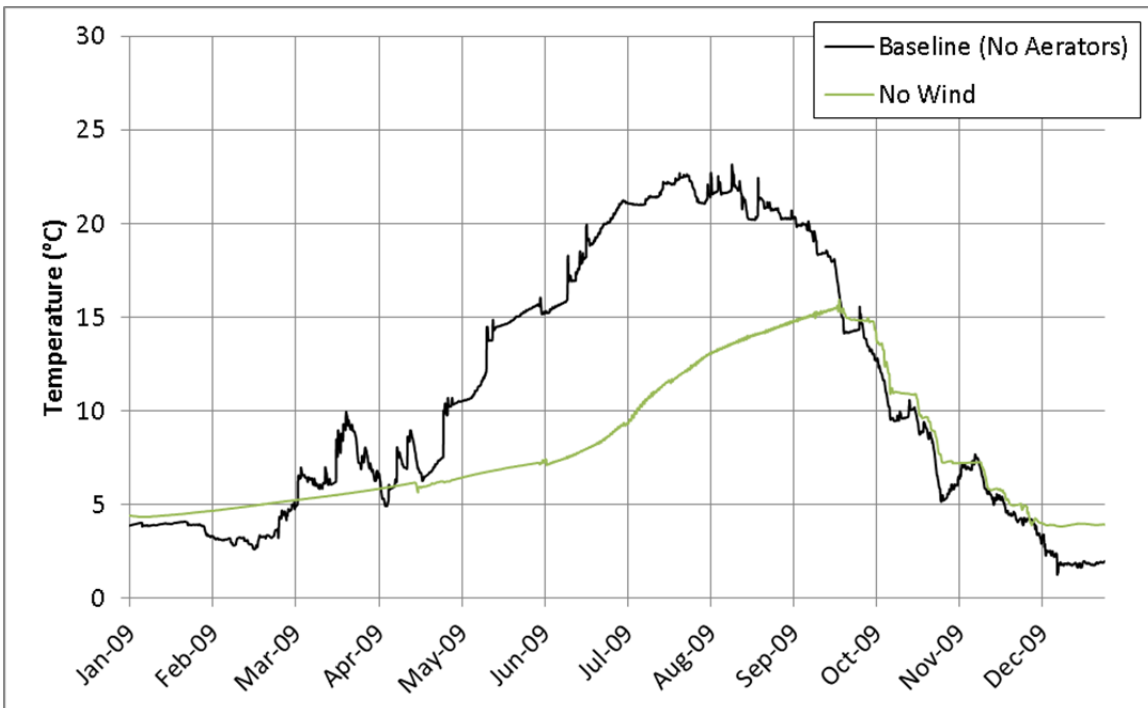


Figure 77. Hourly Simulated Water Temperature at the Bottom for No Wind and Baseline Simulations, CCR2, 2009

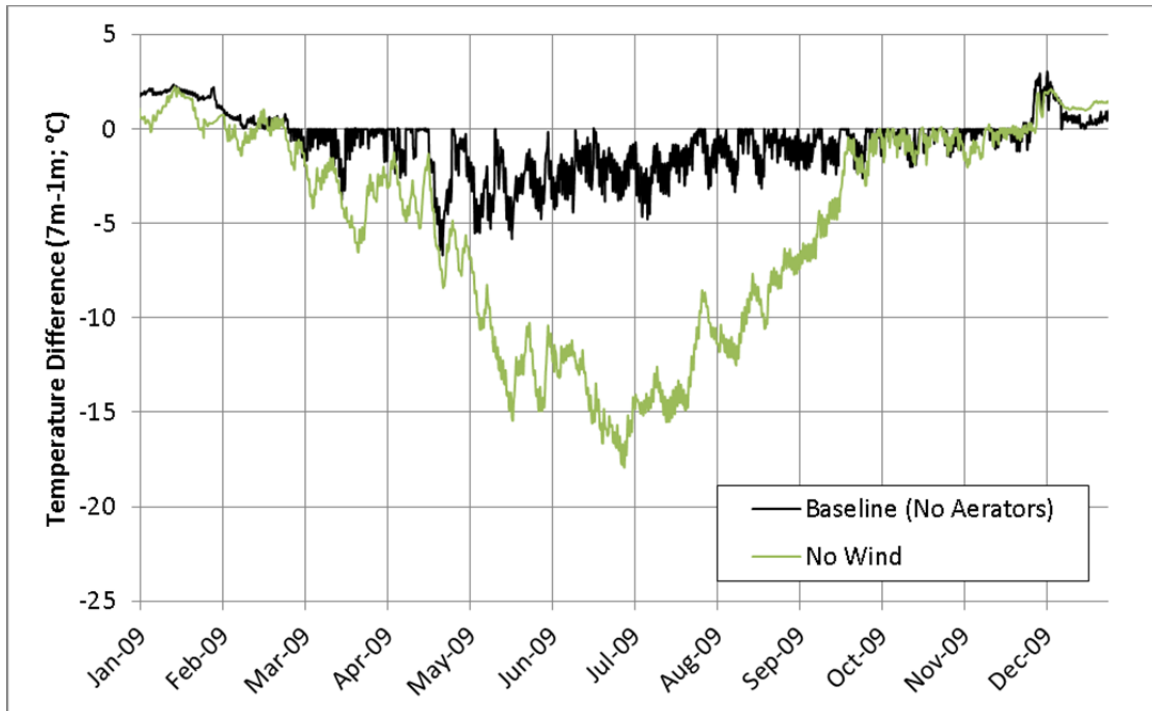


Figure 78. Hourly Simulated Difference in Water Temperature from 1 m to 7 m for No Wind and Baseline Simulations, CCR2, 2009

The stratification (in response to reduced mixing in the No Wind simulation) results in anaerobic conditions at the bottom of the reservoir throughout the summer (Figure 79). Further, dissolved oxygen concentrations are simulated to reach levels near or just below 5 mg/L at the top of the reservoir most years during fall turnover for the No Wind scenario.

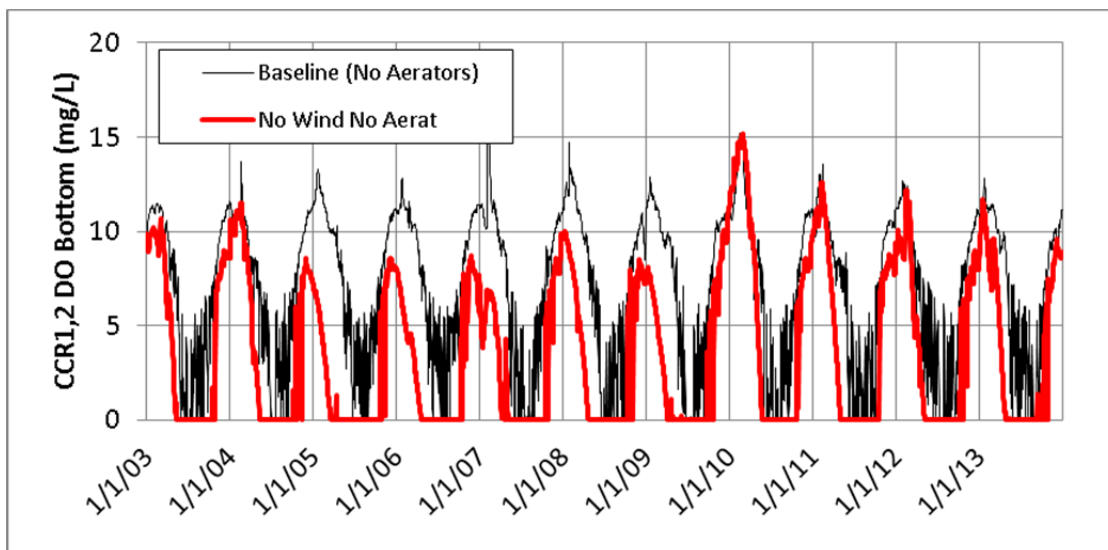


Figure 79. Simulated DO at the Bottom of the Reservoir (CCR1,2), No Wind and Baseline Simulations, 2003-2013

(No Wind Simulation Results Shown in Red to Make Pattern More Apparent)

As a result of these lower DO concentrations simulated at the bottom, the period of anaerobic nutrient loading of ammonia and PO₄ increases. The anaerobic release rate is somewhat lower due to cooler temperatures at the bottom; however, the net effect is an increase in nutrient release. Because there is reduced mixing from top to bottom for this No Wind simulation, nutrient concentrations build up at the bottom of the reservoir until fall turnover (Figure 80). Summer nutrient concentrations at the surface, exhibit smaller changes with no wind in most years.

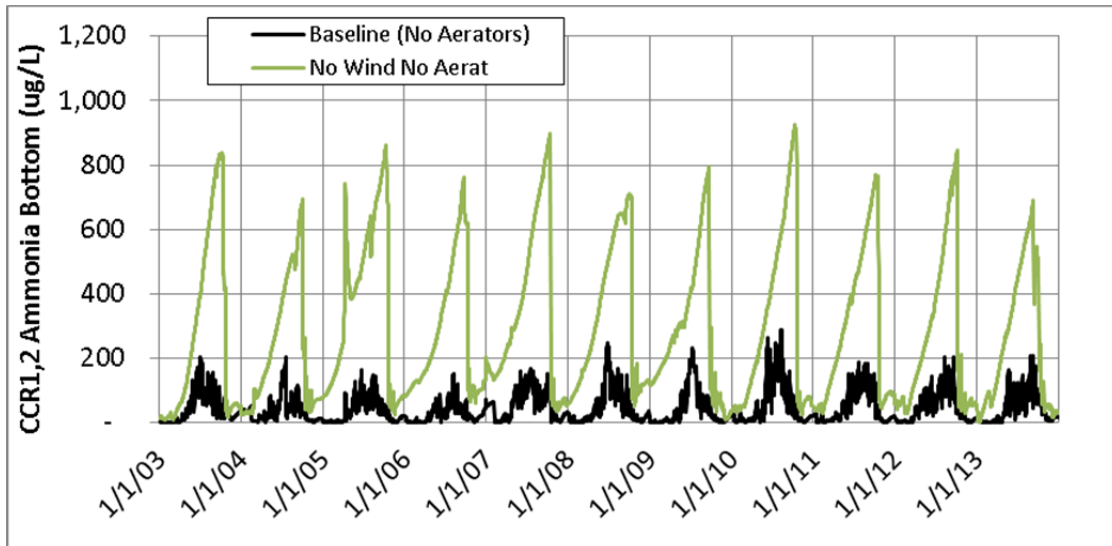


Figure 80. Simulated Ammonia Concentration at the Bottom of the Reservoir (CCR1,2), No Wind and Baseline Simulations, 2003-2013

While there is greater anaerobic nutrient release from sediments, there is also less mixing of nutrients from the bottom of the reservoir to the top through much of the summer. This results in a change in timing of algal blooms. Summer blooms still occur, particularly in response to mixing and loading caused by inflows; however, larger blooms occur in spring and fall (Figure 81). There is also some diffusive transport of nutrients from the bottom to the top in the No Wind scenario, driven by the high concentration gradient. Overall, the greater internal loading of the No Wind scenario results in higher average summer chlorophyll *a* in most years (Figure 81), though the timing of blooms in some years (e.g., 2008, 2010, and 2013) is shifted enough to result in slightly lower summer average chlorophyll *a*. The greatest effect of the no wind scenario on increased summer chlorophyll *a* was observed in 2007 and 2009. During these years, there was greater flow through the reservoir (see Figure 10 and Figure 11), resulting in more mixing. This allowed expression of more of the increased anaerobic internal load to the surface in the summer months in these years, resulting in increased algal growth.

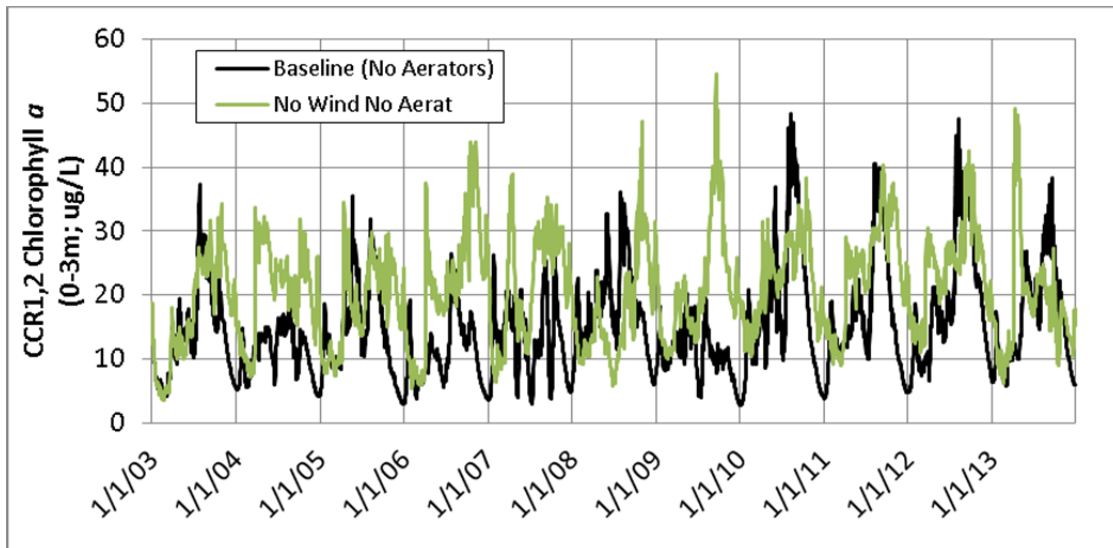


Figure 81. Simulated Chlorophyll α (CCR1,2), No Wind and Baseline Simulations, 2003-2013

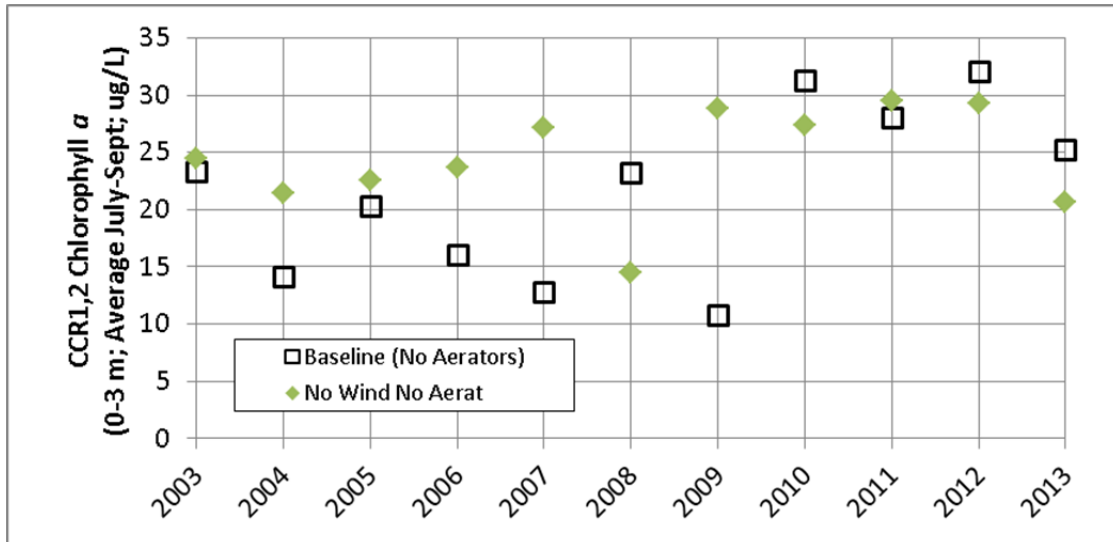


Figure 82. Simulated Average Summer (July-September) Chlorophyll α (CCR1,2), No Wind and Baseline Simulations, 2003-2013

Based on this, it is conceptually important to understand the relative role of wind on the reservoir. The wind is responsible for minimizing stratification and for mixing nutrients from the bottom to the top. The role of the wind is much greater than that of the current destratification system in terms of vertical mixing and brings oxygen to water at depth.

5.2.3 Inflow Nutrient Loading

The third set of sensitivity runs was designed to give an indication of the relative sensitivity of water-quality response to nutrient loading from the two major inflow tributaries, Cherry Creek and Cottonwood Creek. Two runs were performed and compared to the Baseline simulation:

- **Half Cherry Creek Load:** Inflow concentrations of ammonia, nitrate, and PO₄ were halved for inputs in this run.
- **Half Cottonwood Creek Load:** Inflow concentrations of ammonia, nitrate, and PO₄ were halved for inputs in this run.

As would be expected, given the larger relative magnitude of loading from Cherry Creek, particularly for PO₄, the water-quality effects of a 50 percent decrease in nutrient loading from Cherry Creek are generally greater than those for Cottonwood Creek. Decreased nutrient loading from Cherry Creek resulted in an overall decrease in reservoir productivity over the simulated period. As a result of decreased autochthonous organic matter to decay, simulated DO at the bottom of the reservoir was increased slightly above Baseline (Figure 83). Though it is difficult to see in the figure, halving nutrient loading from Cherry Creek resulted in an 8% decrease in the number of days with DO below 2 mg/L at the bottom of the reservoir. A similar effect was not apparent for the smaller net nutrient reductions for Cottonwood Creek. There were no significant changes to temperature or dissolved oxygen at the top of the reservoir in response to either of these sensitivity runs.

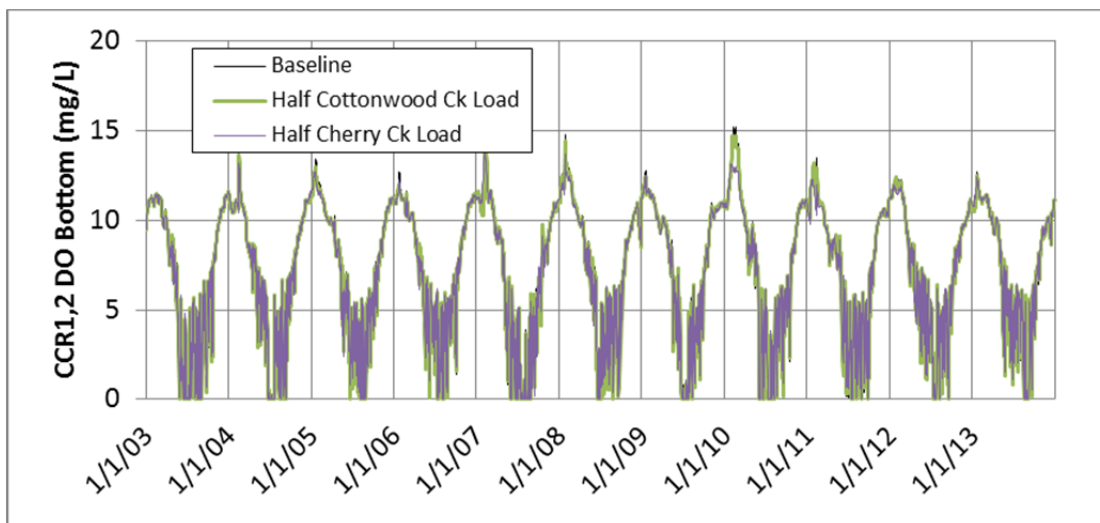


Figure 83. Simulated DO at the Bottom of the Reservoir (CCR1,2), Half Tributary Nutrient Loading and Baseline Simulations, 2003-2013

Nutrient concentrations simulated at the top of the reservoir decreased somewhat with the decreased inflow load, with the greatest effects apparent in PO₄ for halving the loading from Cherry Creek (Figure 84). Greater effects were apparent in years with greater inflow volumes (i.e., 2007, 2009, and 2013). Similar decreases were observed at the bottom of the reservoir. This effect on PO₄ concentrations throughout the water column indicates the significance of inflow tributary loading to PO₄ concentrations observed in the reservoir in some years.

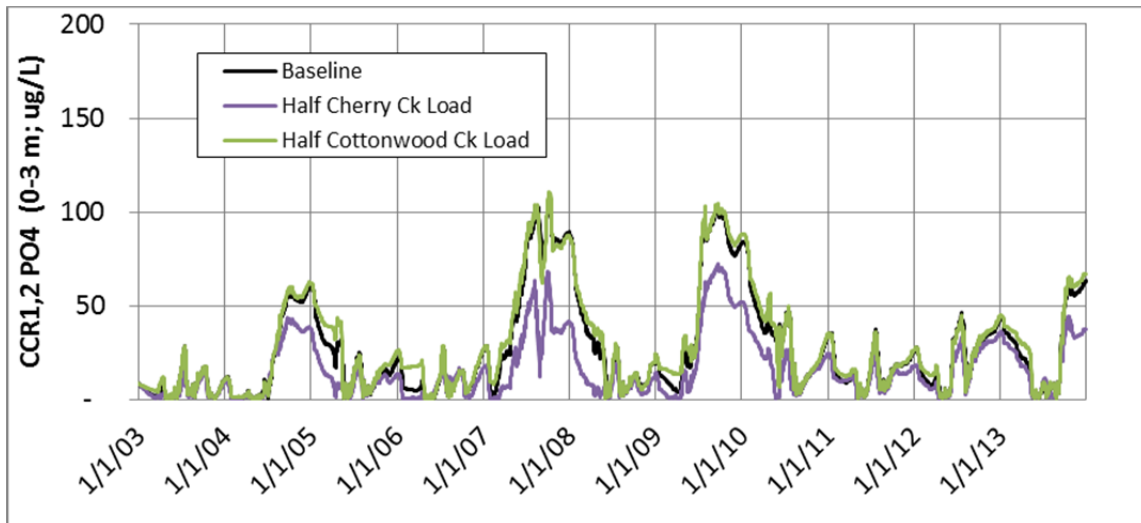


Figure 84. Simulated PO4 at the Top (0-3 m) of the Reservoir (CCR1,2), Half Tributary Nutrient Loading and Baseline Simulations, 2003-2013

The algal response halving of nutrient loading from Cherry Creek is greater (Figure 85), as would be expected. Reducing the nutrient loading from Cherry Creek by one-half decreased average summer chlorophyll *a* by an average of 3.2 ug/L, with a maximum effect of 10 ug/L in 2010. In the recent four years, including 2010, the model predicts that the chlorophyll *a* standard would not have been met.

One thing not reflected in these modeling results is a possible long-term change in the anaerobic PO4 loading rate from the sediments after years of lower inflow PO4 concentrations. If this occurred, the algal concentrations would be expected to be even lower than simulated over the long term, possibly producing algal concentrations below the standard for this 50% inflow loading reduction scenario.

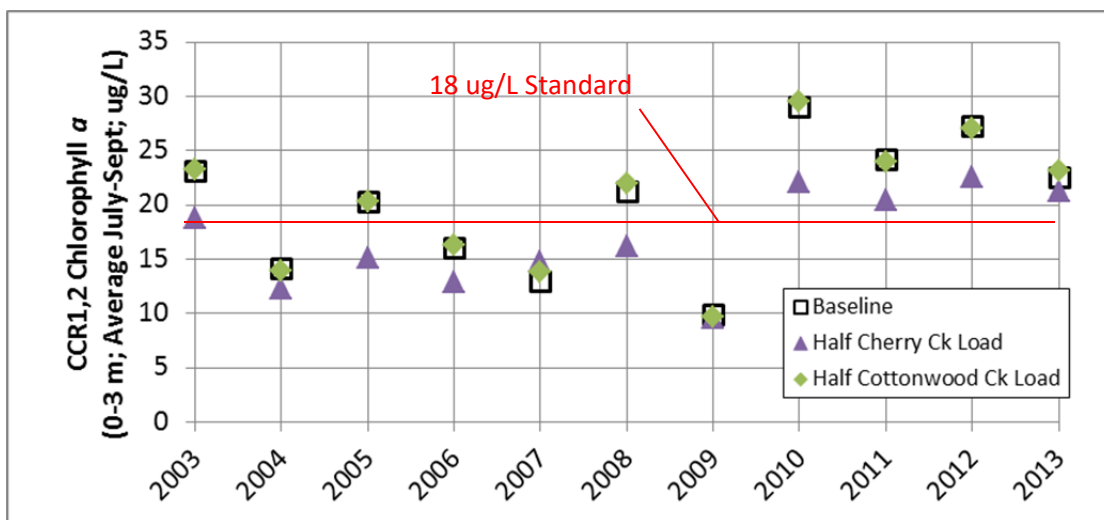


Figure 85. Simulated Average Summer (July-September) Chlorophyll *a* (CCR1,2), Half Tributary Nutrient Loading and Baseline Simulations, 2003-2013

Interestingly, halving the nutrient load from Cottonwood Creek resulted in small (<1 ug/L) simulated increases in chlorophyll *a* in many of the simulation years. In the modeling, this is the result of reducing the nitrate and ammonia loading from Cottonwood Creek, which has historically exhibited higher concentrations of these nutrients, relative to Cherry Creek. This decrease in nitrogen nutrient loading, without a larger decrease in phosphorus loading (PO₄ concentrations in Cottonwood Creek tend to be much lower than in Cherry Creek), resulted in simulation of a small increase in nitrogen-fixing algae, and a subsequent overall increase in summer chlorophyll *a*. This response reflects the strongly nitrogen-limited nature of the reservoir. Based on this and the patterns described in Section 3.5 indicating higher TIN:PO₄ inflow ratios from 2004-2009, it is recommended to consider the role of the inflow TIN:PO₄ ratio as part of future management planning. Specifically, major reductions in nitrogen loading without corresponding reductions in phosphorus loading could have unintended consequences, encouraging additional nitrogen-fixing cyanobacteria.

These results may be useful in evaluating the potential benefits of realistic watershed nutrient reduction targets relative to the site-specific chlorophyll *a* standard. Very large reductions in inflow nutrients may be needed to consistently meet the current chlorophyll *a* standard in this shallow, polymictic, productive reservoir.

5.2.4 Internal Loading and SOD

As noted in Section 4.4, internal loading of nutrients from the sediments to the water column consists of aerobic internal loading (1st-order sediment loading) and anaerobic internal loading (0-order sediment loading). Through calibration and review of model flux output, both are expected to be important in Cherry Creek Reservoir. This makes conceptual sense because, while SOD is high and dissolved oxygen conditions become hypoxic/anoxic at times in the summer months, there are also oxic periods at the bottom due to intermittent mixing events. In more strongly stratified reservoirs, the aerobic processes at the sediment-water interface can be less important through summer months if DO is consistently depleted at the bottom.

Two sensitivity analysis simulations were conducted to learn more about the roles of these processes in water-quality response in the calibrated model:

- **No Aerobic Internal Load:** The 1st-order sediment module in W2 was turned off.
- **No Anaerobic Internal Load:** The 0-order sediment module was turned off. This was done by setting the SOD value to zero. As a result anaerobic release of ammonia and PO₄ was eliminated, and the temperature-based anaerobic oxygen demand was also stopped.

Both aerobic and anaerobic sediment decay processes consume oxygen. Turning off the anaerobic internal loading resulted in a much greater increase in DO at the bottom of the reservoir. Figure 86 shows that in the absence of the anaerobic sediment effects, summer DO concentrations at the bottom would remain above 4.5 mg/L. In the absence of the aerobic sediment effects, the number of days per year with DO less than 2 mg/L would decrease relative to the baseline by 13%. This indicates that oxygen depletion at the bottom of the reservoir is

greater due to sediment oxygen demand simulated by the 0-order module, though aerobic processes are not insignificant.

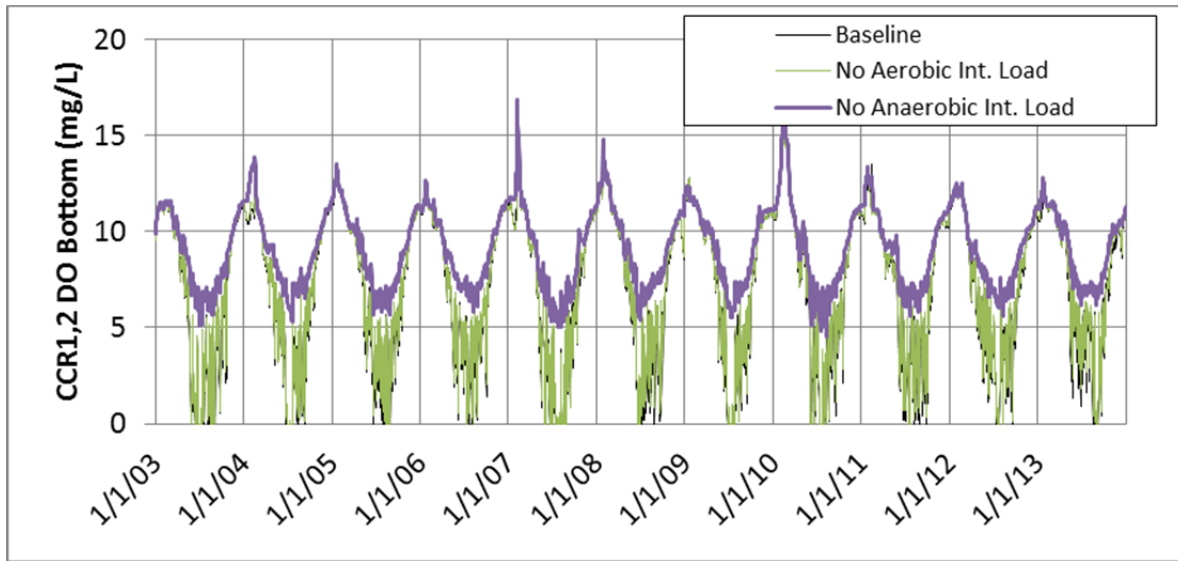


Figure 86. Simulated DO at the Bottom of the Reservoir (CCR1,2), Aerobic and Anaerobic Internal Loading and Baseline Simulations, 2003-2013

Reduced internal loading of nutrients is apparent for both of these sensitivity runs; however the effect is greater for the No Anaerobic Internal Load simulation (Figure 88 and Figure 88). It should be noted that in the event of greater oxygen at the bottom of the reservoir in summer months, greater nutrient loading from aerobic decay processes at the sediment-water interface would be expected. Currently, however, anaerobic processes dominate the dissolved oxygen and nutrient release effects.

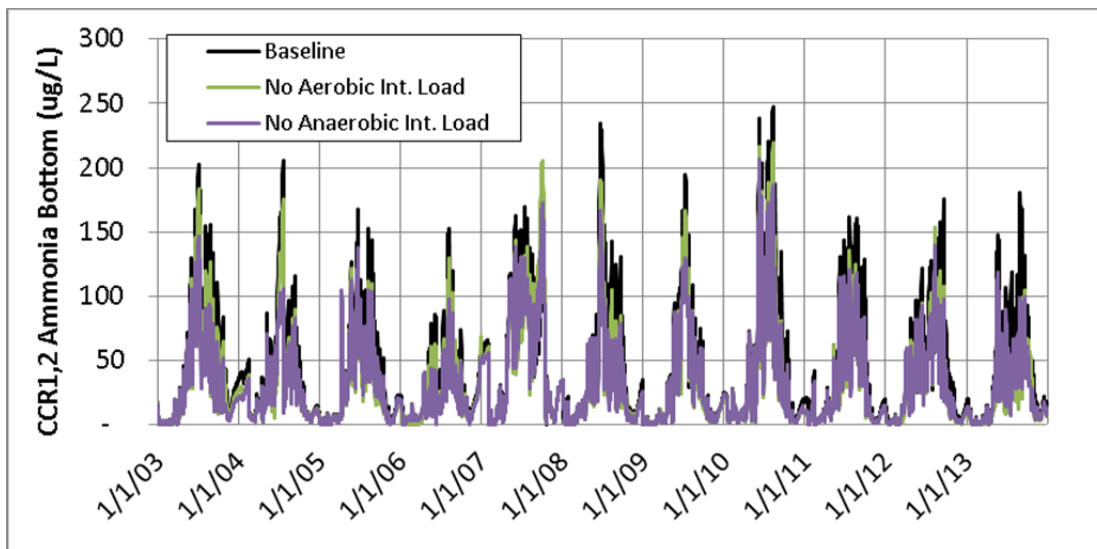


Figure 87. Simulated Ammonia at the Bottom of the Reservoir (CCR1,2), Excluding Aerobic and Anaerobic Internal Loading and Baseline Simulations, 2003-2013

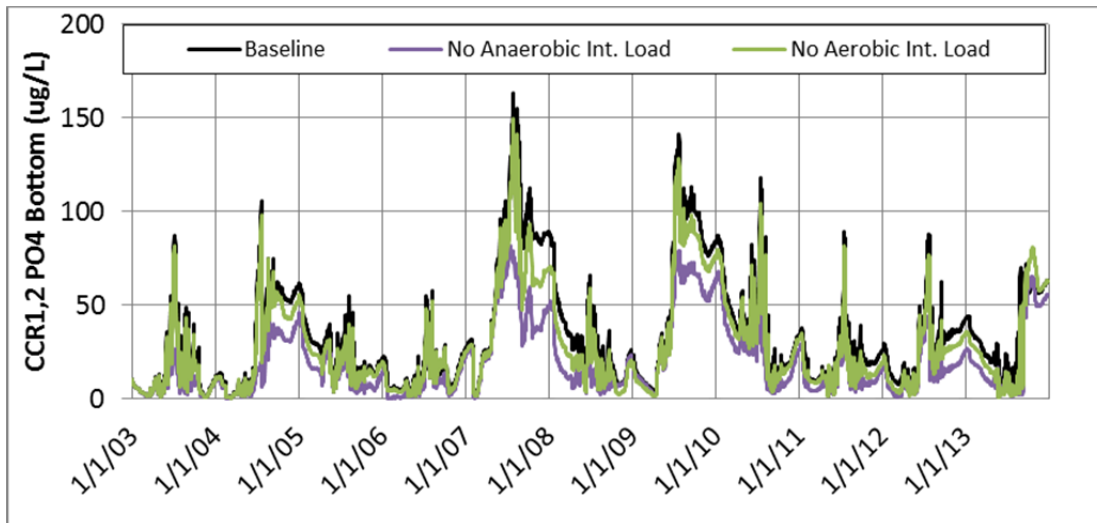


Figure 88. Simulated Orthophosphate at the Bottom of the Reservoir (CCR1,2), Excluding Aerobic and Anaerobic Internal Loading and Baseline Simulations, 2003-2013

In response to the lower nutrient concentrations at the surface of the reservoir for these reduced internal loading simulations, reduced algal growth was also simulated. Summer algal concentrations decreased in response to both reduced internal loading simulations, but the greater effect was simulated for removing anaerobic effects (Figure 89). The effects of reduced internal loading on chlorophyll *a* were less in years more dominated by inflow loading (e.g., 2007¹⁰ and 2009).

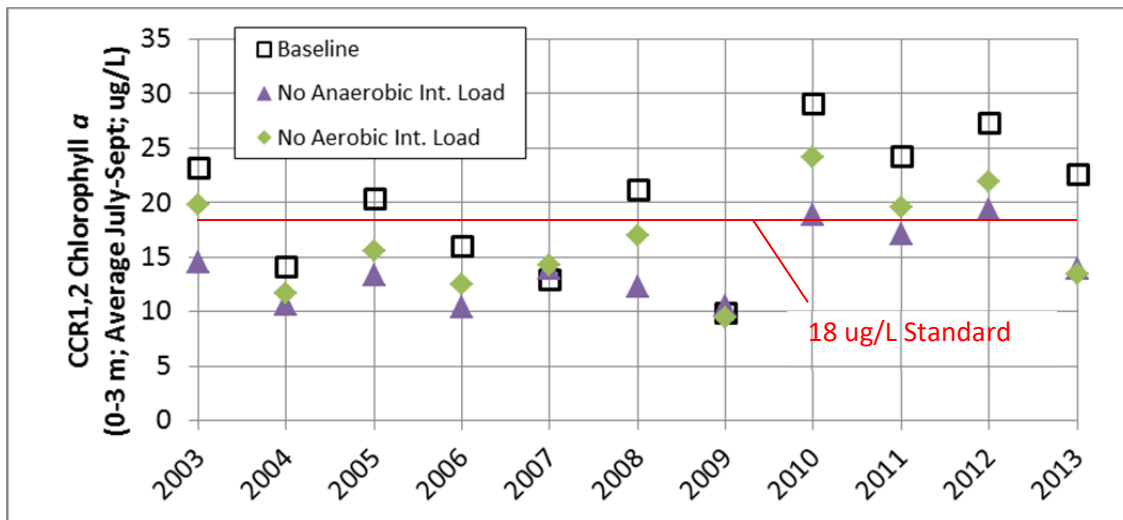


Figure 89. Simulated Average Summer (July-September) Chlorophyll a (CCR1,2), Aerobic and Anaerobic Internal Loading and Baseline Simulations, 2003-2013

¹⁰ In 2007, reductions in internal loading also affected the timing of cyanobacteria blooms by generating an earlier condition of depleted inorganic nitrogen at the surface. The net result was a small (<1 ug/L) increase in the summer average chlorophyll *a*.

In the absence of the anaerobic internal loading, the simulation indicates that the reservoir would meet the site-specific standard in most years, but some years would be very close (e.g., 2010 and 2012; Figure 89). This finding is important because the destratification system is designed to address anaerobic loading. In the event that the destratification system was re-engineered to achieve adequate mixing to keep sediment aerobic, there may still be occasional years with average summer chlorophyll *a* concentrations greater than 18 ug/L. This finding agrees with the results of the 10x Aerator Mixing simulation discussed in Section 6.2.1.

6 Management Runs

Following completion of calibration and the sensitivity analysis, the Authority held a meeting on September 22, 2016 to identify specific model runs to support future management planning. During this meeting, findings from model development and sensitivity runs were considered in light of water-quality goals for the reservoir. From that meeting, five model runs were identified. The runs include adjustments to 1) inflow nutrient concentrations, 2) destratification system mixing effectiveness, and 3) inflow nutrient nitrogen-to-phosphorus ratios (Table 10).

Table 10. Management Runs

Run #	Run Description	Question Addressed
1	Best Anticipated Watershed Control of Nutrients	How would the reservoir respond to the best currently-anticipated reduction of nutrients (nitrate [NO ₃], ammonia [NH ₄], and orthophosphate [PO ₄]) through watershed controls?
2	Increased Destratification System Mixing	How much increased vertical mixing is needed for the destratification system to meet the original bottom DO design target of 5 mg/L?
3	Best Watershed Controls Plus Increased Destratification	How would the reservoir respond to a combination of the best anticipated watershed controls and destratification mixing that achieves 5 mg/L DO at the bottom?
4	Inflow PO ₄ % Reduction to Meet Chlorophyll Standard	What percent reduction in inflow PO ₄ concentration is needed to meet the 18 ug/L chlorophyll <i>a</i> standard value for all simulated years?
5	Nitrogen-to-Phosphorus Ratio	Does the model indicate an adverse effect of increased cyanobacteria in response to disproportionate reduction of inflow nitrogen (NO ₃ and NH ₄) relative to PO ₄ in this nitrogen-limited system?

Inflow nutrient concentration assumptions for Cherry Creek and Cottonwood Creek were developed by Leonard Rice Engineers (LRE, 2016) for 2003 through 2013, for use in Runs 1, 3, and 5. The assumed average annual nutrient loads for Cherry Creek and Cottonwood Creek are summarized in Figure 90 and Figure 91, respectively. The daily concentrations developed by LRE for inputs are plotted in Attachment F.

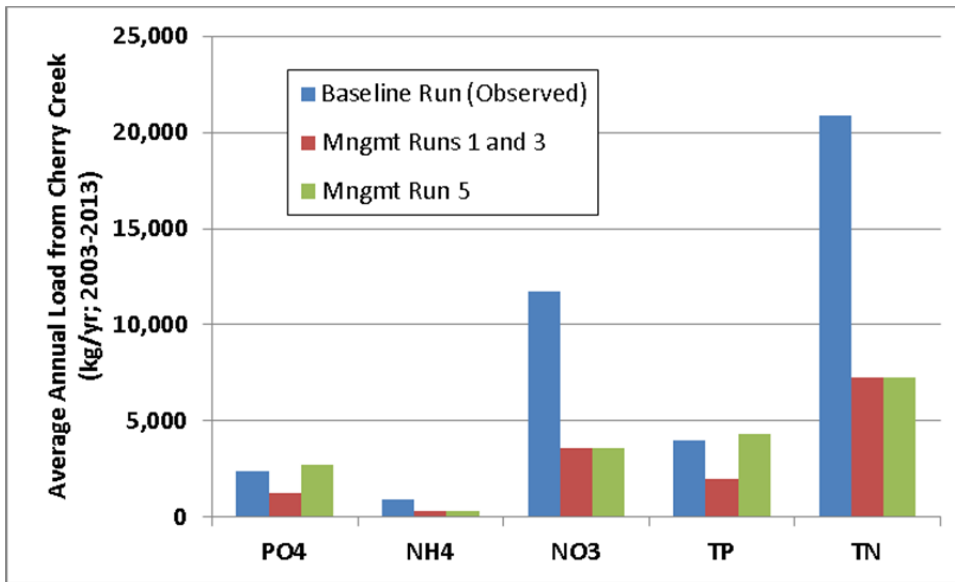


Figure 90. Comparison of Average Annual Cherry Creek Nutrient Loads for Management Runs 1, 3, and 5 (Model Runs Involving Provided Watershed Control Estimates)

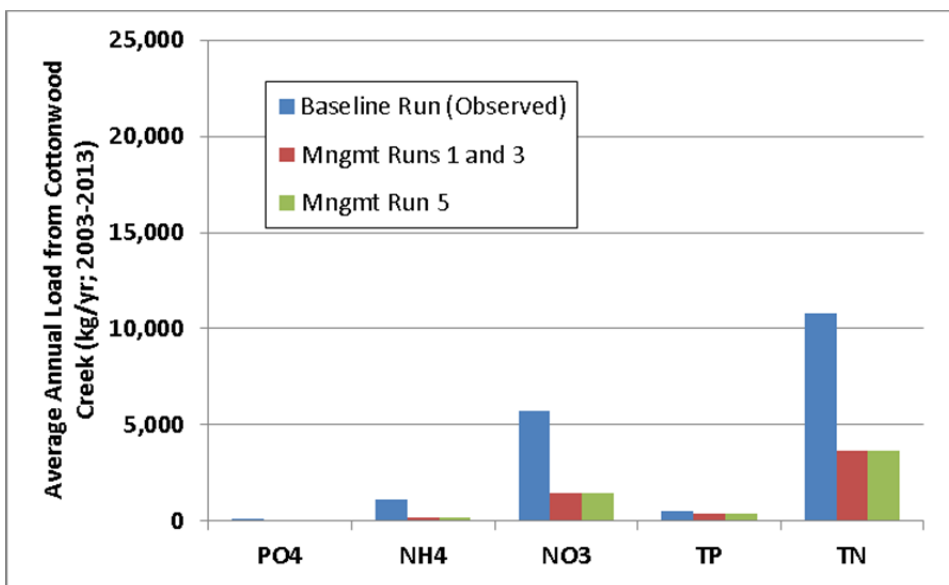


Figure 91. Comparison of Average Annual Cottonwood Creek Nutrient Loads for Management Runs 1, 3, and 5 (Shown at same vertical scale as Cherry Creek, Figure 1, to support comparison)

Each management run was simulated for the full eleven-year calibration period (2003-2013) to cover a range of hydrologic and meteorological conditions. For each run, model results were summarized for average summer (July-September) chlorophyll *a*, dissolved oxygen, and the simulated frequency and magnitude of summer cyanobacteria blooms. The following subsections present the setup and results of each run.

6.1 Run 1 – Best Anticipated Watershed Control of Nutrients

The Authority is interested in understanding how effective best-case-scenario reductions in inflowing nutrients could be for controlling summer chlorophyll *a* in Cherry Creek Reservoir. To

test this, LRE developed estimated inflow concentrations for 2003 through 2013 assuming the most effective available watershed controls were in place for both Cottonwood Creek and Cherry Creek (LRE, 2016). These inflow concentrations suggest that large reductions in both phosphorus and nitrogen can be achieved in Cherry Creek (load reductions of 48% for PO₄, 70% for NO₃, and 64% for NH₄; Figure 90), and large percent reductions in nitrogen can be achieved in Cottonwood Creek (average load reduction of 75% for NO₃ and 82% for NH₄; Figure 91).

To complete the run, the model was setup to simulate reservoir water-quality response to these estimated best-case inflow nutrient concentrations. All other model settings and inputs from the calibration run were unchanged for the simulation, with one exception. In the calibrated model, an increased organic matter load to the sediment was applied to reflect effects following the fish kill in August of 2012 (described in Section 3.6). Based on test runs and review of oxygen concentrations, it was assumed that the fish kill of August 2012 would not have occurred for this management run. Therefore, for Run 1 as presented here, no increased organic matter load to the sediment was applied in August of 2012.

Model results indicate that the assumed major reductions in inflow nutrient concentrations would decrease July through September chlorophyll *a* concentrations by an average of 6.4 ug/L over the simulated years. Further, the model indicates that the average summer chlorophyll *a* concentrations would be at or below the site-specific standard value of 18 ug/L in all of these years (Figure 92). Lower summer cyanobacteria peak concentrations are also predicted (Figure 93).

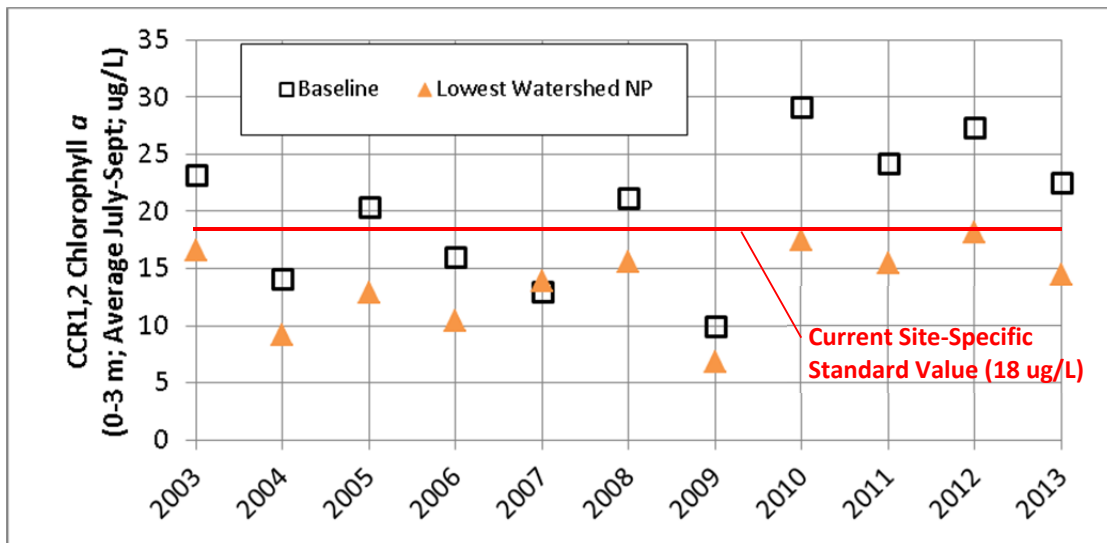


Figure 92. Simulated Average July-September Chlorophyll *a* – Maximum Watershed Controls on Nutrients (NP) (Baseline and Hypothetical Best-Case Reduced Inflow Nutrient Concentrations)

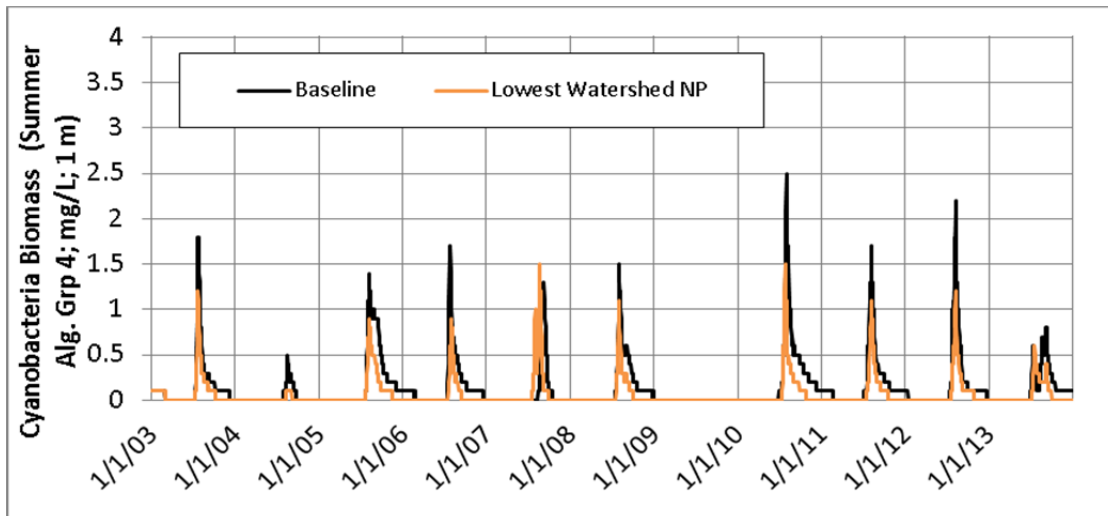


Figure 93. Simulated Average Summer Cyanobacteria Biomass – Maximum Watershed Controls (*Baseline and Hypothetical Best-Case Reduced Inflow Nutrient Concentrations*)

Based on model calibration over a wide range of conditions, these results are expected to be reasonable predictions of water-quality response in the reservoir to the simulated changes in inflow concentrations. However, cautious interpretation of this and all of the management run model results requires recognition of a two key simplifications in these simulations:

- First, changes in inflow water quality included only nutrient concentrations and did not include changes in inflow suspended solids, organic matter, or other constituents that would likely also be affected by assumed watershed management practices. Such additional changes are expected to be captured by watershed modeling for use in future reservoir model runs.
- Second, it is reasonable to expect that, with drastic reductions in inflow nutrients and in-reservoir algal growth, sediment oxygen demand and internal loading would decrease to some extent over time. This effect is reflected in the aerobic sediment decay in the simulations, but cannot be reflected in the anaerobic sediment decay, the behavior of which is set through calibration. As a result, in the long-term, predictions of algal growth might be even lower than those simulated in this run. If simulation of long-term sediment behavior is desired for long-term response refinement, the sediment diagenesis modeling capabilities within CE-QUAL-W2 could be utilized.

6.2 Run 2 – Increased Destratification System Mixing

Through data analysis and model development, it was concluded that the destratification system for Cherry Creek reservoir was under-designed to meet its objectives for oxygen concentrations at the bottom. The goal of this management run is estimate how much the vertical mixing by the destratification system would need to be increased to meet the original design target of 5 mg/L DO at the bottom of the reservoir. This result can be used to provide perspective on the relative magnitude of increased mixing needed by the destratification system, which may be helpful in consideration of whether system enlargement could reasonably be pursued. However, due to the nature of the destratification-system simulation module in CE-

QUAL-W2¹¹, this result is not a direct estimate of the energy or compressor needs for an increased system. If a new or modified destratification system was of interest to increase vertical mixing, a separate engineering study would be needed to properly design the system.

To determine the relative increase in vertical destratification mixing needed to reach 5 mg/L DO at the bottom, a series of model runs was conducted. The destratification mixing factor was increased progressively in each run until the chlorophyll *a* target was met in all years. Additionally, destratification system operation was assumed to occur in all simulation years from 2003-2013, not just in the actual operation years of 2008-2013. This assumption provided a larger number of years over which to evaluate the effects of increased mixing on DO at the bottom. For 2003 through 2007, the destratification system was assumed to operate continuously from March 1 through October 31, approximating the actual seasonal operation patterns from 2008 through 2013. Finally, the calibrated model adjustment applying increased organic matter to the sediment following the fish kill in August of 2012 (described in Section 3.6) was removed for these runs, recognizing that the fish kill would likely not have happened at these higher DO levels.

Model results indicate that a destratification system with three times the vertical mixing effect of the current destratification system would result in at least 5 mg/L of DO at the bottom of the reservoir at nearly all times from 2003 through 2013 (Figure 94). The model also simulates a corresponding decrease in average summer chlorophyll *a* in all years, though the value is still above the current site-specific standard value in the 2010 (Figure 95). Finally, a decrease in the summer cyanobacteria bloom frequency and magnitude is simulated to occur with such an increase in vertical mixing (Figure 96).

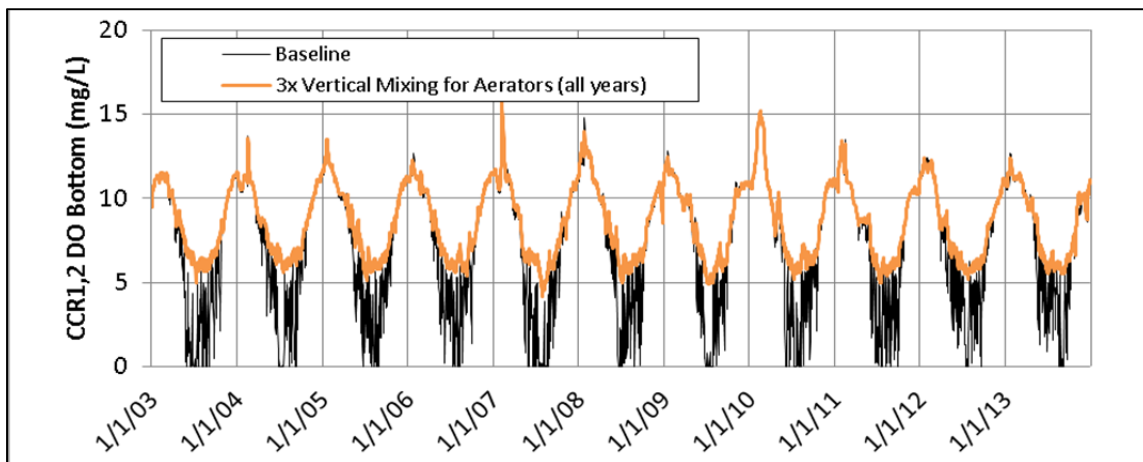


Figure 94. Simulated Dissolved Oxygen Concentrations at the Bottom at CCR1,2 – Destratification Run (Baseline [Existing Destratification Operation] and Hypothetical

¹¹ In the model, vertical mixing by the destratification system is simulated as a multiplier (DZFACT) on vertical mixing in the depth interval above the aerator heads. This module (AERATEC) in the model does not simulate bubble plume dynamics and cannot be directly translated to energy/compressor needs.

De-stratification System with Three Times the Vertical Mixing of the Current System - Applied to All Years)

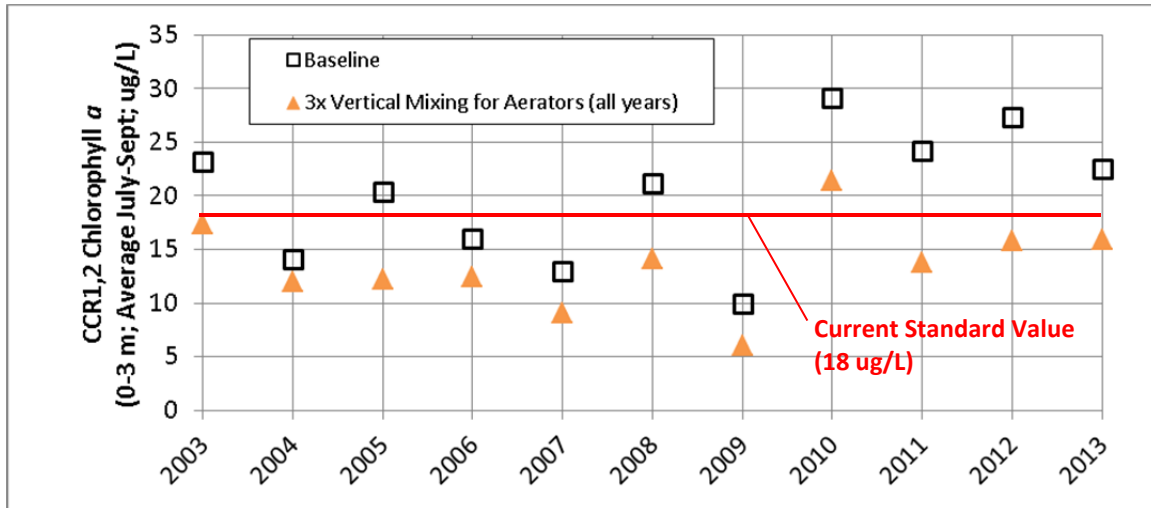


Figure 95. Simulated Average July-September Chlorophyll a – De-stratification Optimization Run (Baseline [Existing De-stratification Operation] and Hypothetical De-stratification System with Three Times the Vertical Mixing of the Current System - Applied to All Years)

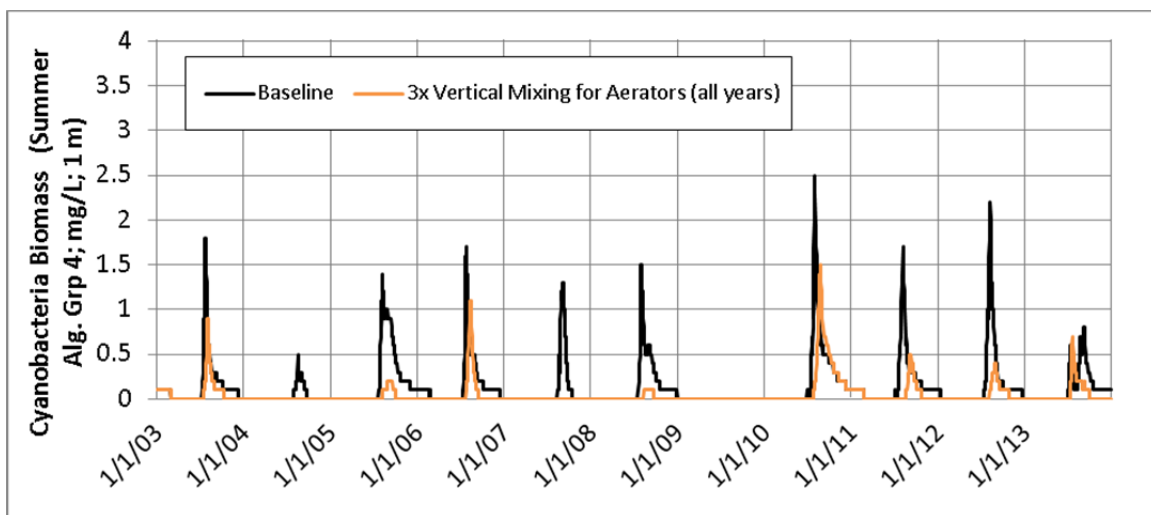


Figure 96. Simulated Average Summer Cyanobacteria Biomass – De-stratification Optimization Run (Baseline [Existing De-stratification Operation] and Hypothetical De-stratification System with Three Times the Vertical Mixing of the Current System - Applied to All Years)

6.3 Run 3 – Increased De-stratification System Mixing and Best Anticipated Watershed Control of Nutrients

To determine how chlorophyll *a* in the reservoir would respond to the combination of the best anticipated watershed controls (Run 1) and de-stratification mixing that achieves 5 mg/L DO at the bottom (Run 2), Run 3 was conducted. This run combined model adjustments described for Run 1 (LRE-provided best-case inflow nutrient concentrations) and Run 2 (de-stratification system mixing tripled relative to the current system and applied to all simulation years).

As would be expected, Run 3 results predict that simulated average summer chlorophyll *a* concentrations would be lower than those of both Run 1 and Run 2. Simulated July through September chlorophyll *a* exhibited an average decrease of 9.4 ug/L over the simulation period, resulting in summer averages at least 4.8 ug/L below the site-specific standard value in all years (Figure 97). Peak summer cyanobacteria concentrations were also sharply reduced (Figure 98). As with Runs 1 and 2, these results assume that three times the current vertical mixing and the assumed best-case reduction in inflow nutrient concentrations can reasonably be achieved.

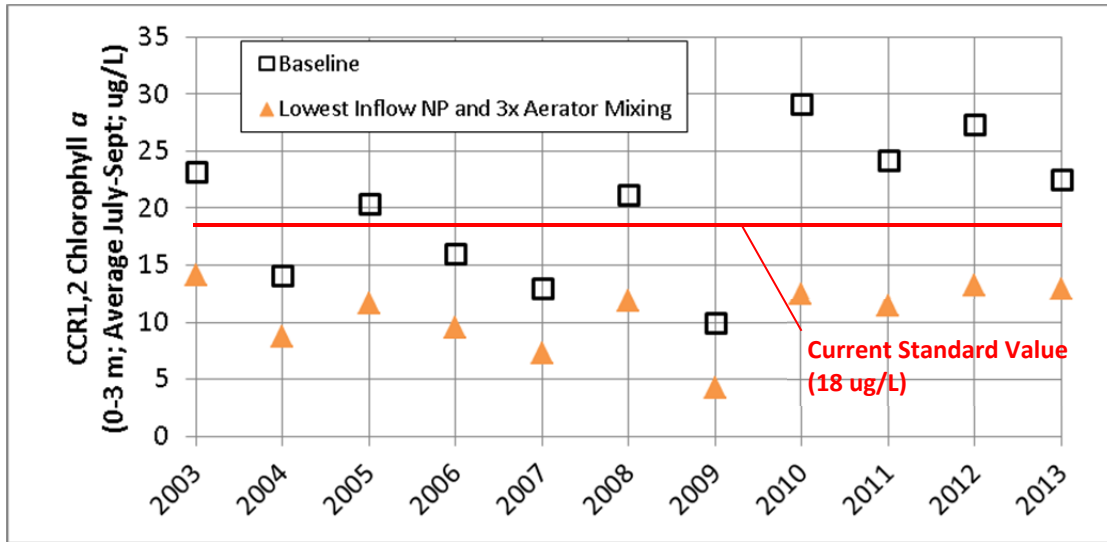


Figure 97. Simulated Average July-September Chlorophyll *a* – Max Watershed, 3x Destratification (Baseline Compared to Best-Case Reduced Inflow Nutrients and Hypothetical Destratification System with Three Times the Vertical Mixing - Applied to All Years)

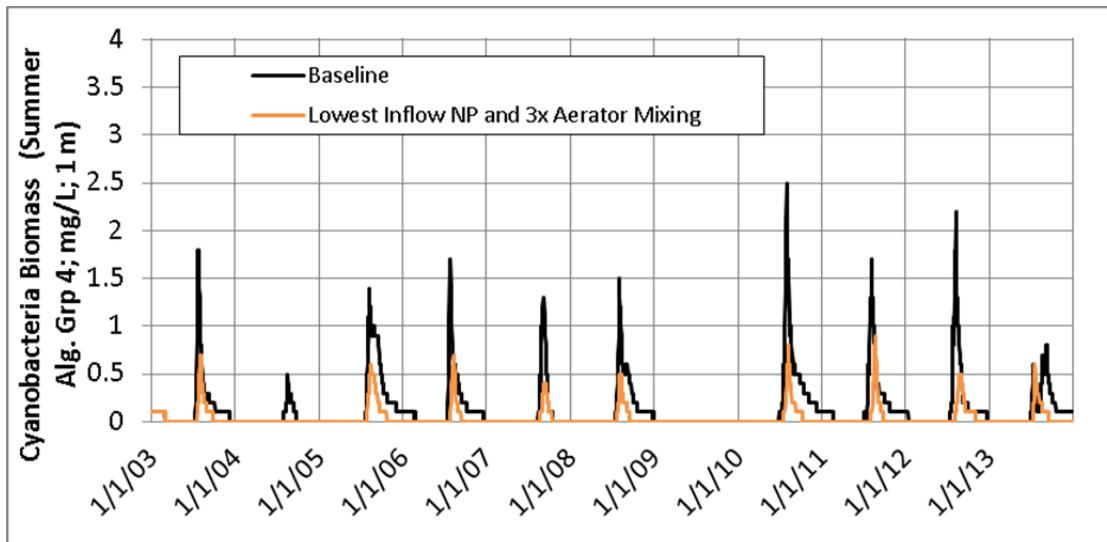


Figure 98. Simulated Average Summer Cyanobacteria Biomass – Max Watershed, 3x Destratification (Baseline Compared to Best-Case Reduced Inflow Nutrients and Hypothetical Destratification System with Three Times the Vertical Mixing - Applied to All Years)

It is unclear how the fishery in the reservoir might respond to such a dramatic reduction in algal productivity as that simulated for Run 3. As described in 2.5.6 and Section 2.6, the zooplankton

populations already exhibit signs of high predation by higher trophic levels, but there is some remaining uncertainty about the relationship of fish to zooplankton populations. The model does not simulate effects on fish; therefore, simulated effects on zooplankton for the management runs should be interpreted cautiously. That said, the model simulates an average 6% reduction in total zooplankton biomass for Run 3 as compared to the baseline run (Figure 99), with a shift in the timing of annual populations peaks. An improved understanding of the fish populations, natural recruitment, and biomass, as noted in Section 2.6, would support better anticipation of the effects, if any, of such a reduction of productivity on the fishery.

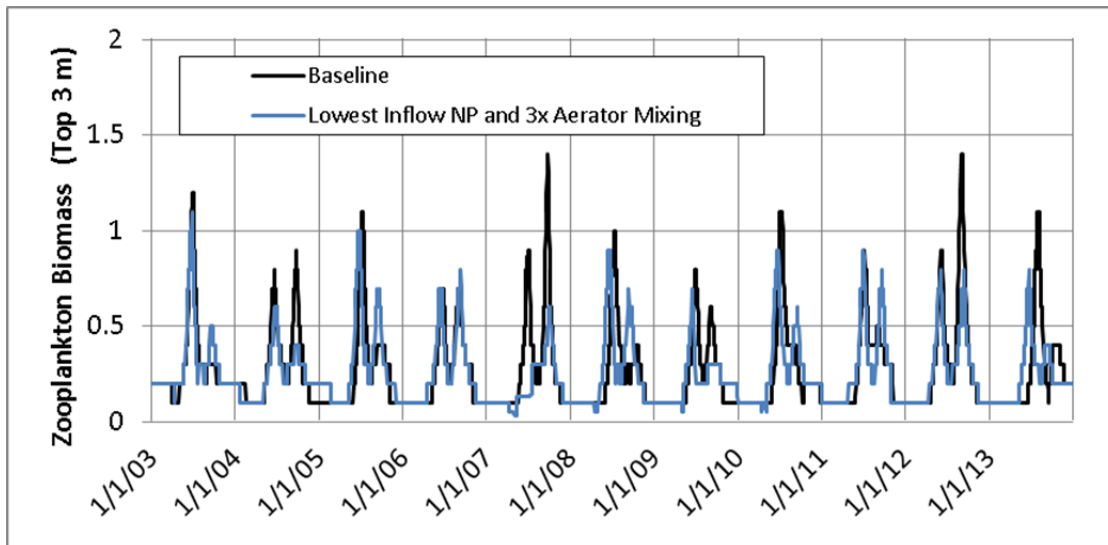


Figure 99. Simulated Zooplankton Biomass Concentrations— Max Watershed, 3x Destratification (Baseline Compared to Best-Case Reduced Inflow Nutrients and Hypothetical Destratification System with Three Times the Vertical Mixing - Applied to All Years)

6.4 Run 4 – Reduction in Inflow Phosphorus Concentration Needed to Meet Chlorophyll *a* Standard

The sensitivity analysis run results (described in Section 5) indicate that a 50% reduction in inflow phosphorus (in the form of orthophosphate [PO₄]) would not alone be adequate to meet the site-specific, in-reservoir chlorophyll *a* standard in all simulated years. The Authority would like to know what percent reduction in inflow PO₄ would be needed to meet that standard. Because the majority of inflow loading of PO₄ is from Cherry Creek, and watershed control work has, to-date largely focused on Cottonwood Creek, the percent reductions tested for this run focused on Cherry Creek.

A series of model runs was conducted progressively increasing the percent reduction in PO₄ concentration in Cherry Creek until the July through September chlorophyll *a* average was less than or equal to 18 ug/L in all of the eleven simulated years. Additionally, the calibrated adjustment applying increased organic matter to the sediment following the fish kill in August of 2012 (described in Section 3.6) was removed for these runs.

The runs indicate that a 75% reduction in inflow PO4 concentrations from Cherry Creek was needed to meet the site-specific chlorophyll *a* standard value in all of the simulated years. That reduction in average annual load compares to the baseline and other management runs as shown in Figure 100. The resulting simulated average summer chlorophyll *a* is provided in Figure 101. The model also simulates that this major reduction in inflow PO4 would result in less frequent and smaller-magnitude summer cyanobacteria blooms (Figure 102).

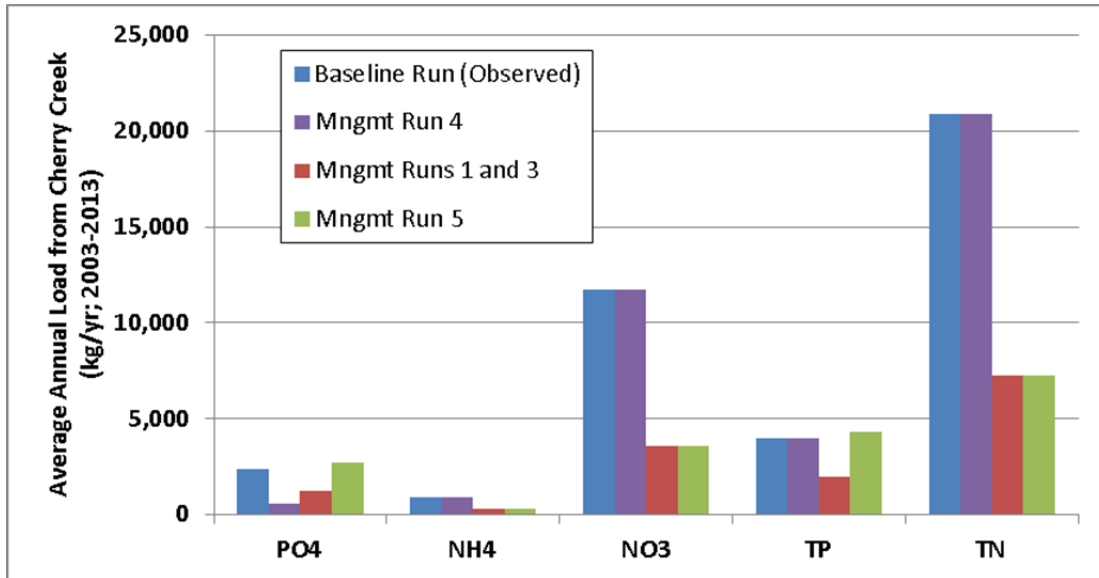


Figure 100. Comparison of Average Annual Cherry Creek Nutrient Loads for Management Runs 1, 3, 4, and 5

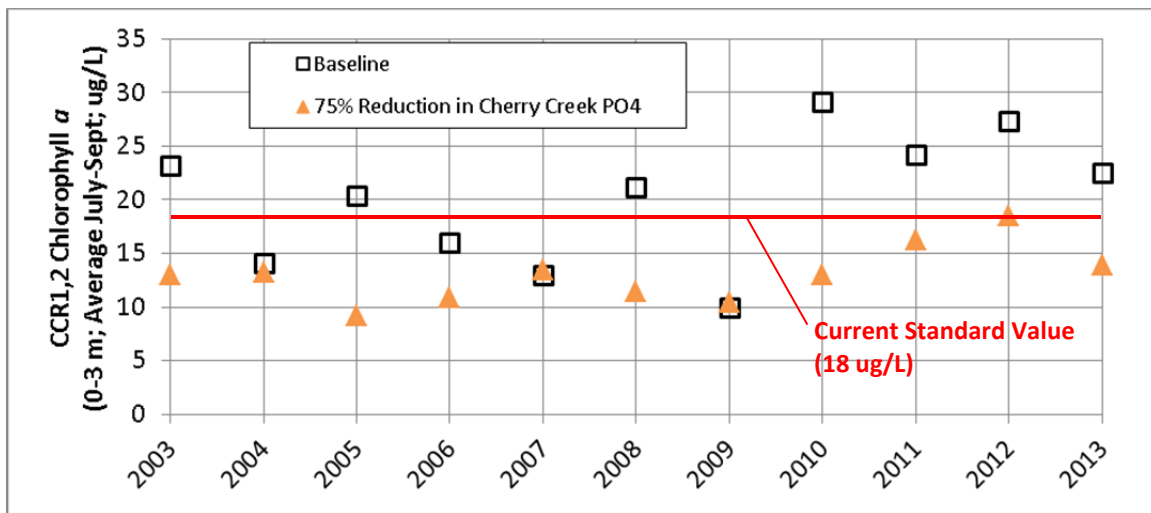


Figure 101. Simulated Average July-September Chlorophyll *a* – Reduced PO4 in Inflow (Baseline [Existing Destratification Operation] and Hypothetical Destratification System with Three Times the Vertical Mixing of the Current System - Applied to All Years)

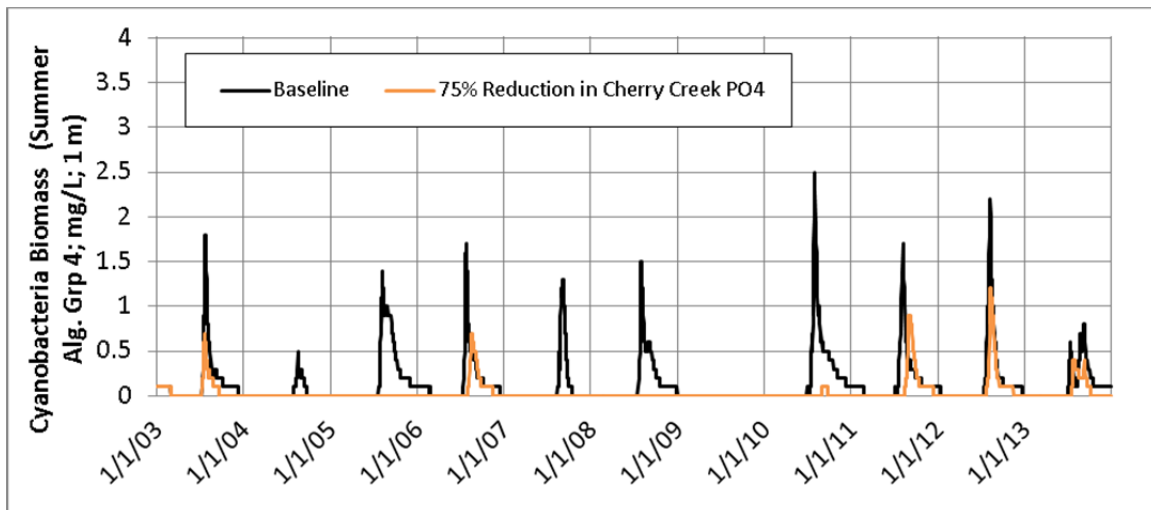


Figure 102. Simulated Average Summer Cyanobacteria Biomass – Reduced PO4 in Inflow (Baseline [Existing Destratification Operation] and Hypothetical Destratification System with Three Times the Vertical Mixing of the Current System - Applied to All Years)

6.5 Run 5 – Nitrogen-to-Phosphorus Ratio

Cherry Creek Reservoir tends to be nitrogen limited in summer months (Hydros, 2016 and others). This creates an advantage for cyanobacteria that can fix nitrogen from the atmosphere. Based on this, a concern has been expressed that further reductions in inflow inorganic nitrogen concentrations could exacerbate nitrogen-limited conditions, potentially increasing cyanobacteria growth. To evaluate the potential significance of this, Run 5 was designed to simulate effects of the maximum potential reduction in total inorganic nitrogen (TIN) loading without a corresponding reduction in phosphorus loading. LRE provided estimated tributary inflow concentrations maximizing watershed controls on TIN but not on PO4 (Figure 90 and Figure 91). The inputs for this run correspond to a 71% reduction in the average TIN:PO4 ratio of the inflows over the 11-year period, with the annual, volume-weighted average inflow TIN:PO4 ratio decreasing from 22 to 6.4. Beyond applying these inflow concentrations for Cherry Creek and Cottonwood Creek, no changes were made in the model settings relative to the baseline condition of the calibration run.

Lower inflow TIN:PO4 ratios resulting in simulation of summer average chlorophyll *a* concentrations similar to the baseline run, with no change in the number of years exceeding the site-specific standard (Figure 103). There was a small overall average decrease in summer chlorophyll *a* of 1.8 ug/L. This decrease is due to the slightly lower inflow PO4 and lower algal growth at times outside optimal cyanobacteria growth temperatures.

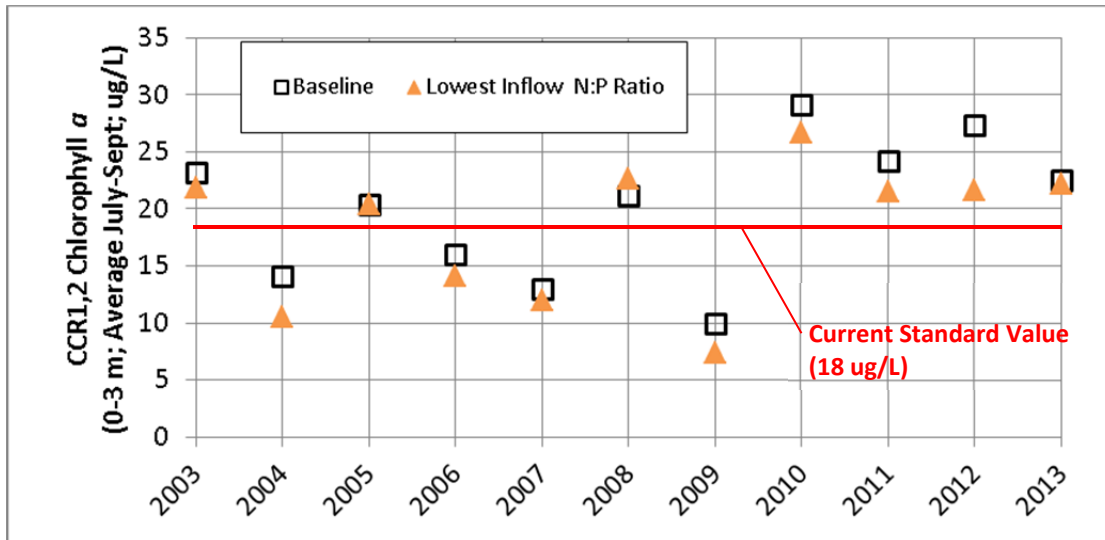


Figure 103. Simulated Average July-September Chlorophyll α – N-to-P Ratio Run
(Baseline and Hypothetical Minimum Nitrogen-to-Phosphorous Inflow Ratio)

The model simulation indicates that in some years (e.g., 2007, 2008, and 2013) summer cyanobacteria may begin to grow sooner in response to the lower TIN:PO₄ ratio, but overall biomass and peaks would be similar to baseline (Figure 104). This suggests that, in this already-nitrogen-limited reservoir, summer cyanobacteria (generally *Aphanizomenon flos-aquae*) already grow whenever temperature and flow conditions are optimal, so even-lower nitrogen-to-phosphorus ratios do not have a large effect. Interestingly, the model simulated a larger growth-stimulating effect on the nitrogen-fixing cyanobacteria that grow in late-spring/fall water temperatures (largely *Anabaena flos-aquae*; Figure 105). Results indicate that reducing the inflow TIN:PO₄ ratio causes TIN to be depleted earlier in the spring, resulting in the potential for larger *Anabaena* blooms at that time in most years¹². In short, based on these simulated results, further reductions to inflow TIN:PO₄ ratios are not expected to have a large effect on summer cyanobacteria, but could increase spring blooms of the nitrogen-fixing cyanobacteria, *Anabaena flos-aquae*.

¹² While the direction of predicted effects on the spring *Anabaena* blooms is expected to be reasonable, there is greater uncertainty in the predicted timing and magnitude of blooms for this algal group, as opposed to the summer cyanobacteria (generally *Aphanizomenon*). This is due to lack of spring *Anabaena* blooms in the calibration period of record with algal biovolume data (2009-2013). Settings in the model for this algal group are based largely on observations of such blooms in the spring of 2014 and 2015; however, future updates of the model to include 2014 and 2015 would allow for more direct refinement of optimum growth and temperature rate settings.

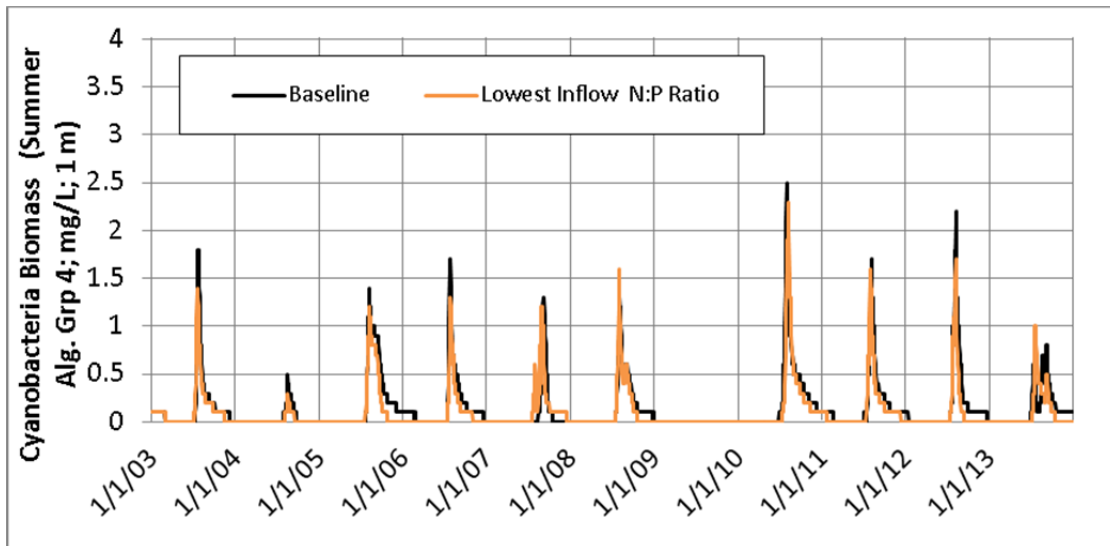


Figure 104. Simulated Average Summer Cyanobacteria Biomass – N-to-P Ratio Run
(Baseline and Hypothetical Minimum Nitrogen-to-Phosphorous Inflow Ratio)

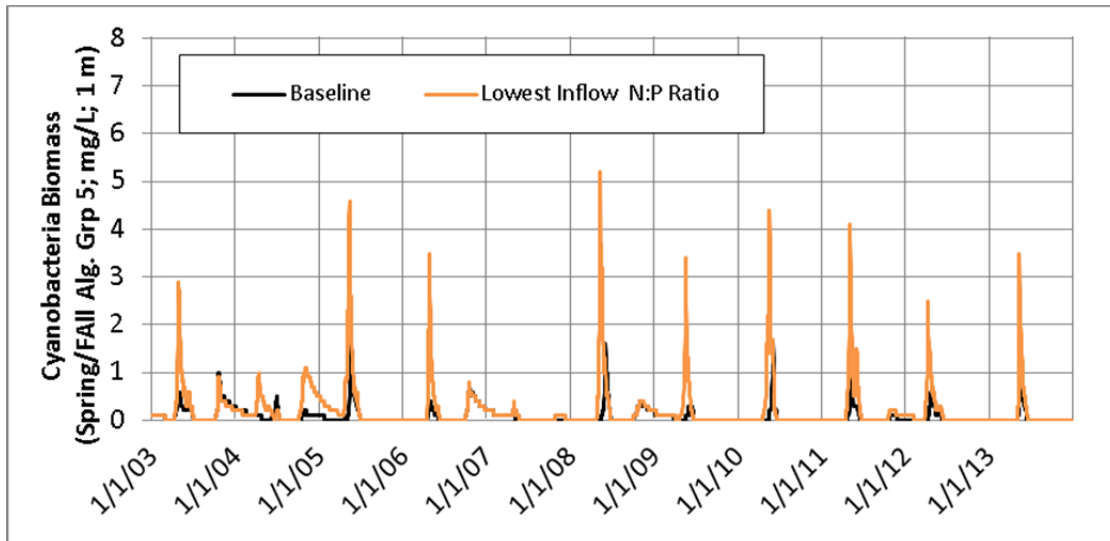


Figure 105. Simulated Average Spring/Fall Cyanobacteria Biomass – N-to-P Ratio Run
(Baseline and Hypothetical Minimum Nitrogen-to-Phosphorous Inflow Ratio)

7 Summary of Findings, Recommendations, and Next Steps

A two-dimensional hydrodynamic and water-quality model of Cherry Creek Reservoir has been developed using CE-QUAL-W2. The model simulates in-reservoir water quality for the years 2003 through 2013 and was calibrated to observed data. The model simulates algal growth, including cyanobacteria, chlorophyll *a*, dissolved oxygen, temperature, light, nutrients, inorganic suspended solids, and organic matter. A sensitivity analysis was conducted with the calibrated model, focusing on water-quality response to major forcing functions for this system, including wind, internal loading, the loading of nutrients from tributaries, and the destratification system. Additionally, five management runs were conducted carrying inflow nutrient loading and the mixing intensity of the destratification system. A summary of findings, monitoring recommendations, and anticipated next steps are presented in this section.

7.1 Study Findings

This study yielded an improved understanding of nutrient loading and algal response in the reservoir, as well as the effectiveness of the current destratification system.

What Drives/Affects Algal Growth in Cherry Creek Reservoir?

- **Polymictic:** Cherry Creek Reservoir is a shallow, eutrophic reservoir that exhibits significant mixing by wind throughout the year (polymictic), resulting in vertical nutrient cycling and increased algal growth throughout the summer.
- **High Internal and External Nutrient Loading:** Both high internal (from sediments) and external (from inflows) loading of nutrients are important drivers with respect to algal growth. Of the external loading terms, Cherry Creek provides the majority of the inflowing nutrient load.
- **Anaerobic and Aerobic Internal Loading:** Both anaerobic and aerobic internal loading from sediments are significant to algal growth, though anaerobic loading is currently greater. This is relevant in consideration of in-reservoir management options.
- **Flushing Flows:** Large spring inflows (flushing flows reducing residence time in the reservoir), such as those observed in 2007, 2009, and 2015, appear to affect summer algal dynamics, resulting in lower chlorophyll *a* concentrations, though not necessarily lower algal biomass.

What Causes Cyanobacteria Blooms in Cherry Creek Reservoir?

- **Nitrogen Limitation:** Cherry Creek Reservoir tends to be nitrogen limited, with elevated orthophosphate and near-absence of inorganic nitrogen at times. This gives a competitive advantage to nitrogen-fixing cyanobacteria.
- **Calm, Warm Conditions:** Summer cyanobacteria blooms tend to occur when the reservoir is calm (low wind and minimal inflows) with warm water temperatures. These conditions set up weak stratification which leads to depletion of inorganic nitrogen in the photic zone, while excess orthophosphate remains.

What is the Current and Potential Effectiveness of the Destratification System?

- **Current System is Under-sized:** The current destratification system is under-sized to achieve the mixing needed to maintain oxic conditions at the bottom of the reservoir. As a result, the current system is not effectively reducing anaerobic internal loading of nutrients. Further, in the deeper areas of the reservoir, data suggest that dissolved oxygen concentrations may be further suppressed due to induced sediment oxygen demand when the destratification system is operating.
- **Minor to No Effects on Cyanobacteria, Algae, or Walleye:**
 - Existing data and modeling indicate there has not been a noteworthy reduction in cyanobacteria since installation of the destratification system.
 - The current destratification system has only a very small effect on algal growth and chlorophyll *a*.
 - There is no clear impact (adverse or beneficial) of the current destratification system on the walleye fishery.
- **Redesign with Increased Mixing Could Have the Desired Effects:**
 - Model runs indicate that a destratification system with three times the vertical mixing effect of the current destratification system is needed to meet the original design target dissolved oxygen (DO) of 5 mg/L at the bottom of the reservoir.
 - This increased mixing would also decrease average summer chlorophyll *a* below the standard and reduce cyanobacteria blooms.
 - A separate study would be needed to appropriately size and design such a system.

What is the Potential Effectiveness of Watershed Controls on Nutrients?

- **Major Inflow Nutrient Concentration Reductions Needed to Meet Chl *a* Standard:**
 - 50% reductions in nutrient loading from either Cherry Creek or Cottonwood Creek alone would not be adequate to meet the chlorophyll *a* standard in all years.
 - The Authority's best-case estimated reductions in inflow nutrient concentrations (47% decrease in orthophosphate and 72% decrease in inorganic nitrogen from the combined tributary load) would result in meeting the site-specific chlorophyll *a* standard in all the simulated years. Further, peak cyanobacteria concentrations would be reduced.
- **Drastic Changes Predicted for Combined Maximum Watershed Controls *plus* Redesigned Destratification System:** The combined effect of sharply reducing inflow nutrient concentrations (Authority-predicted maximum controls) and tripling the vertical mixing of the destratification system would result in summer chlorophyll *a* well

below the standard in all simulated years (an average reduction of 9.4 ug/L) and sharply reduced peak cyanobacteria concentrations.

- **Caution on N:P Ratios and Cyanobacteria:** Major changes to the inflow nutrient ratios (reduced inorganic nitrogen inflow concentrations in the absence of corresponding reductions to inflow orthophosphate) could increase spring cyanobacteria blooms of *Anabaena flos-aquae*. There are not similar concerns for the summer cyanobacteria (typically *Aphanizomenon flos-aquae*).

7.2 Recommendations

Through the course of the study, critical areas of remaining uncertainty were identified that merit ongoing evaluation and/or additional monitoring. Overall, the existing water-quality dataset is an excellent record of conditions in the reservoir and was critical to successful model development, but there are a few critical gaps. The following recommendations are offered to increase confidence in future management decision-making.

- **Continuous / High-Frequency In-Reservoir DO Measurement** – Oxygen conditions at the sediment-water interface are a key indicator of mixing and driver of algal response in the reservoir, yet the observed dynamics are an area of uncertainty given the frequency of current profile collection in this highly dynamic system. It is strongly recommended that the Authority install continuous DO probes at 1 m below the surface and at 0.5 m above the bottom of the reservoir at CCR2. Alternatively, a buoy-based automated profiler, including DO measurement, located at CCR2 would greatly contribute to understanding of DO and mixing dynamics. Even a single year of such data would be invaluable.
- **Wind Data** – Wind is the primary driver of mixing in the reservoir, yet wind data are only available from a 10 m tower located roughly four miles south of the reservoir, leading to some uncertainty in the representativeness of the input. Given the major effects of wind on the water-quality response of Cherry Creek Reservoir, it is recommended that the Authority coordinate with Colorado Parks and Wildlife (CPW) to check and improve wind data collection and data management protocols for the CPW met station located next to the reservoir. Alternatively, a new meteorological station could be installed at the dam. Wind speed and direction data are of primary importance, but including air temperature, relative humidity, and solar radiation would also be helpful.
- **Fish Data** – To better understand food web inter-dynamics with water-quality:
 - A limited amount of fish aging work is needed for validating inferences about fish age-growth. Aging with otoliths is preferred for both walleye and shad, but dorsal spines can also be used in young walleye. Growth of both walleye and gizzard shad appears to be fast enough for the Petersen length-frequency method to be useful, but aging with chronometric body parts is needed to validate the method for use in the future.

- For gizzard shad, in addition to growth investigations recommended above, standardized electrofishing surveys of shad size and abundance in fall, coupled with spring surveys to evaluate overwinter survival are recommended.
- **Critical Sampling to Continue**
 - Continued collection of in-reservoir thermistor data at CCR2 and algal species and biovolume data is critical. Likewise, data collection of organic carbon and zooplankton should be continued.
 - Continued monitoring of the fishery in September is recommended, using standard methods and a statistically valid sampling design. Catch-per-unit effort of vulnerable size classes can be used as an index of recruitment. Accurate measurements of fish weight are required if fish condition indices are to be valid.
- **Possible Sampling to Discontinue** –For the purposes of modeling, water-quality profile collection and grab sampling at location CCR1 could be discontinued. Likewise, thermistor data collection at 1 meter intervals at CCR1 and CCR3 could be discontinued.
- **Investigate pH and Specific Conductivity Trends:** Investigate and continue to track the multi-year trend of increasing specific conductivity and decreasing pH observed in the reservoir and inflows. Ideally, the explanation for these trends will be a finding of the pending watershed modeling.

7.3 Next Steps

It is expected that the next application of the reservoir model will be conducted in conjunction with the watershed model (in development). The watershed model is expected to provide refined predictions of potential improvements to inflow water quality. The reservoir model can then use watershed model predictions as input to generate updated predictions of reservoir response to watershed controls. Prior to that application, it would be valuable to update the data analysis and modeling period to extend through the recent years which have a more robust dataset than early years in the simulation.

8 References

- Allen, R. G., W. Pruitt, J. Wright, T. Howell, F. Ventura, R. Snyder, D. Itenfisu, P. Steduto, J. Gerengena, M. Smith, L. Pereira, D. Raes, A. Perrier, I. Alves, I. Walter, and R. Elliot. 2006. A recommendation on standardized surface resistance for hourly calculation of reference ET_0 by the FAO56 Penman-Monteith method. *Agricultural Water Management*. Vol. 81. March 10, 2006.
- Ashley, K.I. 1983. Hypolimnetic Aeration of a Naturally Eutrophic Lake: physical and chemical effects. *Canadian Journal of Fisheries and Aquatic Sciences* 40 (9), 1343–1359.
- Barica, J., H. Kling, J. Gibson. 1980. Experimental Manipulation of Algal Bloom Composition by Nitrogen Addition. *Canadian Journal of Fisheries and Aquatic Sciences*, 1980, Vol. 37, No. 7. Pgs. 1175-1183.
- Beeman, J.W., D.A. Venditti, r.G. Morris, D.M. Gadomski, B.J. Adams, S.P> VanderKooi, t.C. Robinson, and A.G. Maule. 2003. Gas Bubble Disease in Resident Fish Below Coulee Dam. USGS in Cooperation with U.S. Bureau of Reclamation.
- Bergman, B., E. Flores, H. Bohme, T. Happe, B. Osborne, K. Sivonen, S. Ventura, A. Wilmotte, A. Moth-Wiklund, and P. Cosgrove. 1999. Cyanofix; An ESF Scientific Programme. European Science Foundation. September 1999.
- Boyer, J.M., C. Hawley, and T. Adams. 2014a. Cherry Creek Reservoir Water-Quality Modeling Project: Data Review (Task 1). Technical Memorandum Prepared for the Cherry Creek Basin Water Quality Authority. August 4, 2014.
- Boyer, J.M., C. Hawley, and T. Adams. 2014b. Cherry Creek Reservoir Water-Quality Modeling Project: Model Selection (Task 3). Technical Memorandum Prepared for the Cherry Creek Basin Water Quality Authority. October 7, 2014.
- Brown and Caldwell. Cherry Creek Basin Watershed Phosphorus Model Documentation. Prepared for the Cherry Creek Basin Water Quality Authority. February, 2009.
- Clough, Jonathan S. 2014. Aquatox Release 3.1 plus. Modeling Environmental Fate and Ecological Effects in Aquatic Systems. Volume 1: User's Manual. U.S. Environmental Protection Agency Office of Water, Office of Science and Technology. <https://www.epa.gov/exposure-assessment-models/aquatox-supporting-documentation>.
- Cole, T.M. and S.A. Wells. 2011. CE-QUAL-W2: A Two-Dimensional, Laterally Averaged, Hydrodynamic and Water Quality Model, Version 3.71. User Manual. Instruction Report EL-11-1. Prepared for U.S. Army Corps of Engineers. March 2011.

- Colorado Parks and Wildlife (CPW). 2013. Cherry Creek State Park Brochure. HPCC1104_5K_10/11. Retrieved on May 25, 2013 from: <http://www.parks.state.co.us/PARKS/CHERRYCREEK/MAPSANDDIRECTIONS/Pages/CherryCreekMapsandDirections.aspx>.
- CCBWQA. 2013. Background Information for Reservoir Modeler. Powerpoint Presentation. April 30, 2013.
- Dobberfuhl, D.R., R. Miller, and J.J. Elser. 1997. Effects of a cyclopoid copepod (*Diacyclops thomasi*) on phytoplankton and the microbial food web. *Aquatic Microbial Ecology* 12: 29-37.
- Gantzer, P.A., L.D. Bryant, Little, J.C. 2009. Effects of Hypolimnetic Oxygen Depletion Rates in Two Water Supply Reservoirs. *Water Research* 43. Pgs 1700-1710.
- GEI Consultants, Inc. (GEI). 2014. Cherry Creek Reservoir 2013 Annual Aquatic Biological and Nutrient Monitoring Study and Cottonwood Creek Phosphorus Reduction Facility Monitoring. March 2014. Prepared for the Cherry Creek Basin Water Quality Authority.
- GEI Consultants, Inc. (GEI). 2015. Cherry Creek Reservoir 2014 Annual Aquatic Biological and Nutrient Monitoring Study and Cottonwood Creek Phosphorus Reduction Facility Monitoring. March 2015. Prepared for the Cherry Creek Basin Water Quality Authority.
- Hydros Consulting (Hydros). 2015. Cherry Creek Reservoir Water-Quality Modeling Project: Model Calibration and Sensitivity Analyses. Technical Memorandum to the Cheery Creek Basin Water Quality Authority. July 31, 2015.
- Hydros Consulting (Hydros). 2016. Cherry Creek Reservoir Water-Quality Modeling Project: Data Analysis to Support Task 3B Recoding and Recalibration. Technical Memorandum to the Cheery Creek Basin Water Quality Authority. June 30, 2016.
- Johnson, B. 2014. Environmental Conditions for Walleye in Cherry Creek Reservoir. Prepared for Cherry Creek Basin Water Quality Authority. Rev. August 11, 2014.
- Leonard Rice Engineers Inc. (LRE). 2016. Memorandum: Derivation of Scenarios 1, 3, and 5 Nutrient Inputs for Cherry Creek and Cottonwood Creek. Sent from K. Fendel (LRE) to J.M. Boyer (Hydros). December 1, 2016.
- Lewis, W.M., Saunders, J.F., and McCutchan, J.H. 2004. Studies of Phytoplankton Response to Nutrient Enrichment in Cherry Creek Reservoir, Colorado. Prepared for Colorado Department of Public Health and Environment Water Quality Control Division. January 22, 2004.
- Lewis, W.M., McCutchan, J.H., and Saunders, J.F. 2005. Estimation of Groundwater Flow into Cherry Creek Reservoir and its Relationship to the Phosphorus Budget of the Reservoir. Prepared for the Cherry Creek Basin Water Quality Authority and the Colorado

- Department of Public Health and Environment Water Quality Control Division. March 7, 2005.
- May, M. 2014. Memorandum on Phytoplankton Analysis. From M. May (CPW) to C. Reid (CCBWQA). November 14, 2014.
- McCutcheon, S.C. 1990. Water Quality Modeling: River Transport and Surface Exchange. Volume 1. CRC Press. January 5, 1990.
- Moore, B. C., Chen, P.-H., Funk, W. H. and Yonge, D. 1996. A Model for Predicting Lake Sediment Oxygen Demand Following Hypolimnetic Aeration. JAWRA Journal of the American Water Resources Association, 32: 723–731.
- Risley, J.C. and M.W. Gannett. 2006. An Evaluation and Review of Water-Use Estimates and Flow Data for the Lower Klamath and Tule Lake National Wildlife Refuges, Oregon and Californian. USGS Scientific Investigations Report 2006-5036; Prepared in Cooperation with the Bureau of Reclamation.
- Smith, V. 1983. Low Nitrogen to Phosphorus Ratios Favor Dominance by Blue-Green Algae in Lake Phytoplankton. Science. New Series. Vol 221, #4611. August 12, 1983.
- Schindler, D.W. R. Hecky, D. Findlay, M. Stainton, B. Parker, M. Paterson, K. Beaty, M. Lyng, S. Kasian. Eutrophication of Lakes Cannot Be Controlled by Reducing Nitrogen Input: Result of a 37-Year Whole Ecosystem Experiment. Proceedings of the National Academy of Sciences. Vol 105, #32. August 12, 2008.
- Soltero, R.A., Sexton, L.M., Ashley, K.I., McKee, K.O., 1994. Partial and Full Lift Hypolimnetic Aeration of Medical Lake, WA to Improve Water Quality. Water Research 28 (11), 2297–2308.
- St. Amand, A. 2014. Advanced Algal Identification Workshop: QA/QC. PhycoTech, Inc. St. Joseph, MI.
- Walter, I., Allen, R., Elliott, R., Jensen, M., Itenfisu, D., Mecham, B., Howell, T., Snyder, R., Brown, P., Echings, S., Spofford, T., Hattendorf, M., Cuenca, R., Wright, J., and Martin, D. 2001. ASCE's Standardized Reference Evapotranspiration Equation. Watershed Management and Operations Management 2000: pp. 1-11.
- Wells, S.A., V.I. Wells, and C.J. Berger. 2008. Water Quality and Hydrodynamic Modeling of Tenkiller Reservoir. Expert Report prepared for the State of Oklahoma. Case No. 05-CU-329-GKF-SAJ. May 2008.
- Wolf, C. 2013. The Effects of Reservoir Destratification on Reservoir Ecology and Beneficial Uses. Presentation to North American Lake Management Society. October, 2013.